5-2014

Beetles, Fungi and Trees: A Story for the Ages? Modeling and Projecting the Multipartite Symbiosis Between the Mountain Pine Beetle, *Dendroctonus ponderosae*, and Its Fungal Symbionts, *Grosmannia clavigera* and *Ophiostoma montium*

Audrey L. Addison
Utah State University

BEETLES, FUNGI AND TREES: A STORY FOR THE AGES? MODELING

AND PROJECTING THE MULTIPARTITE SYMBIOSIS BETWEEN THE

MOUNTAIN PINE BEETLE, *DENDROCTONUS PONDEROSAE*, AND

ITS FUNGAL SYMBIONTS, *GROSMANNIA CLAVIGERA*

AND *OPHIOSTOMA MONTIUM*

by

Audrey L. Addison

A dissertation submitted in partial fulfillment
of the requirements for the degree

of

DOCTOR OF PHILOSOPHY

in

Mathematics

Approved:

_____   _____
Dr. James A. Powell   Dr. Nghiem Nguyen
Major Professor   Committee Member

_____   _____
Dr. Barbara Bentz   Dr. John Stevens
Committee Member   Committee Member

_____   _____
Dr. Luis Gordillo   Dr. Mark R. McLellen
Committee Member   Vice President for Research and
                                                              Dean of the School of Graduate Studies

UTAH STATE UNIVERSITY
Logan, Utah

2014

ABSTRACT

Beetles, Fungi and Trees: A Story for the Ages? Modeling

and Projecting the Multipartite Symbiosis Between the

Mountain Pine Beetle, *Dendroctonus ponderosae*, and

Its Fungal Symbionts, *Grosmannia clavigera*

and *Ophiostoma montium*

by

Audrey L. Addison, Doctor of Philosophy

Utah State University, 2014

Major Professor: Dr. James A. Powell
Department: Mathematics and Statistics

As data collection and modeling improve, ecologists increasingly discover that inter-species dynamics greatly affect the success of individual species. Models accounting for the dynamics of multiple species are becoming more important. In this work, we explore the relationship between mountain pine beetle (MPB, *Dendroctonus ponderosae* Hopkins) and two mutualistic fungi, *Grosmannia clavigera* and *Ophiostoma montium*. These species are involved in a multipartite symbiosis, critical to the survival of MPB, in which each species benefits.

Extensive phenological modeling has been done to determine how temperature affects the timing of life events and cold-weather mortality of MPB. The fungi have also been closely studied to determine how they interact with MPB and how they differ in terms of virulence, response to temperature, and nutritional benefits to developing beetles. Overall, researchers consider *G. clavigera* to be the superior mutualist. Beetles developing near *G. clavigera* are larger, produce more brood, and have higher survival rates. Regarding temperature preferences, *G. clavigera* is considered "cool-loving," growing at cooler temperatures than *O. montium*. These findings lead researchers to wonder 1) why has *G. clavigera* not displaced

O. montium from the mutualism (if it is the superior mutualist) and 2) what will happen to the MPB-fungus mutualism in the face of a warming climate.

In this work we present two models connecting fungal growth in a tree to predictions of MPB emergence: a stochastic, individual-based model and a deterministic, tree-based model. We begin by exploring whether variability in temperature can act as a stabilizing mechanism and find that temperature variability due to MPB periodically transitioning between different thermal environments is the most likely explanation for the continued presence of both fungi in the mutualism. Using the second model, we parameterize and validate the model using attack and emergence observations of MPB and the fungi they are carrying. In the process, we test several submodels to learn more about specific MPB-fungi interactions. Finally, utilizing information from previous fungal growth experiments, we test and parameterize several growth rate curves using Bayesian techniques to determine whether the inclusion of prior knowledge can lead to more realistic fits.

(140 pages)

PUBLIC ABSTRACT

Beetles, Fungi and Trees: A Story for the Ages? Modeling

and Projecting the Multipartite Symbiosis Between the

Mountain Pine Beetle, *Dendroctonus ponderosae*, and

Its Fungal Symbionts, *Grosmannia clavigera*

and *Ophiostoma montium*

Audrey L. Addison

As technology improves, so do modes of data collection and mathematical modeling. With this increased data, ecologists are learning that the success or failure of a given species depends not just on the species, but on those it interacts with as well. A prime example of this is the mountain pine beetle (MPB, *Dendroctonus ponderosae* Hopkins) which spends the majority of its life inside a host pine tree, emerging only to find new trees and lay eggs for the next generation. This beetle is of interest because it is capable of killing healthy pine trees on a landscape scale, causing large economic and ecological impacts. As a result, scientists have spent many years studying and modeling the life cycle and habits of the beetle. In the process, they have found that MPB are highly dependent on two species of fungi, *Grosmannia clavigera* and *Ophiostoma montium*. These three species are involved in an obligate multipartite mutualism in which the beetles benefit the fungi by providing transport to new host trees and the fungi benefit MPB as a supplemental food source during several of their developmental life stages.

Scientists have studied these two fungi to determine how they interact with MPB and how they differ in terms of their ability to grow in a tree, their temperature preferences and tolerances, and the amount and type of nutritional benefits they can provide to developing beetles. Overall, researchers consider *G. clavigera* to be more helpful to MPB. Beetles developing near *G. clavigera* are larger, produce more offspring, and have higher survival rates. Regarding temperature preferences, *G. clavigera* is considered "cool-loving," growing

faster at cooler temperatures than *O. montium* while *O. montium* is considered "warm-loving" and is able to grow faster at higher temperatures. These findings lead researchers to wonder, 1) if *G. clavigera* is better for MPB, why has it not displaced *O. montium* from the mutualism, and 2) what will happen to the MPB-fungus mutualism as temperatures warm.

In this work we present a stochastic, individual-based model and a deterministic, population-level model describing the growth of both fungi in a tree and connect these to existing models or approaches for MPB development as a function of the temperature inside a host tree. Using the first model, we begin by exploring whether variability in temperature can act as a stabilizing mechanism, keeping both fungi present in the mutualism, and find that temperature variability due to MPB periodically transitioning from warmer areas to cooler areas and back again is the most likely explanation for the continued presence of both fungi in the MPB-fungus relationship. Using the second model, we estimate parameters for the model using real-world attack and emergence observations of MPB and the fungi they are carrying. In the process, we test several hypotheses describing the timing of when MPB collect fungal spores (to carry to a new host tree) and find that the fungus present as MPB are preparing to exit the tree is most likely to be the fungus transported to new host trees. Finally, using information from previous fungal growth experiments, we test several growth rate curves to determine which is best able to describe the growth of the fungi. We estimate parameters for these curves using a statistical technique that allows prior knowledge of the fungi (from previous experiments) to be taken into account and determine whether this prior knowledge can lead to more accurate functions describing their growth.

This dissertation is dedicated to my wonderful and supportive husband, Eric; my sweet daughters Luca and Tori; and my two wonderful dogs Koopa and Ganon, who only occasionally complained when we worked at school for too long.

ACKNOWLEDGMENTS

Audrey L. Addison

CONTENTS

LIST OF TABLES

LIST OF FIGURES

CHAPTER 1

INTRODUCTION

In an era of rapidly changing climate, our ability to predict and understand future events will increasingly rely on data collection, modeling efforts, and the ability to incorporate community effects of a system rather than the effects of a single species. One such system is the multipartite mutualism that exists between the mountain pine beetle (MPB, *Dendroctonus ponderosae* Hopkins) and two species of filamentous fungi, *Grosmannia clavigera* and *Ophiostoma montium*.

MPB is an aggressive species of bark beetle that inhabits lodgepole, ponderosa, and whitebark pine trees in the western United States and Canada (Wood, 1982). This insect is a serious pest that has the ability to kill healthy trees and cause landscape-level tree mortality (Meddens et al., 2012), though in the past it has also acted as a natural disturbance agent helping to maintain forest ecosystem structure and function. It accomplishes this task with the use of aggregation pheromones (Raffa, 2001) to ensure new trees are rapidly attacked by high numbers of beetles. This high density allows MPB to overcome host defenses such as resin response mechanisms (Raffa, 2001) and eventually cause host tree mortality by severely disrupting fluid transport in the tree (Bentz et al., 2010). The ability of MPB to kill healthy trees and to devastate thousands of acres of trees during an outbreak, make it a very important species both economically and ecologically. The MPB life cycle commonly takes one to two years to complete (a generation completed in one year is known as univoltine while a generation taking longer is known as semivoltine) depending on temperatures inside the host tree; higher temperatures can lead to faster generation times while cooler temperatures can prolong developmental stages and lead to slower generation times. The MPB life cycle progresses as follows: after attacking a new host tree, mating occurs and adult MPB excavate tunnels in the phloem layer of the host tree (Safranyik et al., 2007), laying eggs to either side. As time progresses, beetle eggs hatch into larvae which create larval galleries or tunnels where they feed in the surrounding phloem (Bentz et al., 2010). The beetles continue to feed and develop inside the tree at a rate based on temperature,

moving through four larval stages and one pupal stage before becoming teneral (sexually immature) adults (Safranyik et al., 2007). The MPB life cycle repeats the following year as new adult MPB tunnel out of the bark layer of the tree and fly in search of a new host tree to colonize (Bentz et al., 2010).

Past studies of MPB primarily focused on modeling the insect's phenology, or developmental timing, as a function of temperature (Bentz et al., 2010; Logan and Powell, 2001) or analyzing the large-scale spatial pattern of its attacks from year to year using aerial survey data (Powell and Bentz, 2014; Chen and Walton, 2011). It is increasingly being recognized, however, that the dynamics of a single species can be greatly affected by those with which it interacts, though information has generally been lacking on how to quantify these effects (Bentz et al., 2010). In the case of MPB, this means that the success or failure of the beetle can be closely tied to the performance of its fungal symbionts.

The issue of phenological overlap is not new; many species interact in ways which bind their fates. In addition to MPB, which must coincide timing of larval development with its fungal symbionts, some plants rely on insects or animals for pollination or seed dispersal. Phenological timing can also be important within a species. In some ant and butterfly species, different development rates or maturation times in males and females can lead to variability in the timing of the reproductive period. This can affect mate preference and potentially which individuals are able to mate (Kaspari et al., 2001), possibly even raising the risk of extinction in small populations (Calabrese and Fagan, 2004). From a disease or parasite modeling standpoint, the spread of a disease generally depends on whether susceptible individuals come in contact with a given pathogen at a certain time (Molnár et al., 2013). Connecting models of phenology and development for multiple interacting species would increase our understanding of the broader effects species can have on one another.

The relationship between MPB, *G. clavigera*, and *O. montium* is considered an obligate multipartite mutualism. The fungi benefit by receiving transport to host trees and some shelter from the environment during transport inside the mycangia, specialized structures

for dispersing spores located on the maxillary cardines of both males and females (Six and Paine, 1998). The benefit to the beetles is less understood. It was previously thought that the fungi aided the beetles by quickly growing throughout the substrate of the new host tree, helping to choke its fluid transport systems and cause mortality (Harrington, 1993; Paine et al., 1997), however, this view is less accepted today. The current hypothesis is that mycophagy, the feeding by beetles as larvae or teneral adults on fungi, is the main benefit received by MPB (Harrington, 2005). Since the majority of the MPB life cycle is completed within the phloem layer of a dying host tree, mycophagy allows for more efficient use of the inner bark by increasing the amount of nitrogen available. The fungi also produce large amounts of ergosterol, a sterol that insects can convert to hormones that support molting and reproduction (Bentz and Six, 2006). Other potential benefits to MPB could include protection from harmful fungi or other organisms. Since MPB host trees are often also colonized by yeasts and other fungi, it is possible that MPB inoculation of a new host with *G. clavigera* and *O. montium* spores allow these mutualistic fungi to take root in the tree and limit the space available for other, possibly harmful, species of fungi (Klepzig et al., 2009).

Like many mutualisms, however, the MPB-fungus system is predicted to be unstable. The two fungi use the same resource at the same time (a freshly killed tree) and ultimately must compete for beetles when it is time to be dispersed. As a result, the fungi are expected to be in strong competition with one another and ecological theory suggests that the stronger competitor should outcompete the weaker competitor over time. Nonetheless, the MPB-fungus mutualism has remained relatively stable over a long period of evolutionary time (Six and Bentz, 2007). To better understand this dynamic, numerous studies have been conducted on beetle-associated fungi. These studies have uncovered differences between the fungi in terms of virulence, temperature preferences and tolerances, and the nutritional benefits they provide. Overall, *G. clavigera* is thought to be more virulent and more tolerant of low oxygen conditions than *O. montium* (Solheim and Krokene, 1998), meaning that it can likely grow better or faster immediately after attack. Growth experiments indicate *G.*

clavigera is the "cool-loving" fungus relative *O. montium* in that it tends to grow faster at low temperatures and can survive at colder temperatures. *O. montium*, on the other hand, is considered to be "warm-loving" with a higher optimum temperature for growth and generally higher growth rates at warmer temperatures. Finally, in terms of nutritional benefits, *G. clavigera* is considered slightly more nutritious to MPB. Beetles developing in the presence of *G. clavigera* are larger, have increased brood development, and higher survival rates (Six and Paine, 1998; Bleiker and Six, 2007).

Based on this synopsis, reasonable questions to ask include: 1) why is *O. montium* still present in the mutualism? and, 2) what will happen to the mutualism in the face of climate change? This work seeks to expand on previous knowledge of MPB and answer these questions by modeling and analyzing the critical symbiosis between MPB and its two fungal symbionts, *G. clavigera* and *O. montium*. Considerable attention has been given to understanding how temperature directly affects MPB developmental timing and cold-weather mortality (Bentz et al., 2010; Safranyik et al., 2010; Hicke et al., 2006; Logan and Powell, 2001). However, little work has focused on how temperature affects the symbiosis that exists between the MPB and its symbionts. Since this symbiosis is critical for the survival of MPB (Six and Bentz, 2007), understanding how temperature affects its fungal partners and how this in turn affects MPB is very important.

Our work seeks to combine previous knowledge and phenological models for MPB with experimental observations of fungus growth (direct fungal measurements) and observations of attacking and emerging MPB and the fungus they are carrying (indirect fungal measurements) to accurately model MPB-fungus dynamics inside a host tree. Using these models, we explore the future of the MPB-fungus system in the face of climate change and attempt to learn more about beetle-fungus interactions. We do this in three parts. In Chapter 2, we create a stochastic, individual-based model for fungi growing on a one-dimensional ring of tree circumference as a function of hourly temperature inside a host tree. This model includes the effect of finite space available to colonize and is combined with a previously developed temperature-driven model for median MPB development. Using this combina-

tion of models, we explore whether variability in temperature (over the course of a year, from year to year, or larger variability due to periodically transitioning between different thermal regions) can act as a stabilizing mechanism for the fungi. In the process, we also test whether differences in MPB attack density (which correspondingly affect the distance between fungal lesions) can help stabilize the mutualism.

In Chapter 3, we adapt the model developed for Chapter 2 to allow more input information such as the distribution of MPB attacks and the proportion of each fungus carried over time. This model computes cumulative fungus growth (on a tree-, rather than individual lesion-based, scale) and utilizes a colonization index to account for finite space available. Other adaptations include taking a distributional approach to determine the teneral adult feeding window (rather than using the timing of the median individual, as used in Chapter 2) and allowing fungal lesions to begin growing at different times (as they would in a tree). This model is then combined with a spectrum of five hypotheses representing the timing of fungal spore acquisition by MPB. Each hypothesis is implemented as a submodel which is parameterized using MPB attack and emergence data collected from 2010 to 2011. The submodels are compared and then tested against a second dataset collected from 2011 to 2012 to determine whether the MPB-fungus model can adequately model the actual system and to determine which mycangial packing hypothesis is most valid.

Finally, in Chapter 4, we use Bayesian statistical techniques in an attempt to improve the fit of fungal growth rate curves for both MPB-associated fungi as well as western pine beetle (WPB, *Dendroctonus brevicomis*) associated fungi. Fungal growth rate curves can take many forms, ranging from linear to nonlinear in nature with many different choices for parameters. Since temperature is thought to be one of the key drivers of success for the MPB and most likely to affect the MPB-fungus mutualism, we focus on several fungal growth rate curves that employ temperature thresholds (i.e., the coldest and warmest temperature where the fungi can grow) as key parameters. Though these temperature thresholds are important and biologically meaningful, a practical issue with their use is that they are difficult to directly measure, however, much expert knowledge exists on their relative location (e.g.,

from past, failed experiments). This fact makes a Bayesian approach ideal for parameter estimation. Two of its major benefits are the ability to include prior knowledge about the system when obtaining parameter estimates and the ability to tune the algorithm to ensure it does not become captured in poor regions of parameter space. We compare this technique to maximum likelihood estimation (MLE) with a built-in optimizer, an extremely common and simple-to-implement technique for parameter estimation, as well as to Bayesian "MLE" (B-MLE) which utilizes the same optimizer for MLE with the addition of prior knowledge in the equation being optimized.

From a broader perspective, this work utilizes mathematical tools to create and validate models for the interaction of three species with overlapping phenologies. These models incorporate previous models or approaches for MPB development and new models for fungus growth in a tree that can be parameterized using direct observations (i.e., fungus growth rates collected in an artificial medium). They are then combined using knowledge of the biological system and further parameterized with indirect observations of fungal prevalence (i.e., records of attacking and emerging MPB and the fungus they are carrying). We posit that predictions about the system as a whole will be made stronger when considering their overlapping phenologies. MPB success is thought to depend on nutritional benefits obtained from feeding on fungus colonized phloem at different stages in its development. Due to differences between its fungal symbionts, the degree of MPB success will also depend on fungal timing. Thus, in order to best predict or understand the future of the MPB-fungus system, inclusive models that quantify the likelihood of fungal presence at the appropriate time are essential.

CHAPTER 2

THE ROLE OF TEMPERATURE VARIABILITY IN STABILIZING THE MOUNTAIN

PINE BEETLE-FUNGUS MUTUALISM[1]

Abstract

As global climate patterns continue to change and extreme weather events become increasingly common, it is likely that many ecological interactions will be affected. One such interaction is the multipartite symbiosis that exists between the mountain pine beetle and two species of fungi, *Grosmannia clavigera* and *Ophiostoma montium*. In this mutualism, the fungi provide nutrition to the beetle, while the fungi benefit by being dispersed to new host trees. Multi-partite mutualisms are predicted to be unstable due to strong direct competition among symbionts or natural selection for superior over inferior mutualists. However, this mutualism has remained stable over long periods of evolutionary time. In this paper, we developed a temperature-based model for the spread of fungi within a tree and connected it to an existing model for mountain pine beetle development. Using this integrated model for fungal growth, we explored the possibility that temperature variability is a stabilizing mechanism for the mountain pine beetle - fungi mutualism. Of the three types of temperature variability we tested, intra-year, inter-year and variability due to transitioning between different thermal habitats (thermal migration), we found that thermal migration was the most robust stabilizing mechanism. Additionally, we found that the MPB attack density or spacing between fungal lesions also had a significant effect on the stability of the system. High attack densities or close lesion spacings also tended to stabilize the system, regardless of temperature.

1

2.1. Introduction

The mountain pine beetle (MPB, *Dendroctonus ponderosae* Hopkins) is a bark beetle native to western North America (Wood, 1982). This insect is a serious pest that also acts as a natural disturbance agent, helping to maintain forest ecosystem structure and function. Although MPB population eruptions have occurred for millenia, the size of current outbreaks is greater than those recorded in the past century (Taylor et al., 2007). The distribution of lodgepole pine (*Pinus contorta*), a primary host for MPB, extends further north than the current MPB range suggesting that MPB is limited by climate. Within the past two decades, outbreak MPB populations have expanded north in British Columbia, Canada, and across the Rocky Mountains infesting a new host jack pine (*Pinus banksiana*) in eastern Alberta (Cullingham et al., 2011). Several factors are playing a role in MPB population success and expansion including warming temperatures and past management strategies that promoted landscape homogeneity (Raffa et al., 2008).

Considerable attention has been given to understanding how temperature directly affects MPB development timing and cold temperature mortality, factors that influence geographic range expansion (Bentz et al., 2010; Safranyik et al., 2010; Hicke et al., 2006; Logan and Powell, 2001). However, little work has focused on how temperature affects the critical symbiosis that exists between the MPB and two fungal symbionts, *Grosmannia clavigera* (*G. clavigera*) and *Ophiostoma montium* (*O. montium*). The symbiosis is critical for the survival of MPB (Six and Bentz, 2007), and thus, understanding how temperature affects the fungal partners is as important as understanding how temperature will directly affect the host beetle.

The symbiosis between MPB and fungi is a mutualism. The beetle provides benefit to the fungi through transport to new host trees. This occurs in specialized structures of the insect exoskeleton called mycangia which are located on the maxillary cardines of both males and females (Six and Paine, 1998). When new adults leave the tree they carry spores of the fungi in the mycangia which are then inoculated into the phloem of the next tree as beetles construct egg galleries. In turn, the fungi aid the beetles by providing critical

nutrients to developing beetles (Six and Paine, 1998; Adams and Six, 2007; Bleiker and Six, 2007).

Nutritional benefits to MPB appear to be of two types. The fungi colonize both the phloem and sapwood of the tree. Mycelium growing in the sapwood picks up nitrogen and moves it into the phloem where the larvae feed and develop. Increases in phloem nitrogen due to the fungi can be substantial (40-50%) and likely account for observations that beetles developing with fungi have much higher survival rates and are significantly larger than those that develop without. The fungi also produce large amounts of ergosterol, a sterol that insects can convert to hormones that support molting and reproduction (Bentz and Six, 2006). MPB have been shown to require feeding on spores of fungi as new adults in order to produce eggs. This requirement may relate to ergosterol consumption (Six and Paine, 1998; Bentz and Six, 2006).

While the two fungi appear to impart the same types of benefits to the beetle, the degree of benefit varies (Six and Paine, 1998; Bleiker and Six, 2007; Goodsman et al., 2012; Cook et al., 2010). Overall, *G. clavigera* appears to be superior in concentrating nitrogen (Goodsman et al., 2012; Cook et al., 2010) and supporting brood development (Six and Paine, 1998; Bleiker and Six, 2007). Beetles developing with *G. clavigera* are larger and have higher survival rates (Six and Paine, 1998; Bleiker and Six, 2007). Larger size of beetles developing with *G. clavigera* may mean greater fecundity and overall fitness indicating that *G. clavigera* is the superior mutualist.

Like many mutualisms, the MPB-fungus system is predicted to be unstable. The two fungi use the same resource at the same time (a freshly killed tree) and ultimately must compete for host beetles when it comes time to be dispersed. Therefore, they are expected to be in strong competition with one another, and that the stronger competitor should outcompete the weaker competitor over time. Likewise, natural selection would be expected to select for the superior mutualist with *G. clavigera* eventually moving to fixation with the beetle (Six, 2012). Nonetheless, the MPB-fungus mutualism has remained relatively stable over a long period of evolutionary time (Six and Bentz, 2007). This indicates that some sort

of stabilizing mechanism exists. The stability of the mutualism may be tied to differential temperature tolerances of the two fungi interacting with a variable habitat. Optimal growth of *G. clavigera* occurs somewhere between 20 and 25°C. *O. montium*, on the other hand, grows best at 25°C (Rice et al., 2008). These differences have led to the hypothesis that the different temperature tolerances of the two fungi minimize direct competition by giving each an advantage at different times. It has also been hypothesized that having two fungal symbionts, each with different temperature optima, may allow the beetle to exist across a broad range of environmental conditions by ensuring it is never without a symbiont (Six and Bentz, 2007). While the differential temperature tolerances of the two fungi may allow the beetle greater environmental amplitude, it may also be a major mechanism supporting the existence of two symbionts in this mutualism.

We hypothesized that variability in temperature acts as a stabilizing mechanism for the mutualism. In particular, we considered three types of temperature variability: intra-year, inter-year and thermal migration. By intra-year variability, we mean day-to-day and seasonal fluctuations in temperature that allow an advantage in growth rate to switch back and forth between the fungi throughout the year. For example, in a typical year, warm summer temperatures allow *O. montium* to grow faster than *G. clavigera*. However, as fall temperatures cool, *G. clavigera* may gain the advantage until late spring or early summer, when *O. montium* regains the advantage.

Another form of variability we considered was inter-year variability, which includes differences in temperatures from year to year. Because some years are cooler and some warmer, this form of variability could result in some years where one species dominates and others where the other species gains the advantage. Over the long term however, because the advantage passes back and forth, the relative prevalence of each may remain stable. The final form of temperature variability we considered was variability due to thermal migration. This variability represented varying thermal environments as fungi-carrying MPB moved between warm and cold environments on a landscape. This will be called the thermal migration hypothesis. Our theory was that *O. montium*, the warm-loving fungus, grows in

prevalence during outbreak years at lower elevation environments and that *G. clavigera*, the cool-loving fungus, may gain in prevalence while the beetle occupies a cooler, high-elevation location. This would cause the relative proportion of each fungi to oscillate but remain essentially stable over time.

In this paper we developed a temperature-driven model for fungal growth that includes effects of competition for space in a tree. This model was parameterized using growth data collected from *G. clavigera* and *O. montium* isolates from the mycangia of emerging MPB collected from Logan Canyon in northern Utah in 2010. To project fungal prevalence into the future, we combined the fungal growth model with an existing temperature-based model for MPB development (Powell and Logan, 2005) to determine the proportion of each fungi present in the pupal chambers as teneral adults prepare to leave the tree. Finally, using this integrated model, we simulated the outcomes for the mutualism for a variety of temperature scenarios (emphasizing intra-year, inter-year or thermal migration variability), and attempted to determine how these differences affected the relative prevalence of *G. clavigera* and *O. montium* in the mutualism. Using these models, our goal was to determine whether variations in temperature, and the differential rates of fungus growth at those temperatures, could explain the continued persistence of both *G. clavigera* and *O. montium* in the MPB-fungus mutualism.

2.2. Model development

2.2.1. MPB/fungus interactions

In summer, adult MPB emerge from the trees within which they developed and fly in search of new host trees. Females initiate attacks and release pheromones to attract other dispersing males and females. This results in a mass attack that often occurs over a period of a few days. In a successful attack, males and females excavate long J-shaped galleries in the phloem layer of the tree. Eggs are laid on the sides of the gallery and spores stored in the mycangia and on the body of the beetles are introduced into the phloem (Safranyik et al., 2007). From this point, the development of beetle brood and growth of the fungi into the tree occurs at a rate based on temperature (Safranyik et al., 2007). The

fungal spores germinate and form hyphae that spread throughout the phloem and sapwood while MPB eggs hatch and the larvae progress through four stages while feeding on both phloem and fungal hyphae in larval galleries they construct (Safranyik et al., 2007). After larval development is complete, they construct pupal chambers where they pupate and then develop into new (teneral) adults. The new adults feed on spores that the fungi produce in a dense lining in the pupal chamber while packing their mycangia with spores (Safranyik et al., 2007; Six and Bentz, 2007). Brood adults then emerge from the tree in search of new hosts. This sequence typically takes one year depending on temperature although multiple years are required in cold environments.

To model the prevalence of *G. clavigera* and *O. montium* in relation to MPB development, we modeled the fungi as they spread outward (and captured space) from beetle galleries and computed the relative proportion of each fungus present in the tree as teneral adult beetles prepared to leave. This proportion was important as it directly influenced the proportion of each fungus being carried by the next generation of MPB. We used these models to describe the relationship between temperature and the rate of fungus growth, developed a model for fungal growth in a tree, and used this model in combination with an existing model for MPB development to project the mutualism into the future.

2.2.2. *Fungal growth rate curves*

Beetle-associated fungi grow by forming a mycelium (network of connected hyphae) that spreads radially outward at a rate governed by temperature. To model growth of the fungi, we developed a relationship between observed fungal growth rates and temperature that allowed us to calculate the area each fungus colonized based on a record of hourly temperatures.

Fungus growth data

Fungi were isolated from the mycangia of beetles emerging from lodgepole pine trees in Logan Canyon, UT in the summer of 2010 and 2011. These fungi were identified to species using morphology (Upadhyay, 1981). To determine the growth rates of each species as well as the variability within species, 3-4 replicates of 24 isolates of *G. clavigera* and

17 isolates of *O. montium* were grown in Petri dishes containing 2% malt extract agar (a growth medium) and held at constant temperatures of 5, 10, 15, 20, 25, 30, and 35 °C. These plates were monitored daily and the amount of area colonized by the fungi traced. "Image J" (Schneider et al., 2012) was used to measure the number of pixels (i.e. area) colonized each day by the fungi. The number of pixels was then converted to area.

Next, the 587 estimates of area colonized were converted to measurements of radius colonized and a line fitted to obtain a single radial growth rate for each Petri dish. Finally, maximum likelihood estimation was used to fit these radial growth rates to a distribution often used for modeling insect development (Logan, 1988; Régnière et al., 2012),

$$r(T) = B\left(e^{\alpha(T-T_0)} - 1\right) - B\left(e^{\alpha(T_m-T_0)} - 1\right)e^{(T-T_m)/b}, \tag{2.1}$$

assuming lognormal error. In this equation, $r(T)$ represents the rate of fungal growth per day in mm based on the temperature T in °C, B is a scaling factor that affects the maximum rate of fungus growth, α affects how quickly the growth rate increases at low temperatures, b is the thickness of the boundary layer between peak growth and the upper temperature threshold, and T_0 and T_m represent the lower and upper temperature thresholds for the fungi in °C (i.e., the lowest and highest temperature where the fungus will continue to grow). These parameter values were obtained using a built-in MATLAB optimizer (the Nelder-Mead simplex algorithm, 'fminsearch') and the constraint that T_0 and T_m have biologically reasonable values ($0 < T_0 < 5$ and $T_m \approx 30$ °C). Figure 2.1 shows the observed radial growth rates for *G. clavigera* and *O. montium* as well as their parameterized rate curves. The parameters for these curves are included in Table 2.1.

2.2.3.   Fungal growth in cross section

Consider a horizontal section of a tree bole, which will be intersected by female MPB constructing egg galleries and depositing *G. clavigera* or *O. montium* spores from their mycangia as they burrow. Each intersection can be represented as a distinct fungal inoculation point distributed evenly around the circumference of the tree with some small additive error at a discrete location, that is, $x_i(0) = \frac{(i-1)\pi d}{n} + \varepsilon$ where $i = 1, 2, ...n$, d is the diameter of

Table 2.1

Parameters for the fungal rate curves (Eqn 2.1). In these rate curves, α affects the rate of increase at low temperatures, b is the thickness of the boundary layer between peak growth and the upper temperature threshold, B is a scaling factor which affects the maximum rate of fungal growth, while T_0 and T_m are the lower and upper temperature thresholds for the fungi in °C. These values were estimated using Maximum Likelihood estimation.

Parameter Values for Fungal Growth Rate Curves					
fungus type	α	b	B	T_0 (°C)	T_m (°C)
G. clavigera	0.0041	8.0407	95.6120	0.9123	32
O. montium	0.0662	7.4949	3.8395	-0.0236	34

Fig. 2.1: Growth rate observations for *G. clavigera*, GC (*), and *O. montium*, OM (∘), are shown with their parameterized growth rate curves. Note that *G. clavigera* (solid line) has a higher rate of growth when temperatures are below 16.3°C, while *O. montium* (dashed line) has the higher rate of growth for temperatures above 16.3°C and that its rate curve extends further to the right than *G. clavigera*. This confirms previous observations that *G. clavigera* is the "cool-loving" fungus while *O. montium* is the "warm-loving" fungus. Parameters for these rate curves are shown in Table 2.1.

the tree in mm, and ε is drawn from a normal distribution with mean zero (see Figure 2.2). These locations were then assigned to be *G. clavigera* with probability p_{gc} or *O. montium* with probability $1 - p_{gc}$. Because we restricted our model to a single dimension, we allowed the fungi to spread from these locations horizontally around the circumference of the cross section of the tree at a rate proportional to their radial growth rate (which is determined by temperature). To allow for the fact that fungal growth in a tree will likely be much slower than fungal growth in a Petri dish we also included a scaling factor, $\beta \in (0, 1]$, in the model (a description of how β was estimated is included in Section 2.2.3). This allowed the movement in the left endpoint of the fungus lesion to be represented by

$$\dot{x}_{i,L}(t) = \begin{cases} -\beta r(T(t)), & \text{if } x_{i-1,R}(t) < x_{i,L}(t) \\ 0, & \text{if } x_{i-1,R}(t) \geq x_{i,L}(t) \quad \text{(i.e. if lesions overlap)}, \end{cases} \tag{2.2}$$

at time t, and the growth of the right endpoint by

$$\dot{x}_{i,R}(t) = \begin{cases} \beta r(T(t)), & \text{if } x_{i,R}(t) < x_{i+1,L}(t) \\ 0, & \text{if } x_{i,R}(t) \geq x_{i+1,L}(t), \end{cases} \tag{2.3}$$

where $i = 1, 2, ... n$ and r represents either r_{gc} or r_{om}, the radial growth rate (which is a function of the temperature at time t) for *G. clavigera* or *O. montium*, depending on the type of fungus growing from lesion i.

In the model, competition by fungi for space within the tree is implemented by setting the fungal growth rates to zero when two fungal lesions meet. This is based on observations that only exploitative, not direct competition, occurs between the fungi (Bleiker and Six, 2007). This mechanism also accounts for the finite area available for fungal colonization within the tree; once available space between lesions is occupied, a fungus can no longer capture more space. Based on temperature, the model allows fungal growth to continue until the entire cross section is colonized or until a specified amount of time has gone by, such as the amount of time necessary for the MPB eggs to develop into teneral adults. After
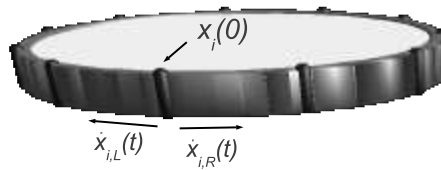
Fig. 2.2: A horizontal cross section of a tree bole that has been intersected by female MPB galleries (represented by dark striations). At each point, either *G. clavigera* or *O. montium* spreads horizontally outward at a rate based on the temperature at time t.

this the proportion of the two fungi present in the tree is calculated and used to update p_{gc} for the next generation of fungus lesions.

Temperature data

To project fungal growth and test our hypotheses, two long-term temperature datasets were used. One was collected in the Stanley Valley of the Sawtooth National Recreation Area (SNRA) in central Idaho and the other at Railroad Ridge (RRR), a high-elevation site located in the White Cloud Mountains in the Challis National Forest of central Idaho. The SNRA temperature dataset consists of hourly phloem temperatures from Julian day (JD) 200 of 1992 to JD 289 of 2004 collected at an elevation of approximately 2,040 m (6,700 ft). These were collected from the phloem of 12 different MPB-infested lodgepole pines (one per year) located throughout the SNRA and combined to form a continuous 12-year temperature record (Powell and Bentz, 2009). This dataset was used to test all three of our hypotheses. The RRR temperature dataset consists of hourly phloem temperatures recorded at the southern weather station established along RRR, a broad east/west running ridge that slopes from approximately 2,900 m (9,500 ft) to 3,400 m (10,500 ft). This dataset was primarily used as the higher elevation site to test the thermal migration hypothesis. Simulations in this paper were performed using south bole aspect RRR phloem temperatures recorded from 1996-2004 (Logan and Powell, 2001).

Estimating the growth scaling parameter

The parameter β included in equations (2.2) and (2.3) was used to scale the rate of fungus growth in a Petri dish to the much slower rate of fungal growth in a tree. A

rough estimate for this parameter was obtained using the observation that beetle larvae will tunnel backwards to older sections of their larval gallery to eat fungus colonized phloem (Adams and Six, 2007). We assumed that the approximate total growth of a lesion could be estimated using the length of MPB larval galleries. For example, using 1994 temperatures from the SNRA dataset, the period from MPB oviposition to pupation took 198 days (using the MPB model which will be described in Section 2.2.4). During that time *G. clavigera* would have grown 28.84cm on agar. To determine a rough estimate of the length the larvae would have colonized as they developed through their four larval instar stages, we measured the length of larval galleries on three pieces of stripped lodgepole bark in the USU Applied Entomology lab and observed larval gallery lengths between 3 and 5cm. We used the mean of these measurements, 4cm, which allowed us to calculate β as approximately $4/28.84 = 0.1387$. We note that this value of β serves only as a rough approximation, as different estimates could be obtained using a different year from the temperature record or if larval gallery lengths vary greatly from our observations. A more data-driven estimate for β is the subject of our next work which will utilize detailed information about MPB attacks and emergence, the proportion of each fungus entering and a tree, and an hourly-temperature record.

2.2.4. The MPB median developmental model

To connect the implications of fungal growth in a tree with the stability of the MPB-fungus mutualism, we used an existing model for MPB development. This model predicts the median emergence date of the MPB from each of their life stages (egg, larvae, pupae and teneral adult) (Powell and Logan, 2005). The model works by taking a year-long temperature record and calculating the corresponding median rates of development through each MPB life stage. Then, based on the median date of MPB attack on a tree, it determines the median date at which MPB transition between life stages. We used this model to determine the window of time during which teneral adult MPB feed on spore layers of the fungi that line the pupal chambers. This window was used to calculate the relative prevalence of *G. clavigera* and *O. montium* available to be carried to the next generation

of host trees. Model details, including integration strategies and rate curve parameters for the eight phases of the MPB life cycle can be found in (Powell and Logan, 2005).

2.3. Model integration

Simulations to project fungal prevalence into the future were done by specifying host tree size, the average distance between fungal lesions (corresponding to the density of attacking MPB), the average proportion of each fungus being carried, the date the majority of MPB began attacking a particular tree (which acts as the date of inoculation for the fungi), and a year-long temperature record. Using these values, the MPB median developmental model described in Section 2.2.4 was used to calculate the teneral adult spore-feeding window. The fungal growth model from Section 2.2.3 was used to determine the relative proportion of *G. clavigera* and *O. montium* present in the tree at that time. The proportion of each fungus available during this window was averaged and used as the proportion carried by beetles to attack new host trees.

To ensure as much realism as possible, we used fungal lesion spacings which corresponded to observed MPB attack densities. A previous study on MPB found that the minimum attack threshold (the lowest density of attacking MPB that will result in a successful MPB generation) for MPB in lodgepole pine is about 40 attacks/m^2, the optimal attack density is 62 attacks/m^2, and a high attack density is considered to be 80 attacks/m^2 (Raffa and Berryman, 1983). Given the fact that MPB parental galleries average 30cm in length and that beetles prefer to attack trees 25cm in diameter or larger (Safranyik et al., 2007), we found that 40-85mm was a reasonable range to include for lesion spacings (where 54mm corresponds to the optimal attack density) assuming the MPB galleries are evenly dispersed across the tree bole. To reduce complexity of the simulations and minimize small sample size effects 1000 cross-sections were spliced together to form a vast mega-section. The number of fungal lesions varied depending on the spacing between lesions used. Table 2.2 shows the approximate relationship between MPB attack density and fungus lesion spacing.

Table 2.2
Approximate correlation between lesion spacing in mm and MPB attack density in beetles/m^2 (assuming female galleries are dispersed evenly across the tree bole).

Relationship between lesion spacing and MPB attack density	
spacing in mm	approximate number of beetles/m^2
40	85
50	67
60	56
70	48
80	42

2.3.1. Hypothesis evaluation

To determine whether temperature variability is allowing both fungi to persist in the mutualism we constructed several vectors of hourly temperature data which included intra-year, inter-year or thermal migration variability and used these to project fungal prevalence into the future. For simplicity, we began each simulation with the relative proportion of each fungus at 50% and examined how different thermal scenarios eroded or enhanced mutualism stability.

Temperature sets to test intra-year variability were constructed by dividing the SNRA temperature dataset into one-year increments and repeating them for a specified number of years. This allowed us to determine whether variability present in a single year's temperature record was enough to maintain both fungi in the mutualism. Inter-year variability was tested by projecting fungal prevalence into the future using our two observed long-term temperature datasets as well as datasets constructed by randomly permuting year-long chunks of observed temperature data from the SNRA or RRR. The final form of variability we considered was variation caused by portions of the MPB population periodically transitioning between different thermal environments. In this case, we selected the number of years the MPB would be at a low elevation or warm environment, n_1, and the number of years they would be at a high elevation or cool environment, n_2, and then randomly selected n_1 years from the Sawtooth dataset and n_2 years from the RRR dataset and repeated this process for the number of cycles we wished to observe. See Table 2.3 for more explanation about

Table 2.3
Method of constructing simulated temperature datasets to test our hypotheses. The hypothesis name is listed on the left while the right column describes how year-long chunks of observed temperatures were used to construct corresponding temperature datasets.

Temperature datasets to test hypotheses	
intra-year	year k, year k, year k, ...
inter-year	1992, 1997, 1995, ...
thermal migration	$SNRA_{1999}$, $SNRA_{1997}$,... $SNRA_{1994}$, RRR_{1996}, RRR_{2000},... RRR_{1997}, ...

how these datasets were constructed.

2.4. Results

2.4.1. Intra-year variability

When projecting fungal prevalence through time, we found that for any given year, one fungus would nearly always gain a slight advantage over the other. Due to the stochastic nature (lesion location and type) of the fungal growth model, this advantage could potentially switch back and forth between the two fungi if the simulation was repeated, particularly if the advantage gained by one fungus was quite small. However, when projected over a long time period, we found that the stability of the mutualism was strongly dependent on how closely the fungal lesions were spaced (i.e. density of MPB attacks). When lesions were close (40mm and below, indicating a very high density of attacking MPB), intra-year variability allowed both fungi to maintain a strong presence in the mutualism in most of the thermal scenarios we tested (Figures 2.3 and 2.4, plots A and B). As lesion spacing increased, we found that the advantage ceased to pass back and forth as often, nearly always allowing one fungus to continue to gain an advantage (Figures 2.3 and 2.4, plots C-J). This would eventually cause the relative prevalence of the other fungus to move toward zero. As lesion spacing increased, the rate at which one fungus began to dominate the mutualism also tended to increase. Exceptions to this with SNRA data occurred in 1994 and 2003 (Figure 2.3, plot J) and RRR data in 2000 (Figure 2.4, plots E-J). These will be discussed further below.
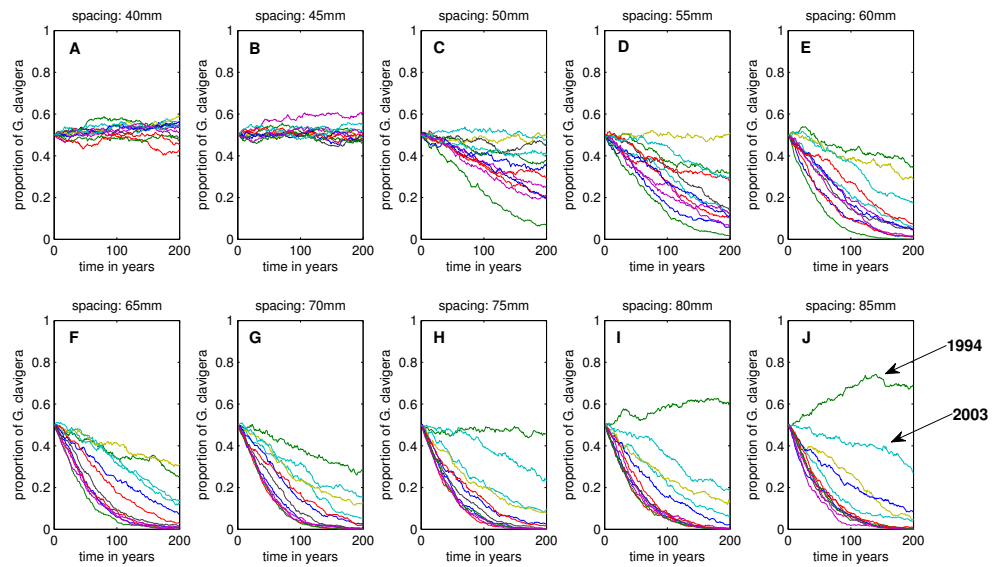
Fig. 2.3: Testing the intra-year variability hypothesis and the effect of lesion spacing on fungal prevalence using SNRA temperature data. Each subplot shows 12 curves (corresponding to the 12 years of temperature observations from the SNRA dataset, south bole) representing the predicted prevalence of *G. clavigera* after iterating the model 200 times using a single year's temperatures. We note that when lesion spacing was small (40-45mm, **A** and **B**, corresponding to very high attack density), both *O. montium* and *G. clavigera* remained present in similar proportions for the entire 200 years. As fungal spacing increased however, more and more years resulted in *G. clavigera* being lost from the mutualism (**C-J**). Interestingly, further increases in spacing allowed 1994 temperatures to favor *G. clavigera* and lessened the advantage *O. montium* was able to obtain for 2003 temperatures (**J**).
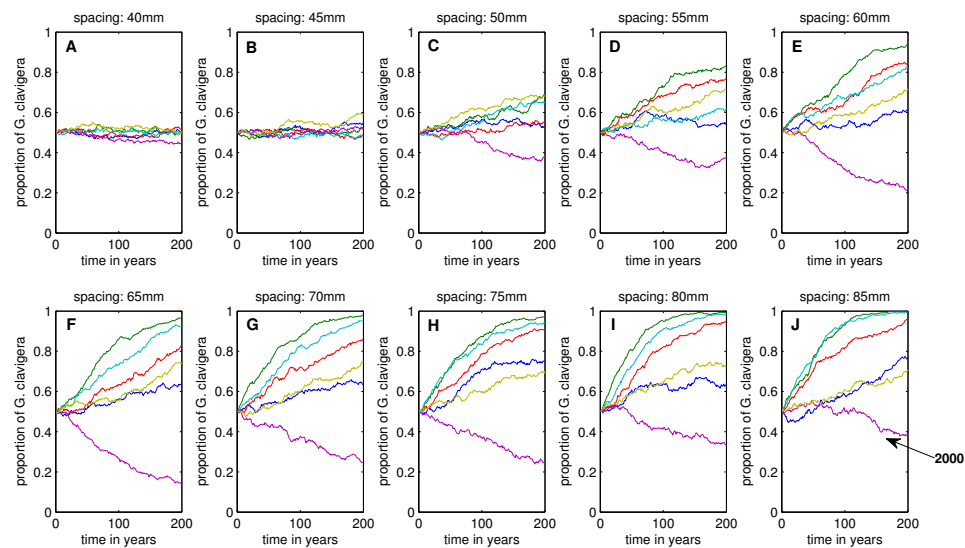
Fig. 2.4: Testing the intra-year variability hypothesis and the effect of lesion spacing on fungal prevalence using RRR temperature data. Each subplot shows 6 curves (corresponding to the 6 years of temperature observations from the RRR dataset, 1996-2001, south bole) representing the predicted prevalence of *G. clavigera* after iterating the model 200 times using a single year's temperatures. As with the SNRA temperatures, when spacing between lesions was small (40-45mm, **A** and **B**) *O. montium* and *G. clavigera* were able to remain present in similar proportions for the entire 200 years. As fungal spacing increased, the coolness of the climate favored *G. clavigera* and *O. montium* began to be lost from the mutualism (**D-J**). An exception occurred for temperatures from 2000, a warm year, in which larger lesion spacings allowed *O. montium* to gain in prevalence and *G. clavigera* to diminish.

Several simulations were performed repeating a single-year temperature series to test whether intra-year variability could stabilize the mutualism. In each case, the simulation began on JD 205 with *G. clavigera* and *O. montium* initially present in the mutualism at a relative proportion of 50%. Projecting their relative proportions forward using a repeated string of yearly temperatures from the SNRA or RRR, we found that when fungal lesions were spaced 40mm apart (equivalent to a very high MPB attack density, ~ 90 beetles/m^2), the mutualism remained stable (Figures 2.3 and 2.4, plot A). However, as lesion spacings increased, stability decreased (Figures 2.3 and 2.4, plots C-J). *O. montium* repeatedly gained an advantage over *G. clavigera* causing the relative proportion of *G. clavigera* to decrease over time. Further increases in lesion spacing allowed *O. montium* to benefit more each year, and *G. clavigera* was lost from the mutualism after a few hundred years. Interestingly, for SNRA temperatures in 1994 and 2003, the behavior of the system changed for very large lesion spacings (80-85mm): 1994 temperatures began to favor *G. clavigera* and 2003 temperatures less strongly favored *O. montium*. Relative to the SNRA dataset, 1994 and 2003 were remarkable only in that 1994 was cooler in late summer/early fall and 2003 had a longer winter, with cooler temperatures beginning in September and lasting through February (versus October-January). A similar result occurred for RRR simulations in that for large lesion spacing, 2000 temperatures began to favor *O. montium*.

2.4.2. Inter-year variability

Simulations testing effects of inter-year variability on the mutualism produced similar results. When projecting fungal prevalence using the observed temperature records from the SNRA and RRR, we found that closely spaced fungal lesions (40mm) allowed the relative proportion of each fungus to stay very near 50% while increases in lesion spacing allowed one fungus to gain an advantage over the other. Generally *O. montium*, the warm fungus, would prevail using SNRA temperatures (Figure 2.5, plot A) while *G. clavigera* benefited slightly more often than *O. montium* (approximately 55% of the time) when using the RRR temperatures (Figure 2.5, plot B), although the change in relative prevalence was often quite small (less than 1%). In repeating these simulations, we found substantial variability.
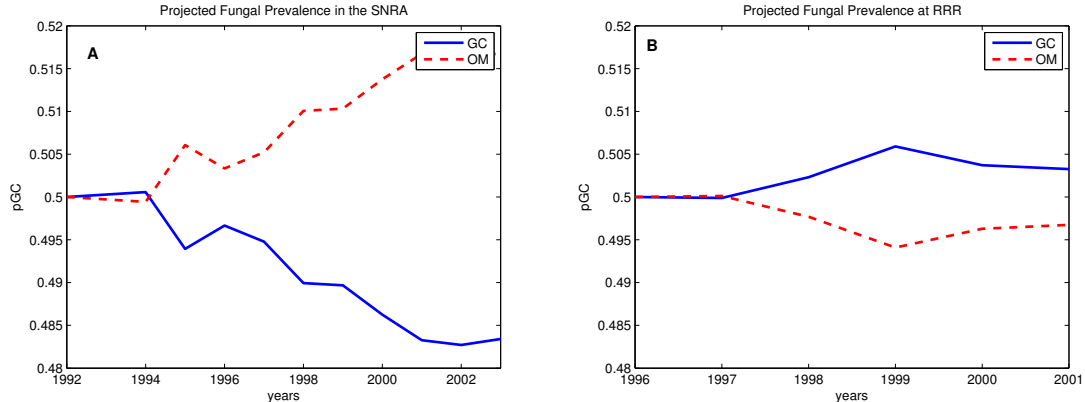
Fig. 2.5: Testing the inter-year variability hypothesis using observed temperature datasets. One realization of the projected proportion of *G. clavigera* (GC, solid line) and *O. montium* (OM, dashed line) present in the mutualism over time in (**A**) the SNRA and (**B**) the higher elevation site, RRR, using a lesion spacing of 54mm. These plots suggest that over time, regardless of inter-year variability, *G. clavigera* may be lost from the mutualism in temperature regimes similar to lodgepole pine stands in the SNRA, while *O. montium* could be lost from the system in higher elevation whitebark pine stands, albeit more slowly.

However, the overall trend indicated that *G. clavigera* will be lost from the mutualism at the low elevation site, while *O. montium* will be lost, although more slowly, at the higher elevation site.

When simulated over a longer timescale using a simulated dataset (200 years, Figure 2.6), we found that this trend continued. Small spacing between lesions (40-45mm) corresponding to high densities of attacking MPB would result in long-term stability. However, as the density of MPB attacks decreased, and spacing between lesions increased, *O. montium* would continue to gain an advantage in the SNRA, slowly forcing *G. clavigera* out of the mutualism while *G. clavigera* would continue to gain an advantage at RRR.

2.4.3. Migration between different thermal environments

When testing the thermal migration hypothesis, we found that the ultimate outcome of the system was sensitive to the number of years (or MPB generations) spent in each habitat but that for certain lesion spacings the outcome became less sensitive to these time periods. In general the relative proportion of *G. clavigera* in the mutualism tended to decrease when MPB occupied the warmer, low-elevation location and increase when MPB
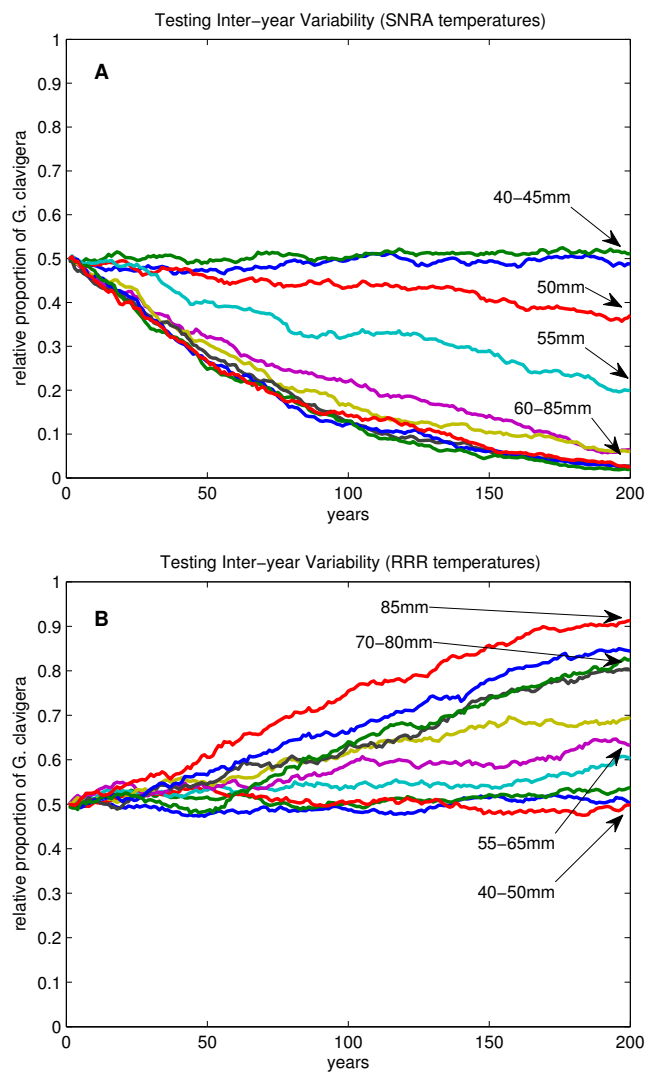
Fig. 2.6: Testing the inter-year variability hypothesis. The projected proportion of *G. clavigera* present in the mutualism over time is shown for the (**A**) SNRA and (**B**) RRR with lesion spacings ranging from 40 to 85mm using a hypothetical dataset created by sampling random year-long chunks from the observed temperature sets. Note that low lesion spacings (40-45mm, indicating high densities of attacking MPB) have the potential to stabilize the system for a long period of time while large lesion spacings (i.e. fewer attacking MPB) can cause *G. clavigera* to be lost from the mutualism in the SNRA, and *O. montium* to be lost from the mutualism at RRR.

occupied the cooler, high-elevation location. Provided the ratio between the low and high elevation periods was appropriate, the overall relative prevalence of the two fungi would oscillate up and down, and the mutualism would not ultimately destabilize except at the most sparse lesion spacings (Figure 2.7, plot A). If the period spent at low elevation became too long, however, then we would see a trend favoring *O. montium* (Figure 2.7, plot B). Conversely, if the period spent at high altitude was too long, then the trend would favor *G. clavigera*. The prevalence of each fungus was less sensitive to MPB attack density in these simulations than in those for MPB remaining in a single thermal environment.

2.5. Discussion/Conclusions

In this study, we developed a temperature-driven model for fungal growth in a tree which includes effects of competition for space. This model was parametrized using fungal growth data and combined with an existing model for MPB development. Using this integrated model, we projected fungal prevalence through time using observed and constructed temperature datasets which allowed us to test whether variability in temperature was capable of stabilizing the MPB-fungus mutualism. We found that of the three hypotheses tested, thermal migration was the most robust stabilizing mechanism for the MPB-fungus mutualism independent of lesion spacing. This type of variability allowed *G. clavigera* and *O. montium* to remain in the mutualism indefinitely given appropriate rates of migration. Our simulations did not indicate that either intra- or inter-year variability alone were capable of stabilizing the mutualism. We acknowledge that inter-year variability could produce similar results as thermal migration, although temperature records used in our model analyses did not include years with sufficiently cool and warm temperatures.

Additionally, we were surprised to find that spacing between lesions (or the density of attacking MPB) influenced stability of the mutualism. All three sources of variability we tested appeared to be plausible stabilizing mechanisms when MPB attack densities were at or above the optimal attack density of 62 beetles/m^2 (corresponding to a lesion spacing of 54mm or closer). As spacing between lesions increased (corresponding to lower MPB attack densities) thermal migration variability emerged as the only temperature mechanism
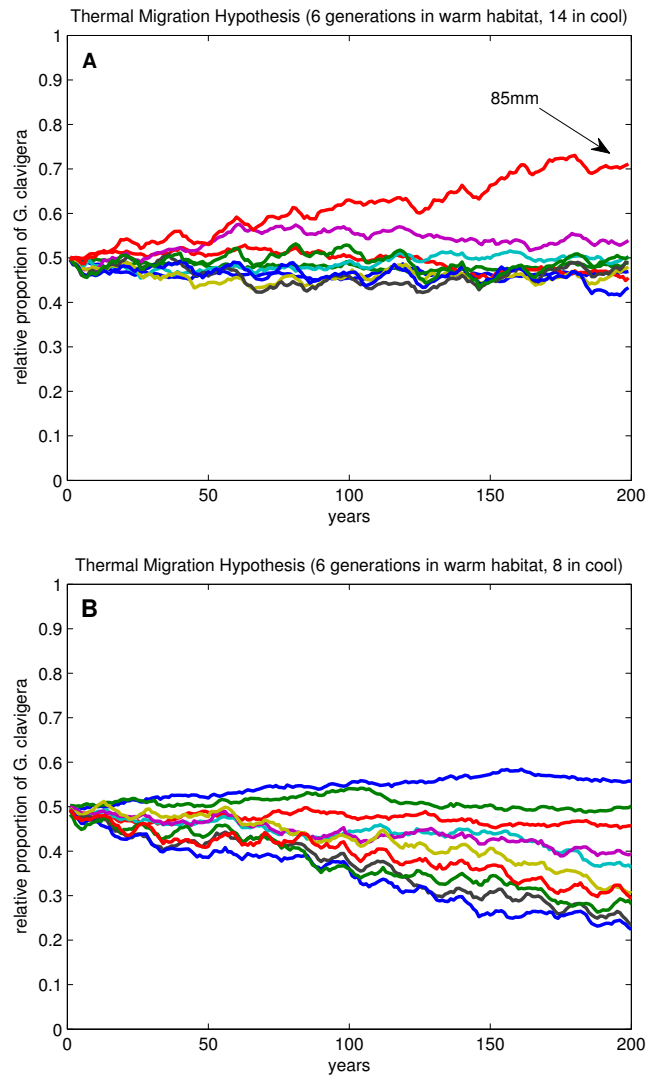
Fig. 2.7: Testing the thermal migration hypothesis as a portion of the MPB population periodically transition between two distinct thermal habitats. We allowed the MPB to alternate between 6 generations in the SNRA (perhaps in an outbreak phase) and 14 generations (∼24 years) in a cooler location, RRR (**A**) and 6 generations in the SNRA and 8 at RRR (∼40 years) (**B**). From these plots, we see that appropriate patterns of transitioning between thermal environments can maintain both fungi in the mutualism for all but the most distant lesion spacings while different ratios of transitioning may lead to destabilization.

capable of stabilizing the system. This raises the question, what about lesion spacing acts to stabilize the mutualism?

How does lesion spacing stabilize fungal prevalence?

To explore the dynamics of lesion spacing, we used the fungal growth rate curves from Section 2.2.2 to plot the competition between two lesions, each of a different fungal species. Using these rate curves, we plotted the cumulative length of phloem each fungus could colonize in an average year (SNRA 1995) to visualize differences between the overall growth of the fungi (when infinite space was available to colonize). Next we plotted the cumulative length *G. clavigera* could colonize coming from one direction and the cumulative length *O. montium* could colonize coming from the opposite direction and varied the initial distance between them (representing different lesion spacings) (Figure 2.8). Displayed this way the point at which the curves cross indicates the time at which the space between two lesions is totally colonized and how much was colonized by each species.

The cumulative growth of the two fungi was quite similar and could be divided into three phases: rapid growth in fall, slow or zero growth in winter, and rapid growth again in spring. Qualitatively, the biggest difference between these curves occurred at the transition between phases ($\sim$60-100 days after attack and $\sim$270-320 days after attack). In these regions, the average growth rate of the fungi was quite different which could have a large impact on where the fungi intersect (Figure 2.8 plot B).

When lesions were tightly spaced, the fungi intersected early in the fall when their growth was roughly linear and average temperatures were near the temperature at which *G. clavigera* and *O. montium* grow at the same rate (where the fungal rate curves in Figure 2.1 intersect, $\sim 16.3°$C based on our parameterization). For example, in the SNRA in 1995 the mean temperature for the first 60 days after attack (JD 205 to JD 265) was 15.23°C. This helped stabilize the mutualism since most of the available space was colonized in the fall when the fungal growth rates were nearly indistinguishable, leaving less potential for winter and spring temperatures to affect the system. As the space between lesions increased, the fungi intersected later in the year, closer to one of the transitions between
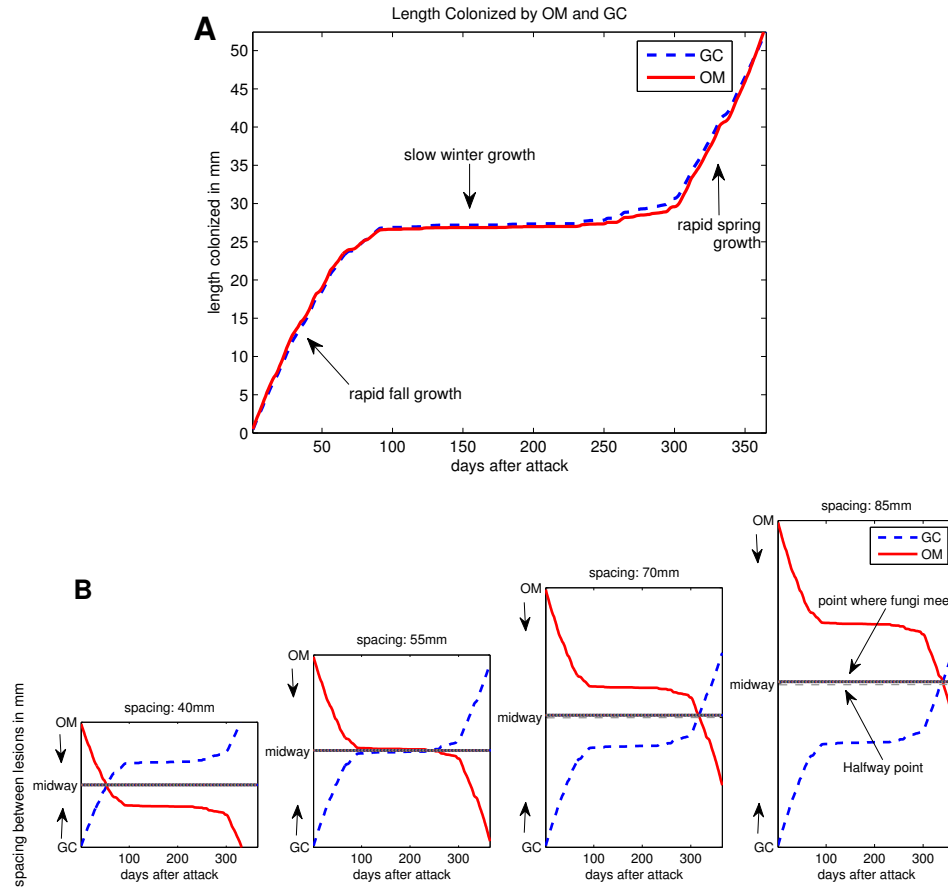
Fig. 2.8: Effect of spacing on the proportion of a tree each fungus is able to colonize. Cumulative growth of *G. clavigera* and *O. montium* (**A**), and the dynamics of two lesions with different fungal type initially 40, 55, 70, and 85mm apart (**B**). We allowed *O. montium*, OM, (solid line) to grow from one direction while *G. clavigera*, GC, (dashed line) grows from the other. Note, the point of intersection of the fungi (horizontal black line) is affected by the initial space between lesions. When the space is small (40mm, on left), the fungi intersect during their initial rapid growth phase (when their growth is nearly identical). Each colonizes approximately 50% of the space available (regardless of winter and spring temperatures) and the mutualism remains stable. As space between lesions increases the fungi intersect in late fall or early spring where the fungi display the most different behavior. For this particular year, wider space between lesions allowed *G. clavigera* to gain a small advantage. This mechanism allows one fungus, depending on temperature, to colonize more space and gain dominance in the mutualism, leading to a destabilization over time. Phloem lengths colonized in this plot were calculated using SNRA 1995 temperatures, an attack date of JD 205 and $\beta = .1387$.

phases where the realized growth characteristics of the fungi were most different. This generally resulted in one fungus claiming slightly more space than the other. Simulations are based on a constant date of attack each year, although in reality attack date will vary annually as temperature influences insect development and emergence timing. Changing date of attack could significantly influence fungal interactions and future work will include using observed MPB and fungal parameters observed at field plots to evaluate and improve the model. Model improvements will also include a coupled competition model for the total area colonized by each fungus under the bark and variability in fungal growth rates.

For the majority of years, temperatures in the SNRA favored *O. montium* (Figure 2.3) and we saw the relative proportion of *G. clavigera* decrease over time for lesion spacings above 45mm. One anomaly, however, was that large lesion spacings altered the outcome in fungal prevalence in 1994 and 2003, causing 1994 temperatures to favor *G. clavigera* and reducing the advantage *O. montium* could obtain in 2003 (Figure 2.3 plot J). To explore this further in the context of lesion spacing, we looked at the overall cumulative growth of each fungi during 1994 and 2003 (Figure 2.9) to see how their growth matched up over these years, and in particular, how the two fungi transitioned between slow winter growth and rapid spring growth (which would affect their point of intersection between lesions with very large space between them).

We found that although 1994 was a cooler year the growth of each fungus was similar during the first 60 days following the MPB attack (Figure 2.9 plot A). As the year went on, there were brief periods which favored *O. montium*, but overall *G. clavigera* held the advantage. This meant that with finite space available, the two fungi could either meet early in the year when the fungi had nearly identical growth, slightly later, perhaps early in the transition between fall and winter phases when *O. montium* had a brief advantage, or later, when *G. clavigera* had a clear advantage. This explained how in simulations for intra-year variability the curve representing 1994 was stable for small lesion spacings (Figure 2.3 plots A-B), began to favor *O. montium* as lesion spacings increased, and how it switched and began favoring *G. clavigera* for the largest spacings (Figure 2.3 plot J). The year 2003 also
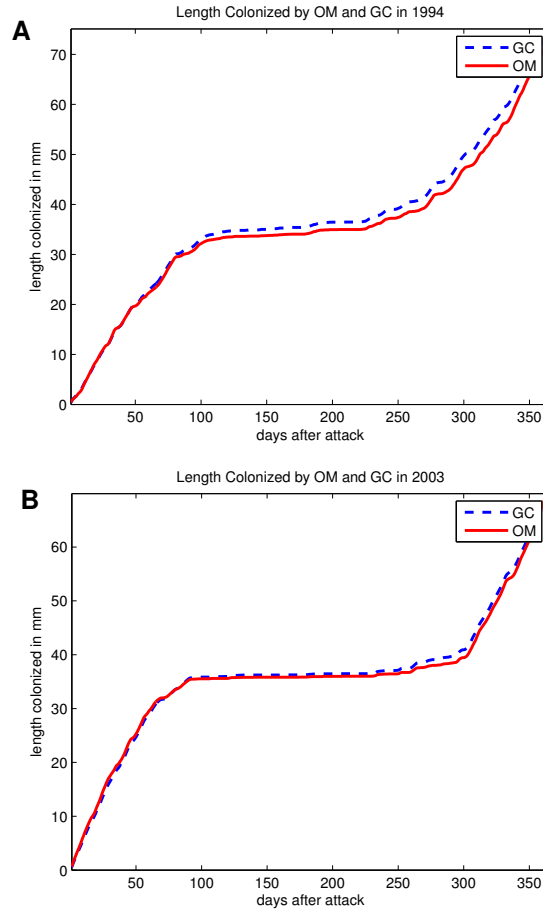
Fig. 2.9: Exploring the effect of lesion spacing on fungus prevalence for two anomalous years, 1994 (**A**) and 2003 (**B**). The relative position of the cumulative growth curves for *G. clavigera*, GC (dashed line), and *O. montium*, OM (solid line), and how they transition between rapid fall growth, slow winter growth and rapid spring growth are able to explain how differences in lesion spacings could affect the outcome of the mutualism.

produced anomalous results in that the relative proportion of *G. clavigera* was somewhat higher after 200 years for large lesions spacings rather than small ones (Figure 2.3). The mechanism behind this also became clear upon inspection of the cumulative length each fungus would have colonized (Figure 2.9 plot B). Both fungi grew quite similarly with the exception of the transition between slow winter growth and fast spring growth which would have altered the outcome of the mutualism for large lesion spacings. Based on this analysis, it seems that for current temperatures lesion spacing is quite a robust stabilizing mechanism, which begs the question: will it maintain stability in an altered temperature regime?

Because global temperatures are projected to warm in the coming decades, we added a warming trend of 1 and 2°C per 10 years and repeated the projections testing the thermal migration hypothesis (Figure 2.10). In doing so, we found that the closest lesion spacings (40-45mm) continued to stabilize the system. When temperature became too warm (i.e. after several decades), MPB development slowed as temperature exceeded the optimal developmental thresholds of larvae and pupae, resulting in substantially delayed teneral adult emergence. We halted simulations once the warming trend caused teneral adult emergence to be delayed beyond the next year. For larger lesion spacings, the warming trend caused *G. clavigera* to lose its advantage in the cooler habitat, removing the possibility for it to make up for losses in prevalence unless MPB attack density remained extremely high. This means that over time, *G. clavigera* will likely be forced from the MPB-fungus mutualism unless there is a stabilizing mechanism distinct from temperature or one that can override the effects of temperature.

Our results indicated that of the three forms of temperature variability tested, the thermal migration hypothesis was capable, on its own, of stabilizing the system over the long term. Inter-year variability could potentially act in the same way, provided there are sufficiently cool and warm years, though none of the observed years in our dataset from the SNRA were cool enough to allow *G. clavigera* to increase significantly in prevalence and the RRR years were not warm enough for *O. montium* to increase in prevalence. We also acknowledge that MPB attack density does not remain constant and it is possible that changes in attack density along with changes in temperature could act to stabilize the system. In particular, attack density increases during population eruptions and the cycle of endemic to outbreak population phases this insect is known for may also help to stabilize the system. Nonetheless, if climate change results in *G. clavigera* being forced out of the mutualism, at least in portions of the MPB range, there could be important ramifications for MPB and pine trees. For one, *G. clavigera* is thought to be nutritionally superior to *O. montium* and supports greater beetle fitness (Six and Paine, 1998). Completely replacing *G. clavigera* with *O. montium* could result in lower fecundity and survival of MPB, affecting
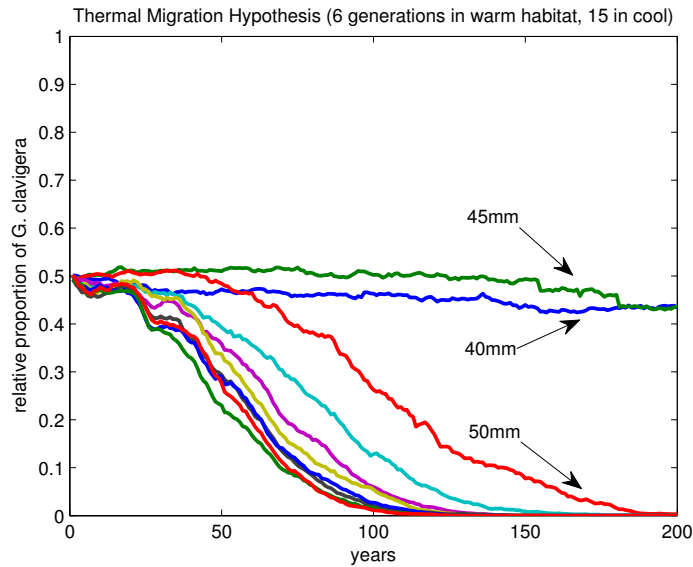
Fig. 2.10: Result of thermal migration simulation after adding a 1°C per 10 year warming trend. Close lesion spacing (40-45mm) continues to stabilize the system. At higher lesion spacings (55-85mm), however, the continued warming caused *G. clavigera* to lose its advantage in the cooler habitat causing it to be lost from the mutualism over time.

its ability to respond to conditions that would normally support an outbreak. It may also diminish environmental buffering by reducing the symbiont community associated with the beetle to one species with a reduced environmental amplitude (Six and Bentz, 2007).

CHAPTER 3

CONNECTING PREDICTIONS FOR SYMBIOTIC FUNGAL PREVALENCE TO

TEMPERATURE AND MOUNTAIN PINE BEETLE DEVELOPMENT[1]

Abstract

The fate of a species is often tied to the phenology and success of community associates. Examples include flowering plants and their pollinators, diseases or pathogens and susceptible individuals, and even males and females of a species whose differential development rates may lead to lack of reproductive success. Despite the prevalence of phenological overlap, however, few methods exist for connecting phenological models for multiple, interacting species. In this paper, we focus on the interactions between the mountain pine beetle (MPB) and two species of mutualistic fungi, *Grosmannia clavigera* and *Ophiostoma montium*. We adapt a model for the growth of these fungi within a tree and introduce the notion of a colonization index. This allows us to combine predictions of tree colonization by fungi to temporal predictions of MPB teneral adult feeding windows and emergence. Using this combined model, we consider a spectrum of strategies for MPB to pack their mycangia with mutualistic fungi, thereby directly influencing the proportion of each fungus carried to new host trees. The models are parameterized using fungal growth rates determined in agar and field observations of MPB, and associated fungi, entering and exiting trees. We found that the models provide good predictions of fungus carried by MPB over time and that the most likely mycangial packing strategy is for MPB to pack their mycangia just prior to emergence from the tree. We also found large differences in the relative growth of the two fungi inside a tree, with the most likely model estimating that *Grosmannia clavigera* can grow approximately 25 times faster than *Ophiostoma montium*, though the veracity of this result is in question due to the anomalously low production of *Ophiostoma montium* in the study trees.

1

3.1.   Introduction

The mountain pine beetle (MPB, *Dendroctonus ponderosae* Hopkins, Coleoptera: Curculionidae, Scolytinae) is currently the most significant insect species affecting pines in western North America. Between 1997 and 2010, MPB caused tree mortality on more than 8.5 million forested ha in British Columbia and the western United States combined (Meddens et al., 2012). Range expansions in Alberta and northern British Columbia are ongoing (de la Giroday et al., 2012) as a result of warming summers and winters (Cudmore et al., 2010; Sambaraju et al., 2012). An important feature of MPB population dynamics and survival, however, is that they are influenced by two fungal symbionts, *Grosmannia clavigera* and *Ophiostoma montium*. Together, these species are involved in an obligate multipartite mutualism. The beetle benefits the fungi by transporting their spores to new host trees in specialized structures called mycangia (Six and Paine, 1998). In turn, the fungi provide benefit to the beetle by transporting nitrogen from the sapwood to the phloem layer of the tree where larvae feed. New (teneral) adults also feed on lipid-rich fungal spores prior to emerging from a host tree, an action that simultaneously provides beetles with nutrients required for reproduction as well as packing spores into mycangia for dispersal (Six and Paine, 1998; Adams and Six, 2007; Bleiker and Six, 2007). Because this association is obligate, the phenologies of the fungi and beetle must overlap. The interdependence of partners in this symbiosis make it is essential to incorporate the dynamics of all three species when modeling or attempting to predict future MPB-caused tree mortality or estimating range expansions or contractions.

The issue of phenological overlap in ecology is not new; many species interact in ways that bind their fates. For example, phenological overlaps between pollinators and flowering are critical for the reproduction of many plants (Gross and Werner, 1983; Murali and Sukumar, 1994). In some ant and butterfly species, different development rates or maturation times for males and females can result in loss of reproductive success under some conditions (Kaspari et al., 2001), and increase the risk of extinction in small populations (Calabrese and Fagan, 2004). For diseases and parasites, spread often depends on phenolog-

ical overlap between the pathogen and susceptible individuals (Molnár et al., 2013). Thus, being able to connect phenological models for multiple, interacting species would increase our understanding of the broader effects species can have on one another and ecological processes.

In this paper, we develop a methodology for connecting temperature-driven phenological models for MPB and its symbiotic fungi, and incorporate five biologically plausible submodels that describe a spectrum of possible ways in which MPB and its fungi interact. While our approach is specific to the MPB-fungi system, elements of our approach can be adapted to connect phenological predictions of other systems with multiple, interacting species. Here we use direct (growth rate) and indirect (fungal prevalence) observations to discriminate among models describing MPB-fungus interactions and to determine values for cryptic parameters scaling laboratory measured growth rates to growth in a tree. This allows us to determine that the fungi present (or sporulating) just prior to emergence (as opposed to the fungus primarily present during the entire teneral adult feeding window) are most likely to be dispersed, and that differential growth rates of the two fungi under bark unexpectedly favor the cold-loving fungus *G. clavigera*, providing a possible mechanism for its persistence at warm sites in spite of a warming climate.

3.1.1. The MPB-fungus system

MPB have evolved complex interactions with two species of mutualistic filamentous fungi, *G. clavigera* and *O. montium* (Adams et al., 2008; Six, 2012). MPB and these mutualistic fungi interact throughout their entire life cycle. Following successful attack and colonization of a host tree, adult MPB excavate tunnels under the bark and lay eggs. During this process, they simultaneously inoculate phloem tissue with fungal spores from their mycangia (Six and Klepzig, 2004). After this, the beetles and fungi develop at rates based on temperature. The larvae feed on both phloem and fungal hyphae as they develop, and prior to emergence the newly eclosed teneral adults feed on fungal spores (Six and Paine, 1998). Sometime during this period of spore feeding, the beetle's mycangia becomes packed with fungal spores which are then dispersed to the next host tree and the next

generation of beetles. The proportion of each fungal species dispersed by each generation is determined by the timing of fungal growth and acquisition of spores in mycangia by adult MPB.

To connect phenological models for the MPB-fungus system, several components need to be considered. These include 1) the presence of not one but two mutualistic fungal species, 2) the fact that phenological outputs are qualitatively different (developmental milestones for MPB versus spatial extent for fungi), and 3) the range of biologically plausible ways in which MPB procure fungal spores. The two symbionts of MPB differ substantially in their effects on beetle fitness. Therefore, their relative prevalence is important, not only in fitness of the fungi but also in how they affect beetle populations. Because the fungi compete for the same spatial resources under bark, their relative rates of growth and resource capture must be included in models. Phenological models for MPB only provide temporal predictions of MPB life stage timing (Bentz et al., 1991; Logan and Bentz, 1999; Régnière et al., 2012). The completion of fungal life stage events is not relevant in this context, so models for the growth of the MPB mutualistic fungi are based on and predict measurements of length colonized (see Chapter 2). These different outputs from beetle and fungal models need to be combined in a tractable way. Finally, interactions between MPB and their fungal symbionts take place exclusively within the phloem layer of a tree. Although some types of interactions have been measured within this cryptic habitat (Adams and Six, 2007; Bleiker and Six, 2007), others such as how MPB pack their mycangia with fungi are completely unstudied. These interactions are important because they influence nutritional acquisition, beetle fitness, and determine the relative proportions of the two fungi that will be transported to new host trees.

From a scientific standpoint, these features make the system interesting. In addition to the large amount of tree mortality caused by MPB, the system is notable because it is a multipartite mutualism that has remained stable over a long period of time. This is at odds with ecological theory, which predicts a superior or more competitive mutualist should eventually dominate the mutualism. In Chapter 2, we explored thermal stabilizing

mechanisms by creating a temperature-dependent model for the spread of *G. clavigera* and *O. montium* within a tree, connecting it with existing MPB development models and simulating MPB-fungi dynamics to determine whether differences in the temperature responses between the two fungi could stabilize the system. Two processes critical to coupling the MPB and fungal growth models were not included: first, how fungal growth rates, originally determined from lab studies in Petri dishes, scale to actual growth rates in a tree, and second, the relationship between fungal prevalence in the tree and the proportion of each species packed in MPB mycangia as a function of the relative timing of the teneral adult feeding window.

3.1.2. Scaling fungal growth on an artificial medium to estimate growth in a tree

Grosmannia clavigera and *O. montium* are species of fungi that spread outward in an infested tree by forming a mycelial network from their initial inoculation point. Because the fungi grow under bark, it is impossible to monitor growth from individual inoculation points in a tree over time. Instead, growth rates were determined in lab experiments by growing the two fungi on 2% malt extract agar in Petri dishes at six temperatures (Moore, 2013). These data were used to develop the fungal growth rate curves and growth rate parameters discussed in Section 3.2.2 and to develop the models in Chapter 2. A concern with using these measurements directly, however, is that conditions inside the tree are different than those in a Petri dish – and likely less hospitable. Fungi are likely to grow slower in the tree than growth rate curves based on lab experiments suggest. The result of inoculation studies also suggest that *G. clavigera* is a better first invader of a tree (Krokene and Solheim, 1998) than *O. montium* because it is more virulent and so can better tolerate tree defences. To account for this in our model, we incorporate growth rate scaling parameters for each fungus.

3.1.3. MPB-fungus interaction and mycangial packing

Timing of MPB mycangial packing will influence which fungus is transported from a brood tree to a new tree. MPB feed on fungal spores as teneral adults (Adams and Six, 2007). Teneral adults pack their mycangia with fungal spores sometime following eclosion

from the pupa but prior to emerging from the host tree (Six and Paine, 1998). The feeding window for teneral adults may last weeks, however, and during this time fungal prevalence may change drastically. This makes the timing and efficiency of mycangial packing an important factor in developing accurate models. To better predict fungal acquisition by teneral adults, we hypothesize and test five possible strategies for the timing of mycangial packing. These strategies describe a spectrum of behaviors ranging from model 1, in which MPB immediately pack their mycangia with the first fungus available, to model 5, in which they delay mycangial packing until just prior to emerging from the tree.

Our goal is to determine the most likely model describing mycangial packing and deduce under-bark growth rates from field data. Using derived fungal growth rate scaling parameters and five mycangial packing hypotheses, we construct likelihood functions connecting mathematical hypotheses with observations of fungi carried by emerging MPB adults from observations in the field. We also validate the model and determine which mycangial packing strategy is most likely. Finally, we discuss our findings in relation to the MPB-fungus system and suggest follow-up studies that would aid in our understanding of mechanisms involved in mycangial packing and ultimately fungal prevalence in the following year and with the next generation of beetles.

3.2. Methods

3.2.1. MPB, fungi and temperature data collection

The timing of MPB attacks on trees and adult emergence the following summer was monitored on three lodgepole pine (*Pinus contorta*) in 2010-2011 and four lodgepole pine in 2011-2012 at a site in Logan Canyon, UT (41.9528, -111.55290, 2190m). The MPB population in the vicinity of the site was considered incipient epidemic with approximately one tree per square kilometer infested. In addition to monitoring timing of attack and emergence of adult MPB, the identity of fungal associates (i.e., *G. clavigera* and *O. montium*) carried by MPB entering and exiting trees, and present with the beetle in trees over the one year development period, was determined through phloem sampling and mycangial dissection of adults.

MPB attack timing

On August 2, 2010, an aggregation lure (Synergy Semiochemicals Corporation, Burnaby, BC, Canada) was placed on the north side of each tree. After 10-15 MPB attacks were observed on a tree (i.e., 1 to 3 days) the lure was removed to allow the MPB attack process to continue naturally. Attacks were monitored daily on each tree between 1 and 5 feet above the ground, by bole quadrant (i.e., north, south, east and west). MPB attacks are visible as frass or resin exuding from small entrance holes through the bark. The number of attacks was recorded for each day and each day's attacks marked with a different colored straight pin. This process was repeated in 2011 in the same vicinity using new live trees.

Fungal samples from attacking MPB

Our protocol assumed that fungi introduced into a tree by individual MPB will be present in the phloem surrounding its entry site. To allow adequate time for the fungi to grow into the phloem following adult MPB attacks, we waited 10 days after the first attacks to begin sampling trees. On the 10th day following the first day of attack, 12 attack sites were randomly chosen from all attacks that occurred on a single tree over the first three days. These areas were prepared for fungal sampling by smoothing the bark just above the entry hole (MPB tunnel upward after entry). We then sprayed the area with 70% ETOH. Using a ETOH sterilized 9mm cork borer, a core containing bark and phloem was removed from just above the entry hole. The phloem portion was placed into a sterile-autoclaved microcentrifuge tube that was labeled with the tree number, date of MPB attack, and date of sampling and then placed on ice and transported to the laboratory. This process was repeated for each tree every 3 days throughout the attack period, resulting in up to 120 samples per tree.

To identify the fungal species present in each phloem sample, a sample was placed onto the center of a Petri dish containing 2% malt extract agar amended with Streptomycin and cycloheximide and stored at room temperature for 1 week to allow fungal growth. Isolates were then identified using cultural characteristics and morphology of conidia and conidiophores.

MPB emergence timing

In both years following successful attack, mesh cages were placed on all four quadrants of each tree covering the entire sample area. The following summer, emerging univoltine beetles were collected from cages daily. Beetles were transported to the laboratory where they were placed in sterile Petri dishes with filter paper moistened with distilled water and stored at $3°C$ for less than 1 week. Each adult beetle's sex was determined and the width of its pronotum measured. Both mycangia of each live beetle were dissected and placed individually on opposite sides of a Petri dish containing 2% malt extract agar amended with Streptomycin and cycloheximide. Each dish was labeled with a unique code that identified a single beetle so that fungal identification could be cross-referenced to the tree, bole quadrant, emergence date, size and sex. A maximum of 20 adult MPB from each of the four quadrants of each sampled tree were dissected per sample day (i.e., 80 beetles per day). Fungal cultures were grown at room temperature ($\sim21°C$) and then identified to species.

Length of the MPB life cycle in trees attacked in 2010 was predominately univoltine (i.e., one generation in a single year), although $\sim20\%$ of the population was semivoltine (i.e., one generation every two years) (Bentz et al., 2013). MPB in trees attacked in 2011 were 100% univoltine. Only data from univoltine beetles from 2010 attacks were used in model parameterization, and data from trees attacked in 2011 were used in model validation.

Temperature measurements

Ambient air temperature was measured at the study site using a radiation-shielded temperature probe placed at 1.4 m above the ground on the north side of a tree to reduce direct sun exposure (Campbell Scientific Inc., Logan UT). North and south bole aspect phloem temperatures were measured using thin-tipped (0.34 mm^2) thermocouple temperature probes (Omega Engineering, Inc., Stamford, DT) inserted under the bark and into the phloem layer. Hourly air and phloem temperatures were collected continuously over both sampling years (May 27, 2010 through November 8, 2012) using a datalogger (Campbell Scientific Inc., Logan UT). Model performance was tested using each of the temperature records to explore the effect of north versus south bole temperatures and to determine how

the model might perform for a different site if only ambient temperatures are available.

3.2.2. Fungal growth model

The model we develop here is a modification of the model presented in Chapter 2 in which fungal growth is tracked around a cross section with fungus lesions stochastically, but uniformly, placed around the tree. Lesions were indexed individually and allowed to grow at a rate based on temperature until they contacted the neighboring lesion. When parameterizing the model to fungus input and output observations, however, we found this approach was too rigid. The assumption that fungus lesions could not cross prevented rapid changes in fungal prevalence observed in the field. Thus we moved to a deterministic model that includes a colonization index. To account for the fact that the fungi will not grow into an area already colonized while still allowing fungi to grow around more slowly-growing lesions, we do not explicitly place lesions but instead calculate the cumulative effect of each fungus based on the number (and timing) of attacking MPB carrying each type of fungus. Under-bark colonization rates are proportional to parameterized fungal growth rate curves which describe the length each fungus can colonize based on temperature. We then use a maximum likelihood approach to fit the model to observed data from the field. This includes estimating the value of parameters scaling fungal growth from agar to tree as well as parameters describing the timing of MPB mycangial packing (described below).

Fungal growth in a tree

Using field observations of MPB attack timing and the proportion of each fungus carried by attacking beetles, we allowed a lesion of type *G. clavigera* and a lesion of type *O. montium* to begin growing on each inoculation day at a rate based on temperature. The size of these lesions was scaled by the observed number of attacking MPB carrying that particular fungus. After accounting for each day of MPB attacks, the contribution of each lesion was summed to get a measure of the total distance colonized by *G. clavigera* and *O. montium* from attack to day t_k. Growth rate was based on hourly temperature, and was calculated for the two fungal species separately using growth rate curves parameterized in Chapter 2. That is, the growth rate r of the fungi in millimeters per day was computed as a function of the

temperature T,

$$r(T) = \begin{cases} B(e^{\alpha(T-T_0)} - 1) - B(e^{\alpha(T_m-T_0)} - 1)e^{(T-T_m)/b}, & T \in (T_0, T_m) \\ \\ 0, & T \notin (T_0, T_m). \end{cases} \qquad (3.1)$$

Parameters α, b, B, T_0, and T_m dictate the shape of the curve and were estimated using maximum likelihood estimation (MLE) techniques to best match observed fungal growth data (see Chapter 2). Specific parameter values used for the two fungi are shown in Table 3.1.

Distances colonized by each fungus on each day were multiplied by parameters β_{GC} and β_{OM} (whose values will be estimated using MLE as described in Section 3.2.2) which scale agar growth to growth in a tree. The distances were then added together to get a measure of the total length colonized by both fungi in the tree. That is,

$$G(t_j) = \beta_{GC} \cdot Cum_{GC}(t_j) + \beta_{OM} \cdot Cum_{OM}(t_j),$$

where $G(t_j)$ is the total length colonized in millimeters on day t_j (accounting for all fungal lesions) and $Cum_{GC}(t_j)$ and $Cum_{OM}(t_j)$ represent the unscaled cumulative length colonized by *G. clavigera* and *O. montium* on day t_j calculated using Eqn 3.1 and observed hourly temperatures.

As in our previous model for fungus growth, computations were simplified by considering growth around a tree cross-section. Assuming that MPB attack the tree with roughly even spacing (vertically and horizontally), the average fungus lesion can grow linearly away from its initial inoculation point a maximum distance depending on the size of the tree and the density of MPB attacks. We assume that the two fungi do not colonize the same area. To change distances to a dimensionless quantity suitable for integrating with dimensionless MPB phenology, we divide by C, the average space between fungal lesions. This normalizes our growth G and represents the proportion of the tree that is colonized. Considering only MPB attack densities high enough to cause tree mortality, the average space between fungal lesions C can range from approximately 40mm to approximately 85mm (see Chapter 2). For

Table 3.1
Parameters for the fungal growth rate curves: α affects the rate of increase at low temperatures, b is the thickness of the boundary layer between peak growth and the upper temperature threshold, B is a scaling factor which affects the maximum rate of fungal growth, while T_0 and T_m are the lower and upper temperature thresholds for the fungi respectively in °C. These parameters were estimated in Chapter 2.

Parameter Values for Fungal Growth Rate Curves					
fungus type	α	b	B	T_0 (°C)	T_m (°C)
G. clavigera	0.0041	8.0407	95.6120	0.9123	32
O. montium	0.0662	7.4949	3.8395	-0.0236	34

simulations in this paper, we allowed $C = 54$mm corresponding to an optimal MPB attack density of 62MPB/m^2 (Raffa and Berryman, 1983). Note that the actual colonization index may vary from tree to tree, affecting values of β_{GC} and β_{OM}. For this reason we will also report the ratio between these parameters, β_{GC}/β_{OM}, which is independent of C.

Finally, to obtain a prediction describing the amount of each fungus in the tree on day t_j, we compute the day p in which $G > C$, which is when the total growth G of the fungi will have outgrown the space available. The space between lesions therefore depends on β_{GC} and β_{OM}, the observed hourly temperatures, and the observed attack distribution. The proportion of each fungus in the tree on day t_j is

$$p_{GC}(t_j) = \begin{cases} \beta_{GC} \cdot Cum_{GC}(t_j) & \text{for } t_j < p, \\ \beta_{GC} \cdot Cum_{GC}(p) & \text{for } t_j \geq p, \text{ and} \end{cases} \quad (3.2)$$

$$p_{OM}(t_j) = \begin{cases} \beta_{OM} \cdot Cum_{OM}(t_j) & \text{for } t_j < p, \\ \beta_{OM} \cdot Cum_{OM}(p) & \text{for } t_j \geq p. \end{cases} \quad (3.3)$$

That is, the proportion of each fungus in the tree on a given day is equal to the cumulative growth of the fungi (based on observed growth rates measured in a Petri dish) multiplied by the respective growth rate scaling parameter and then normalized. Given the proportion of each fungi present in the tree over time, we next needed to determine the probability that

a MPB would be feeding as a teneral adult beginning on a given day.

Predicting the timing of teneral adult feeding on fungi

Which fungus resides in the mycangia of a particular emerging adult beetle is affected by the timing of its eclosion to the teneral adult stage and the length of time it feeds on fungal spores. A distribution of likely teneral adult feeding windows is therefore necessary. That is, we wish to know the range of possible days t_j when a teneral adult could have begun feeding, given emergence day t_k. We were also interested in the relative likelihood of day t_j relative to the other days. The feeding window distribution was determined by working backward from a distributional MPB phenology model (Régnière et al., 2012) using observed hourly temperatures and known attack and emergence dates. This was done by expressing the "hang time" or "observed" development time of MPB as $t_k - t_j = \delta \cdot \tau$ where t_j and t_k are the predicted beginning and end dates of the observed teneral adult feeding window, τ is the median emergence time for teneral MPB adults, and δ is the multiplicative variability between observed and median development times. Solving this equation for δ we find that

$$\delta = \frac{t_k - t_j}{\tau} = \int_{t_j}^{t_k} r(T(t')) \, dt', \tag{3.4}$$

where r represents the teneral adult development rate of MPB as a function of temperature T in degrees C. We follow Régnière et al. (2012) and make the assumption that δ follows a lognormal distribution with mean 1 (that is, $\delta \sim ln\mathcal{N}(-\sigma^2/2, \sigma^2)$ where σ is an additional parameter to be estimated). This ensures $\delta \geq 0$, i.e., that development times and rates are never negative; it can be easily inverted; and its asymmetrical shape with a longer right-hand tail is commensurate with observations of MPB development (Régnière et al., 2012). Making this lognormal error assumption, the cumulative distribution function (CDF) of development time is given by,

$$P(t > t_j) = \Phi \left[\frac{\ln(\delta) + \sigma^2/2}{\sigma} \right],$$

so the probability density function (pdf) is

$$\frac{dP}{dt_j} = \frac{1}{\sqrt{2\pi\sigma^2\delta^2}} \exp\left(-\frac{(\ln(\delta)+\sigma^2/2)^2}{2\sigma^2}\right) \cdot \frac{d(\delta)}{dt_j} \ .$$

Taking into account the definition of δ (Eqn 3.4), we find that

$$\frac{d(\delta)}{dt_j} = -r(T(t_j)).$$

Putting all of this together, we find that the probability that a beetle emerging at time t_k was feeding at time t_j as a teneral adult is given by

$$pdf_k(t_j) = \frac{r(T(t_j))}{\sqrt{2\pi\sigma^2 R(t_j,t_k)^2}} \exp\left(-\frac{(\ln(R(t_j,t_k))+\sigma^2/2)^2}{2\sigma^2}\right), \tag{3.5}$$

where

$$R(t_j,t_k) = \int_{t_j}^{t_k} r(T(t'))dt' \ .$$

For purposes of computation, the continuous function pdf_k is approximated by a matrix of probabilities, $Pfeed$, calculated by discretizing the time domain into hour-long segments and then reporting the probability of feeding on day t_j given that the beetle emerges on day t_k, that is,

$$Pfeed(t_j,t_k) = pdf_k(t_j). \tag{3.6}$$

An example of the resulting distribution of teneral adult feeding can be seen in Figure 3.1 where the distribution of possible feeding start days is shown for a particular day of emergence. This calculation was repeated for all emergence days t_k. Note that this calculation reflects the probability that an adult could emerge on day t_k, given that it happens to be under the bark on day t_j. It does not reflect the actual probability of teneral adults appearing on day t_j under the bark given observed attacks. It therefore may assign a nonzero probability to teneral feeding windows beginning the previous fall or early spring (Figure 3.1), which are unrealistic in the context of observed attacks.

Assigning fungi to emerging MPB

Utilizing the matrix of probabilities, $Pfeed$, computed from Eqn 3.6 in Section 3.2.2 and the proportion of each fungus available in the tree (p_{GC} and p_{OM}) over time, we can construct submodels to compare the five mycangial packing hypotheses. The strategies describe a spectrum of behaviors ranging from model 1, in which MPB immediately pack their mycangia with the first fungus available, to model 5, in which they delay mycangial packing until just prior to emerging from the tree. In the following discussion, p_1, p_2 and p_3, will be used to represent the proportion of MPB emerging on day t_k with *G. clavigera*, *O. montium*, and no fungus respectively. The specific method for calculating p_1, p_2 and p_3 will differ based on the mycangial packing assumption and will be described individually below.

1) First fungus contacted – this model assumes that the fungus present in the mycangia of an emerging adult MPB is the first fungus contacted by the beetle within the pupal chamber. The model is implemented by calculating all probable feeding windows (similar to the one depicted in Figure 3.1) for MPB emerging on days in which emergence was recorded. For each emergence day t_k, the probabilities p_1, p_2 and p_3 are:

$$
\begin{aligned}
p_1(t_k) &= \sum_{t_j} p_{GC}(t_j) p_{feed}(t_j, t_k), \\
p_2(t_k) &= \sum_{t_j} p_{OM}(t_j) p_{feed}(t_j, t_k), \text{ and} \\
p_3(t_k) &= 1 - p_1(t_k) - p_2(t_k)
\end{aligned}
$$

using information obtained from equations 3.2, 3.3 and 3.5.

2) Mostly the first fungus contacted – this model assumes that the majority of MPB pack their mycangia with the first fungus available, but that some proportion pack their mycangia in subsequent days, with a diminishing probability each day according to an exponential distribution with parameter λ which represents the mean time to
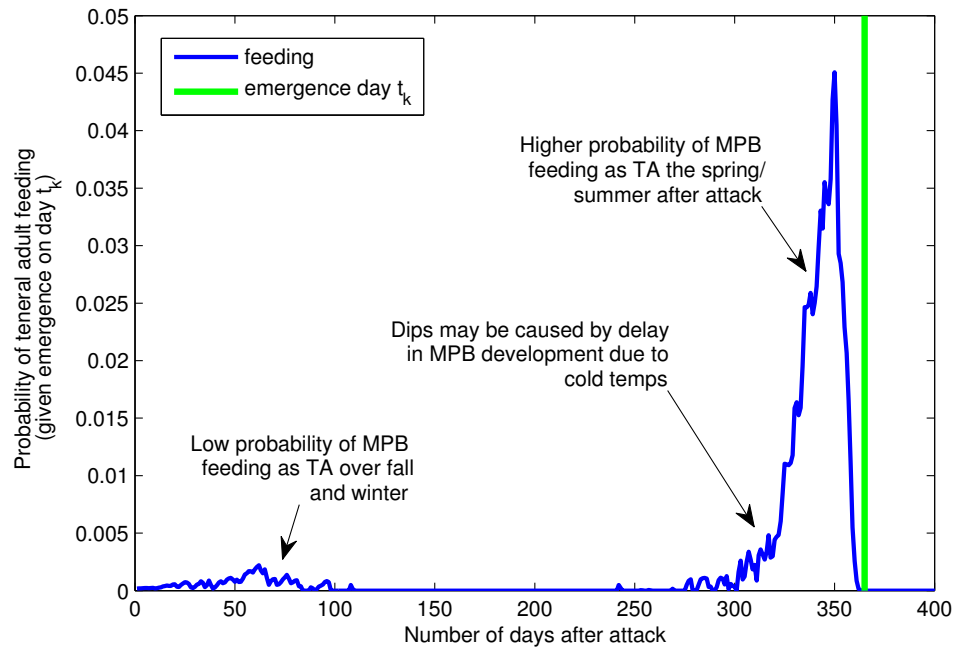
Fig. 3.1: Predicted probability of beginning feeding as a teneral adult given emergence on a particular day t_k. The solid blue curve represents the probability of beginning feeding as a teneral adult on a particular day given that the MPB emerged from the tree 365 days after attack (i.e., JD 204 of 2011). The emergence day is shown as a vertical line (dashed green). This demonstrates that the most likely time for an MPB to be feeding on fungal spores in the teneral adult stage is in the weeks leading up to emergence from a tree (though there is some nonzero, but very low, probability – based on the phenology model – that this could occur in late fall or early spring). The dips in the curve are a result of delays in movement from the pupal to teneral adult stage, perhaps due to cold temperatures.

encounter or pick up a fungal spore (as $\lambda \to 0$, this model represents model 1). Using this distribution, the probability P of first encountering a fungal spore after t days is given by

$$P(\text{first encounter at } t \text{ days}) = e^{-t/\lambda},$$

so the probability of not encountering a fungus until time t is given by

$$F(t) = P(\text{no encounter} \le t) = 1 - e^{-t/\lambda}.$$

This was used to calculate the probability that an MPB packed its mycangia during a given period. That is,

$$p_{pack}(t_j + t) = F(t_j + t) - F(t_j + t - 1) \tag{3.7}$$

is the probability that an individual packed its mycangia between JD $t_j + t - 1$ and JD $t_j + t$. In order to arrive at the probabilities of an MPB emerging with $G.\ clavigera$, $O.\ montium$ or no fungi, probabilities of collecting each fungus, $p_{GC,coll}$ and $p_{OM,coll}$, were calculated

$$p_{GC,coll}(t_j) = p_{GC} \cdot p_{pack} \quad \text{and} \quad p_{OM,coll}(t_j) = p_{OM} \cdot p_{pack}.$$

Then

$$
\begin{aligned}
p_1(t_k) &= \sum_{t_j} p_{GC,coll}(t_j) p_{feed}(t_j, t_k), \\
p_2(t_k) &= \sum_{t_j} p_{OM,coll}(t_j) p_{feed}(t_j, t_k), \quad \text{and} \\
p_3(t_k) &= 1 - p_1(t_k) - p_2(t_k).
\end{aligned}
$$

3) A delay in mycangial packing – this model uses the Laplace probability distribution in place of the exponential probability distribution used in model 2. It allows for an initial delay in mycangial packing following eclosion to the teneral adult stage. This

delay could be due to slow fungal growth and sporulation in the pupal chamber. A delay could also be a result of time required for maturation of teneral adults prior to feeding. Mycangial packing would then increase, reach some peak packing probability, and diminish. Mathematically, this changes the probability of not encountering a fungus until time t to

$$P(\text{no encounter} \leq t) = \begin{cases} \frac{1}{2}e^{\frac{t-\mu}{\lambda}}, & \text{for } t < \mu \\ 1 - \frac{1}{2}e^{\frac{t-\mu}{\lambda}}, & \text{for } t \geq \mu, \end{cases} \tag{3.8}$$

where μ represents the delay in days after eclosing to a teneral adult until peak mycangial packing occurs (or the delay until the greatest presence of spores to be packed is available) and λ determines the spread in mycangial packing around this date. The remaining calculations for p_1, p_2 and p_3 are identical to those for model 2.

4) Mostly the last fungus contacted – this model is the opposite of model 2. It assumes that MPB do not pack their mycangia until they are nearly done feeding, with most MPB mycangial packing occurring just prior to emergence. It is also implemented using an exponential probability distribution where the probability of not encountering fungal spores until day t is given by

$$P(\text{no encounter} \geq t) = 1 - e^{-(t_k - t)/\lambda}.$$

As in model 2, $t = 1, 2, 3, \ldots$ represents the number of days that the teneral adult has been feeding, t_k is the number of days that the teneral adult will feed prior to emerging from the tree, and λ represents the spread in the number of days of mycangial packing. Using this CDF, the remaining calculations for p_1, p_2 and p_3 are identical to those for model 2.

5) Last fungus contacted – this model assumes that MPB pack their mycangia just prior to emerging from the tree with whichever fungus is available at the time. We allow

$$
\begin{aligned}
p_1(t_k) &= p_{GC}(t_k), \\
p_2(t_k) &= p_{OM}(t_k), \text{ and} \\
p_3(t_k) &= 1 - p_1(t_k) - p_2(t_k).
\end{aligned}
$$

This means that the fungus carried by MPB emerging from the tree on day t_k is simply the proportion of each fungus available in the tree on day t_k.

Differences among models in the timing of probability of feeding are shown in Figure 3.2 with $\lambda = 4.1$ for models 2 and 4 (representing the mean time to encounter/pick up fungi) and $\lambda = 1.3$, $\mu = 5.4$ for model 3. In model 3, the parameter μ represents the delay in days until peak mycangial packing occurs and λ dictates the spread in mycangial packing around that day.

Likelihood function for parameterizing the fungus growth model

To parameterize the fungal growth models and reconcile emergence observations with the values for p_1, p_2 and p_3 computed above, MPB field observations were divided into categories in which n_1 represented the number carrying *G. clavigera*, n_2 represented the number carrying *O. montium*, n_3 represented the number carrying no fungi, and $N = n_1 + n_2 + n_3$ represented the total number of MPB emerging for each observed emergence day. These values were used in a maximum likelihood framework with a multinomial distribution to obtain the best parameter estimates for the fungal growth rate scaling parameters β_{GC} and β_{OM} (as well as λ for mycangial packing hypotheses 2, 3 and 4 and μ for model 3). The likelihood for the multinomial probability distribution is written as

$$
\mathcal{L} = \prod_{t_k} \frac{N(t_k)!}{n_1(t_k)!\, n_2(t_k)!\, n_3(t_k)!}\, p_1(t_k)^{n_1(t_k)} p_2(t_k)^{n_2(t_k)} p_3(t_k)^{n_3(t_k)} . \tag{3.9}
$$

In this likelihood, N, n_1, n_2 and n_3 come from the observations while p_1, p_2 and
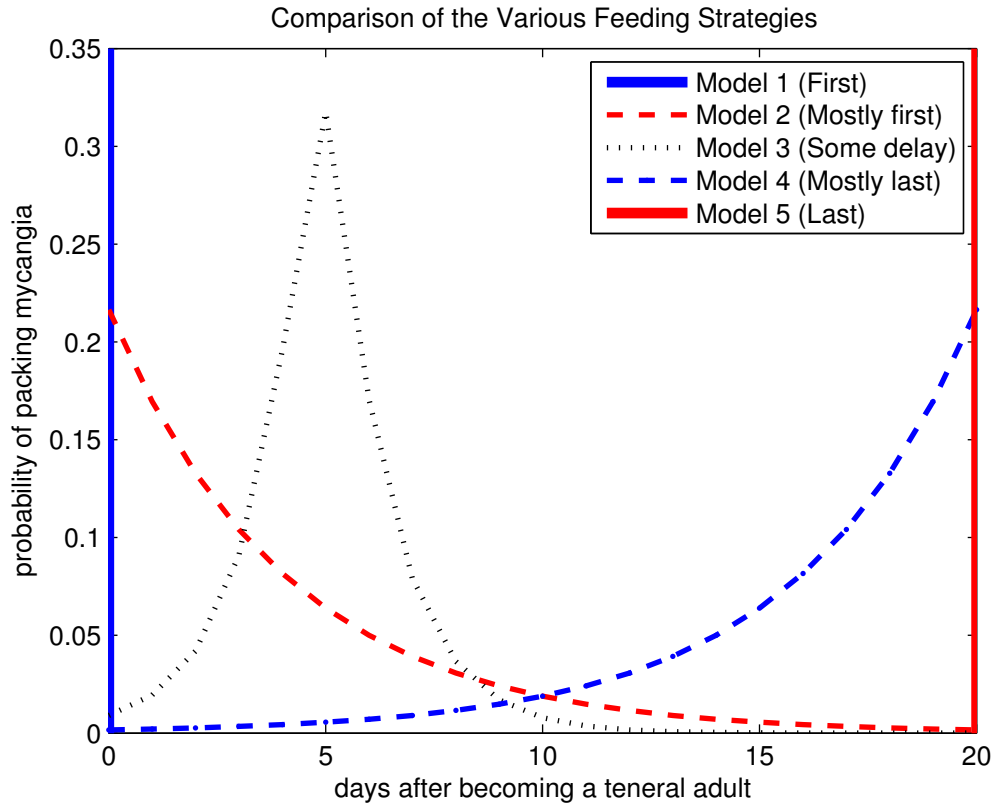
Fig. 3.2: Comparison of the different probability distributions used to construct mycangial packing models 1-5. In model 1, mycangial packing takes place on day 1 of teneral adult feeding (solid blue vertical line), in model 2 (dashed red exponential curve), mycangial packing begins immediately after eclosion to the teneral adult stage, model 3 (dotted green Laplace curve) allows a delay then a peak in mycangial packing, model 4 (dashed blue exponential curve) results in little mycangial packing until just before adult emergence (in this case occurring 20 days after entering the teneral adult life stage), and model 5 (solid red vertical line) is where mycangial packing takes place on the final day before emergence. For these plots, $\lambda = 4.1$ for models 2 and 4 and $\lambda = 1.3$ and $\mu = 5.4$ for model 3. Note that increasing λ has the effect of stretching the curves horizontally, prolonging the potential period of mycangial packing while altering the value of μ in model 3 will change the timing of peak mycangial packing.

p_3 are computed using the fungal growth model combined with the mycangial packing strategies described in Section 3.2.2. The values of p_1, p_2 and p_3 represent the proportion of *G. clavigera*, *O. montium*, and no fungi, respectively, available in the tree on a given emergence day. These three values incorporate the effects of parameters β_{GC}, β_{OM}, λ and μ which allow us to obtain estimates using a built-in MATLAB optimizer (the Nelder-Mead simplex algorithm, 'fminsearch') to minimize the negative log likelihood (negative log of Eqn 3.9).

Of all the parameters and unknowns, the two that have the largest potential to impact overall predictions are β_{GC} and β_{OM}, the growth rate scaling parameters for *G. clavigera* and *O. montium*, respectively. Though we lack field measurements or observations for these values, we will constrain and assess their values based on several assumptions:

1) We hypothesize that fungi grow slower in a tree than in a Petri dish and that they will not decrease in prevalence (this requires β_{GC} and β_{OM} to lie between 0 and 1);

2) Based on observations of MPB occasionally tunneling backwards in their larval galleries to eat fungus colonized phloem (Adams and Six, 2007), we obtained a rough estimate for a single growth rate scaling parameter, $\beta = 0.1387$, for both fungi in Chapter 2; and

3) *G. clavigera* is known to be more aggressive at growing in a freshly killed tree (Krokene and Solheim, 1998) and may be less susceptible to cold induced mortality than *O. montium* (Rice et al., 2008) which leads us to expect that β_{GC} will be larger than β_{OM}.

Condition 1 was used to constrain the parameter estimates whereas conditions 2 and 3 will be used later to assess their values. This constraint was implemented by setting the negative log likelihood to an arbitrarily large positive number when $\beta < 0$, and an arbitrarily large number times β when $\beta > 1$. This caused the optimization algorithm to move away from the extremes and explore the valid region of parameter space. The optimization procedure was repeated 1,000 times for each model with random initial guesses for each parameter.

Parameters resulting in the lowest negative log likelihood were selected as the best parameter estimates for each model.

3.2.3.   Bootstrapping the data

To quantify the sensitivity of parameter estimates, we employed bootstrapping, constructing a new set of observations (i.e., MPB emergence date and species of fungus carried, that is, $n_1(t_k)$, $n_2(t_k)$ and $n_3(t_k)$) of the same size as the original dataset by sampling the original dataset with replacement. After obtaining a new set of observations, the model and MLE procedure was repeated 1,000 times to generate a 95% confidence interval for the parameters for each of the five mycangial packing hypotheses.

3.2.4.   Testing model sensitivity to temperature

Sensitivity of the models to temperature was tested by running models 1-5 using their respective parameter estimates (Table 3.3) with ambient temperature as well as north and south bole phloem temperatures collected at each of the study trees. We also ran models 1-5 using observed temperatures from trees attacked in 2010, increased and decreased by -1.5 to 1.5°C (incremented by 0.05°C). For each of the modified temperature sets, model predictions for all five models were compared against observed MPB emergence.

3.2.5.   Model evaluation

Output from the five mycangial packing models were compared using Akaike Information Criterion (AIC), defined as

$$AIC = -2\log(\mathcal{L}(\theta|y)) + 2K,$$

where $\mathcal{L}(\theta|y)$ is the likelihood of the model and parameters given the data and K is the number of parameters (Burnham and Anderson, 2002). This value quantifies the amount of information lost by the model and allows for model competition via AIC. Models were also compared using R^2.

A weak validation was conducted by starting the model with observed 2010 attacks and running it forward with estimated parameters to predict fungal prevalence then comparing

with observed prevalence on emergence. This was combined with probable MPB teneral adult feeding windows. A second, stronger validation was then conducted using an independent dataset that consisted of observed temperatures and MPB attack and emergence data with fungus carried collected on trees attacked in 2011.

3.3. Results

3.3.1. Parameter estimates for the five mycangial packing models

MPB attack and emergence observations and associated data on the prevalence of fungi from trees attacked in 2010 (Table 3.2) were used to obtain estimates of the growth rate scaling parameters β_{GC} and β_{OM} and mycangial packing parameters λ and μ (as applicable) for the five mycangial packing models (Table 3.3). Model parameterization was repeated for ambient air temperatures as well as north and south bole phloem temperatures for the various attacked trees. While there were slight differences in parameter estimates, the models performed equally well regardless of temperature. For consistency, we chose to parameterize the models using north bole phloem temperatures. The results of this parameterization show some variability between β_{GC} and β_{OM} across models (and across acceptable parameters for model 4), however, the ratio of the two parameters β_{GC}/β_{OM} remains quite steady, ranging from just 24.16 to 24.92. Comparing the estimates for β_{GC} and β_{OM} shown in Table 3.3 with assumptions described in Section 3.2.2, all the estimates seem reasonable. Each value for β_{GC} and β_{OM} lies between 0 and 1, the average of the parameters lies reasonably close to our former estimate of $\beta = 0.1387$ (see Chapter 2), and the estimates for the *G. clavigera* scaling parameter are much greater than for *O. montium*. This difference between the β_{GC} and β_{OM} estimates reflected the MPB emergence observations (Table 3.2), which were heavily biased toward *G. clavigera*. MPB that attacked trees in both 2010 and 2011 were observed carrying a nearly equal mix of *G. clavigera* and *O. montium* whereas emerging MPB from these trees were carrying predominantly *G. clavigera*. For example, more than 38% of MPB attacking trees in 2010 were carrying *O. montium*, yet only 4.3% of adults emerging from these same trees were observed with *O. montium* in their mycangia. A similar pattern was seen in trees attacked in 2011 (Table 3.2).

Table 3.2
Comparison of the percentages of MPB carrying *G. clavigera* (GC), *O. montium* (OM), both fungi, or no fungi into and out of trees attacked in 2010 and 2011.

Attack and Emergence Data					
	# of MPB analyzed	%GC	%OM	%Both	%None
2010 Attacks	263	21.8	38.6	4.9	34.7
2010 Emergence	1099	90.4	4.3	3.5	1.9
2011 Attacks	193	26.9	28.8	1.3	42.9
2011 Emergence	908	63.9	10.8	6.2	19.2

Table 3.3
Comparison of the growth rate scaling parameter estimates β_{GC} and β_{OM} and feeding distribution parameters λ (the mean waiting time to encounter fungi; models 2, 3 and 4), and μ (the peak receptivity to fungal spores; model 3), obtained using maximum likelihood for 2010 data. Parameter estimation for model 4 was slightly less consistent than for models 1-3 and 5, so the midpoint of the acceptable parameters that resulted in the best AIC has been reported. Note that the ratio of the growth rate scaling parameters was largely steady across all models.

2010 Growth Rate Scaling Parameter Estimates					
	Model 1	Model 2	Model 3	Model 4	Model 5
β_{GC}	.9336	1.0000	1.0000	.8959	.6355
β_{OM}	.0376	.0401	.0401	.0364	.0263
β_{GC}/β_{OM}	24.81	24.92	24.92	24.62	24.16
λ	na	3.7054	1.2883	4.1333	na
μ	na	na	5.4168	na	na

3.3.2. Model performance

Using parameterized data, model fit statistics including ΔAIC (Table 3.4) and R^2 (Table 3.5) were computed, where R is the correlation coefficient of the model predictions ($p_1 * N$, $p_2 * N$ and $p_3 * N$) versus the observations (n_1, n_2 and n_3) over all observed emergence days. We found that all five models performed well, in terms of visual fit (Figure 3.3) and high R^2 (Table 3.5), when predictions were compared to field observations used for model parameterization. Model 5, representing the case where MPB pack their mycangia with the last fungus contacted, performed best in terms of producing the lowest AIC (Table 3.4) and model 4 also performed quite well. Differences in R^2 were trivial (Table 3.5).

3.3.3. Model validation

After bootstrapping and reparameterizing the models 1,000 times using data from trees attacked in 2010 (i.e., the data used in the original parameterization), the 95% confidence intervals were compared (Table 3.6). These intervals showed small amounts of variability across parameter estimates for models 1, 2, 3 and 5 and greater variability in model 4. This was expected for model 4 due to the range of viable parameter estimates obtained from the original dataset, perhaps indicating a very shallow likelihood surface.

When each model was run for a range of temperature shifts from -1.5 to 1.5°C, we found that the AIC values for each model fluctuated in different ways. Models 1 and 5 were the most variable, and model 4 was the least variable (Figure 3.4). Over the entire temperature range, the AIC values for model 4 varied by 3.83, models 2 and 3 varied by

Table 3.4
Comparison of $\Delta AIC = AIC - AIC_{low}$ computed for the various mycangial packing hypotheses for 2010 data. Models are arranged from packing early (model 1) to packing late (model 5) and the best ΔAIC values are marked in bold. Model 5 produced the lowest AIC for 2010, $AIC_{low} = 247.4722$ with model 4 producing a very similar AIC, indicating mycangial packing occurs late in the teneral adult feeding window.

Comparison of ΔAIC (for parameterization Data)				
Model 1	Model 2	Model 3	Model 4	Model 5
4.9927	7.1009	6.3786	**2.4208**	**0**

Table 3.5
Comparison of R^2 fit for each model where the best values are marked in bold. Here the number of MPB emerging carrying *G. clavigera*, *O. montium*, and no fungus were compared to each model's predictions (arranged from packing early, model 1, to packing late, model 5). Note how the R^2 values for *G. clavigera* are very high across all models whereas they are lower for *O. montium* and quite poor for "no fungi". We suspect that this difference could partially be attributed to the high number of *G. clavigera* emergence observations for 2010 which caused the optimization method to put more weight on fitting the *G. clavigera* data.

Comparison of R^2 (for parameterization Data)					
	Model 1	Model 2	Model 3	Model 4	Model 5
R^2_{GC}	**.9973**	**.9973**	**.9973**	.9791	**.9972**
R^2_{OM}	.6600	.6573	.6603	.6086	**.6624**
R^2_{none}	.0758	.0711	.1399	**.1521**	**.1521**

Table 3.6
95% confidence intervals for parameter estimates obtained using bootstrapped data from the 2010 dataset. Here we see some variability in the parameter estimates for models 1 ("first fungus contacted"), 2 ("mostly first fungus contacted"), 3 ("some delay in mycangial packing") and 5 ("last fungus contacted"); greater variability for model 4 ("mostly last fungus contacted") parameters (which is expected since the model 4 parameter estimates were found to be variable using the original 2010 dataset).

Confidence Intervals for Parameters obtained via Bootstrapping					
	Model 1	Model 2	Model 3	Model 4	Model 5
β_{GC}	(.9167,.9377)	(1,1)	(.9981,1.000)	(.7209,.8853)	(.5896,.6377)
β_{GC}	(.0354,.0477)	(.0369,.0512)	(.0373,.0515)	(.0323,.0391)	(.0240,.0328)
$\frac{\beta_{GC}}{\beta_{OM}}$	(17.22,28.98)	(17.57,31.27)	(16.38,30.43)	(17.44,29.52)	(17.66,29.96)
λ	na	(3.6053,4.5847)	(.5777,1.5862)	(4.0081,4.9052)	na
μ	na	na	(3.1076,7.9357)	na	na
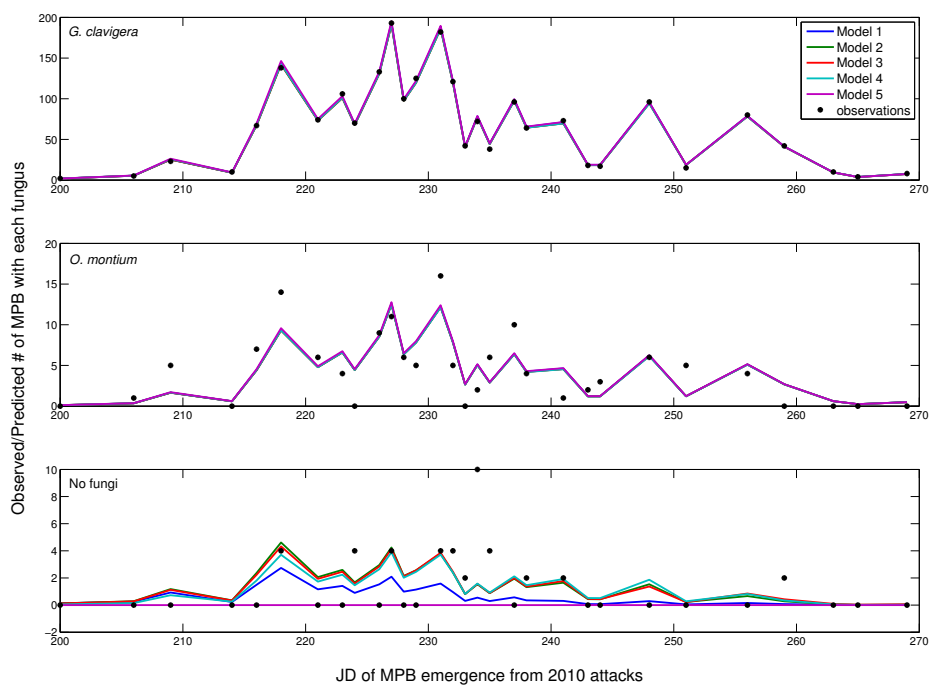
Fig. 3.3: Comparison of the five model predictions for fungi carried by emerging beetles versus actual observations using the parameterization dataset (2010). Models are arranged in order of mycangial packing with model 1 representing immediate packing and model 5 presenting packing just prior to emergence from the tree. Here we see all models perform very well for predicting *G. clavigera* with emerging beetles, as well as for beetles emerging with *O. montium* but have more difficulty predicting when beetles emerge with no fungi (in part because model predictions for "no fungi" are directly affected by predictions for *G. clavigera* and *O. montium*).

Table 3.7

Comparison of $\Delta AIC = AIC - AIC_{low}$ computed for the various mycangial packing models (arranged from packing early, model 1, to packing late, model 5) for 2011 validation data with the best value marked in bold. For the validation data, model 4 produced the lowest AIC, $AIC_{low} = 1383.2$.

Comparison of ΔAIC (for Validation Data)				
Model 1	Model 2	Model 3	Model 4	Model 5
1170.1	122.9	155.5	**0**	838.3

Table 3.8

Comparison of R^2 fit for each model (arranged from packing early, model 1, to packing late, model 5) against the validation data where the best values are marked in bold.

Comparison of R^2 (for Validation Data)					
	Model 1	Model 2	Model 3	Model 4	Model 5
R^2_{GC}	.9635	.9637	.9636	**.9642**	**.9642**
R^2_{OM}	.9261	.9258	.9256	.9257	**.9262**
R^2_{none}	.1962	.6617	.6397	**.7079**	**.7174**

23.69 and 24.16, respectively. Models 1 and 5 were the most sensitive with an overall change in AIC of 67.59 and 284.31. The sensitivity in model 5 was quite pronounced, even with a small change in temperature of -0.1 to 0.1°C. The change in AIC over this range was 205.20.

The models were further evaluated using an independent dataset based on observed MPB attack and emergence, fungus carried, and hourly temperatures for trees attacked in 2011. ΔAIC (Table 3.7) and R^2 values (Table 3.8) were computed. These provided somewhat conflicting results with model 4 ("mostly last fungus contacted") providing the best AIC value by a sizeable margin and model 5 ("last fungus contacted") providing the best R^2 values. Model predictions were less accurate than when visually compared to the observed data used in model parameterization (Figure 3.3). All five models overpredicted *G. clavigera* with emerging beetles and underpredicted emergence with *O. montium* and no fungi (Figure 3.5). This is not represented in the R^2 values for the models, however, because R^2 is a measure of whether the timing of increases and decreases is accounted for, not the scale.
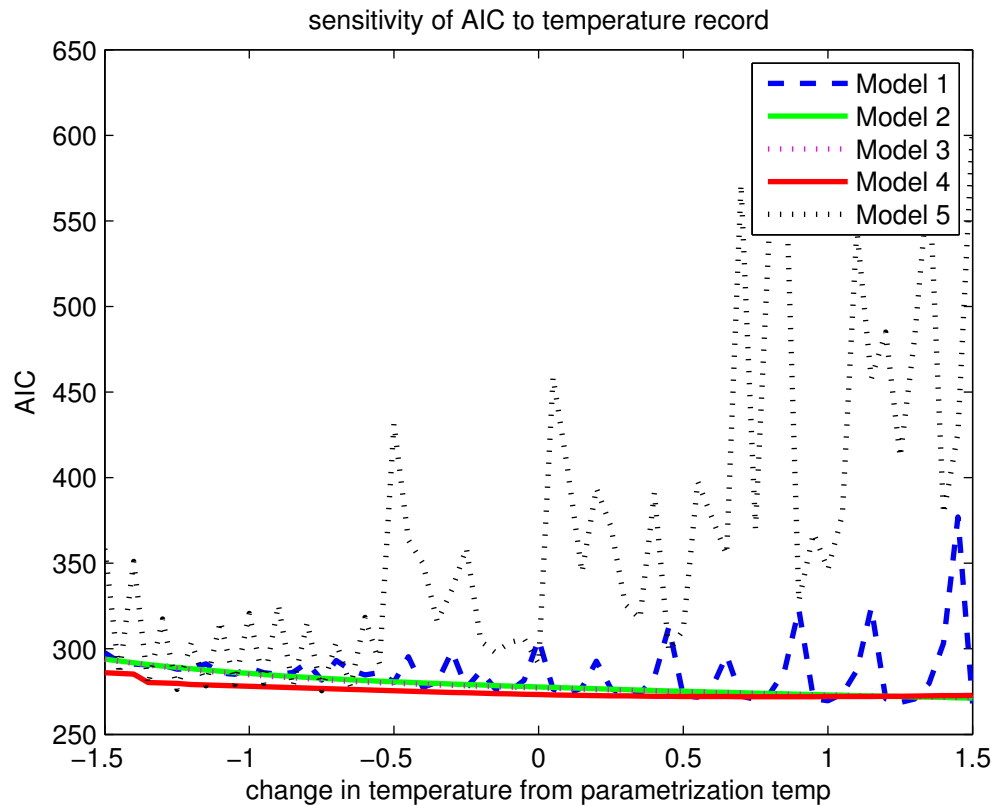
Fig. 3.4: Variability in AIC when models 1-5 were run with temperature data used in model parameterization with a small +/- change in temperature. Note the high degree of sensitivity of model 5 ("last fungus contacted," dotted black line) and, to a lesser degree, model 1 ("first fungus contacted," dashed blue line). Models 2 ("mostly first fungus contacted," solid green line), 3 ("some delay in mycangial packing," dotted magenta line), and 4 ("mostly last fungus contacted," solid red line) were much less sensitive with model 4 being the most robust to small fluctuations in temperature.
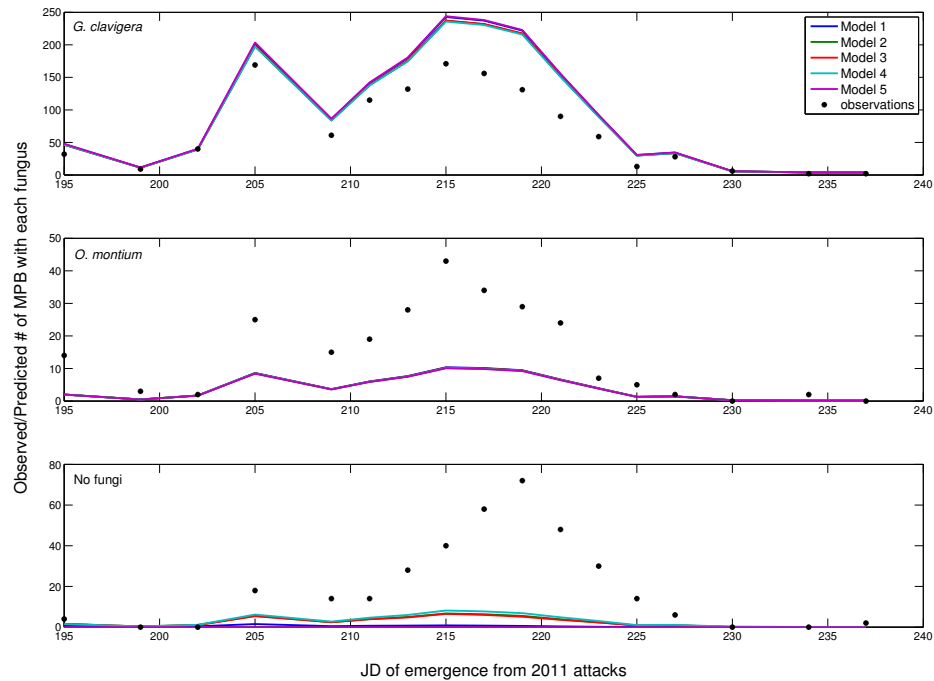
Fig. 3.5: Comparison of the five model predictions for fungal emergence versus observed emergence using the validation dataset from trees attacked in 2011. Models are arranged in order of mycangial packing with model 1 representing immediate packing and model 5 presenting packing just prior to emergence from the tree. We note that temperatures in 2011-2012 were warmer than in 2010-2011 which resulted in slightly higher relative emergence by *O. montium*. This resulted in an overprediction in the number of MPB emerging with *G. clavigera* and an underprediction of the number of beetles emerging with *O. montium* and no fungi. The differences in model predictions are most noticeable in plot C) where the predicted emergence of MPB carrying no fungi is shown. Note that models 1 and 5 ("first fungus contacted" and "last fungus contacted") predict nearly zero beetles will emerge with no fungi (likely due to full tree colonization by the fungi).

3.4. Discussion

3.4.1. Mycangial packing hypotheses and model fit

Using the parameterization dataset, all five models describing various mycangial packing strategies provided good predictions of emerging MPB carrying *G. clavigera*, and reasonable predictions for MPB carrying *O. montium*. The model that assumed MPB packed their mycangia with the last fungus encountered (model 5) had the lowest AIC and two of the best R^2 values. None of the models did a good job of predicting MPB emergence with "no fungi", likely because few beetles emerging from trees attacked in 2010 (i.e., data used for model parameterization) had no fungi. The overwhelming majority of MPB emerging from 2010 attacks were found to be carrying *G. clavigera* which put more weight on matching *G. clavigera* emergence in parameter estimation. In addition, our model defined the proportion of "no fungi" in the tree as the proportion of the tree not already colonized by the two fungi, making "no fungi" predictions very reliant on predictions for the other two fungi.

The two models assuming either the first or last fungus encountered were packed in the mycangia were the most sensitive to temperature changes. Altering the hourly temperatures could effectively alter the prevalence of a particular fungal species at the time of emergence, particularly if the tree was still being colonized by the fungi near the time of MPB emergence from the tree. This was the case for model 5. The growth rate scaling parameters estimated for this model did not result in full tree colonization until approximately JD 180 of the next summer (using actual 2010 temperatures; Figure 3.6 Plot D). Altering the temperature series by warming or cooling had the potential to change the timing of tree colonization, dramatically changing model predictions of the fungal species being carried out of the tree which could change the fit of the model (Figure 3.4). Allowing the mycangial packing to be spread out over time (with an exponential or Laplace distribution, i.e., models 2, 3 and 4) buffered fluctuations in fungal prevalence to small changes in temperature. In addition, fungal growth rate scaling parameters for these models were larger, which led to higher tree colonization by fungi during the teneral adult feeding window (literally leaving

less room for fluctuations in fungal prevalence and hence, model fit; Figure 3.4). This figure also demonstrates the way in which "no fungi" predictions are tied to predictions of *G. clavigera* and *O. montium*. Models 1 and 5 have the shared property that all MPB pack their mycangia (either when they first eclose from the pupal chamber or just prior to emergence from the tree), so predictions of no fungi must come from area available in the tree to be colonized. The models with mycangial packing spread over time (models 2, 3 and 4), however, allow some portion of MPB to never pack their mycangia depending on the length of the teneral adult feeding window and the value of the parameter λ – despite the tree being fully colonized by fungi. This explains how models 2, 3 and 4 are able to predict higher numbers of beetles emerging with no fungi than models 1 and 5.

Repeating the model comparisons using an independent dataset for temperature, MPB attacks, emergence and associated fungi (i.e., trees attacked in 2011), we found a much starker contrast between models in terms of AIC (Table 3.7). Model 4, where observed fungi comes from more recent feeding, produced the lowest AIC by a substantial margin (119.5 lower than the next model, model 2). Model 5, which performed best in terms of AIC when the data used in parameterization was also used for validation, had the highest R^2 but the lowest AIC of all five models (Table 3.8). R^2 may not be the best statistic for model selection, however, since it describes errors in the timing of increases and decreases in fungal prevalence rather than actual magnitudes. A visual inspection of predictions versus observations (Figure 3.5) shows that all models overpredict prevalence of *G. clavigera* and underpredict *O. montium* emergence, although the shapes of the distributions are qualitatively correct. Model 4 overpredicted *G. clavigera* and underpredicted "no fungi" by the smallest margin of the five models, thereby producing the lowest AIC.

Based on the two validation exercises, models 4 and 5 provided the best fit. In addition, β_{GC} estimates for models 1, 2 and 3 were all unrealistically large. These results suggest that the most likely fungus for dispersal is the fungus available just prior to emergence and that the most likely value for β_{GC} ranges from approximately 0.6 to 0.8. Model 5 was highly sensitive to slight changes in temperature (Figure 3.4), however, lowering its reliability.
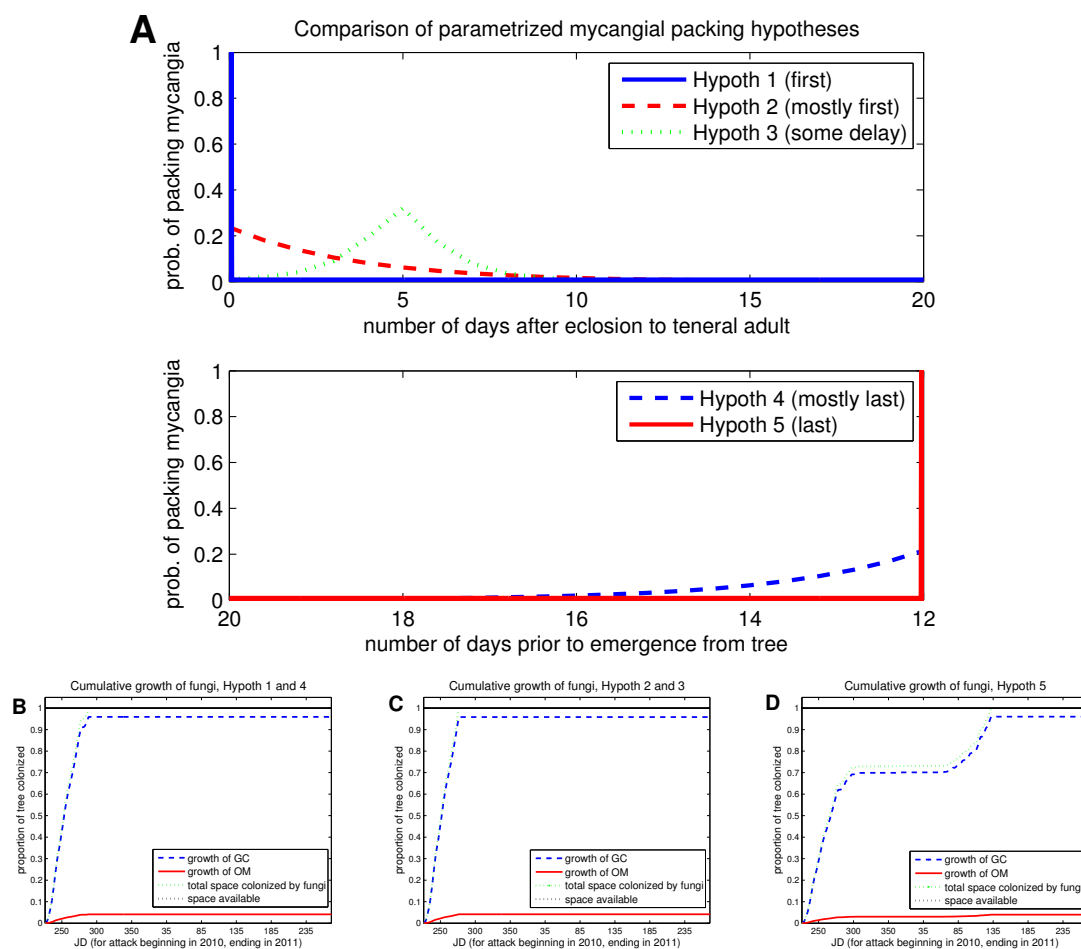
Fig. 3.6: This figure demonstrates how the various mycangial packing strategies and corresponding fungal growth profiles combine to produce various predictions. Plot A is a graphical depiction of the five models while Plots B-D show the corresponding fungal growth profiles. Due to the similarity of beta parameters, Plot B represents the growth of fungi using model 1 and 4 ("first fungus contacted" and "mostly last fungus contacted"), Plot C represents the growth of the fungi using models 2 and 3 ("mostly first fungus contacted" and "some delay in mycangial packing") and Plot D represents the growth of the fungi with model 5 ("last fungus contacted").

Therefore, the best choice is model 4 which assumes that adult MPB acquire mostly the last fungus it encounters, although with an exponential decay in acquisition.

3.4.2. Additional thoughts

It is unclear why the number of MPB emerging from study trees and carrying *O. montium* was so low, especially given that more attacking beetles in both years were carrying *O. montium*. A possible explanation includes factors related to the location of the study area. The study trees were located in a cool drainage, and therefore potentially favored growth of the cool-loving *G. clavigera* once beetles were in the tree. MPB-attacked trees on a nearby south-facing slope may have provided many of the beetles that attacked trees used in our study and may have provided a more conducive growing environment for the warm-loving *O. montium*. Cooler temperatures in the study trees, however, favored growth of *G. clavigera*, causing it to dominate the emergence data.

Differences in the β estimates between the fungal species could also be attributed to the lack of beetles observed carrying *O. montium* as they emerged from trees. Since the growth rate scaling parameters were estimated by determining parameter values which best fit the model to the data, low numbers of beetles emerging with *O. montium* necessarily led to low estimates for the *O. montium* growth rate scaling parameter, β_{OM}.

In Chapter 2, we hypothesized that variability in temperature could allow both *G. clavigera* and *O. montium* to remain present in the MPB-fungus mutualism while also exploring the effect of various lesion spacings (i.e., densities of attacking MPB). We found that both fungi could remain if MPB periodically transitioned between warm and cold environments. Growth rates of the two fungi, scaled using above β estimates (Table 3.3), provide an additional explanation. Although lab data suggests that *O. montium* can grow faster than *G. clavigera* at temperatures above 15°C, when growth is scaled by β, *G. clavigera* grows significantly faster until 30°C (Figure 3.7). The faster growth of *G. clavigera*, even at warm temperatures, would allow *G. clavigera* to persist in the mutualism under a wide range of conditions. It is unclear if these same differences in growth scaled to a tree would persist at a different field location.
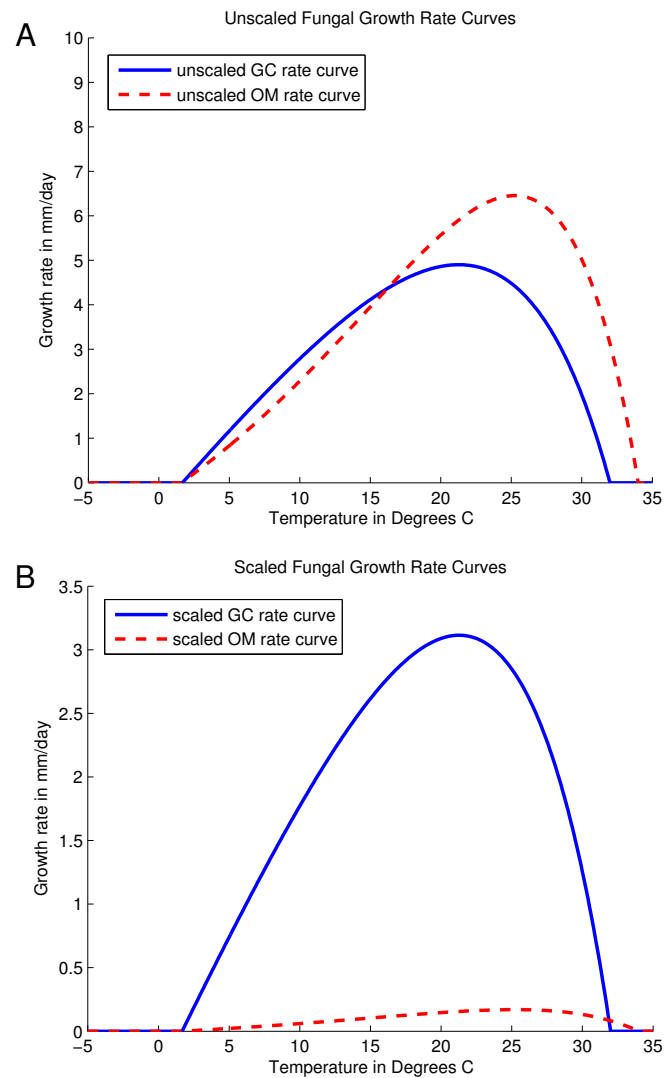
Fig. 3.7: Unscaled (i.e., rates observed in culture; Plot A) and scaled (Plot B) rates of growth for the two fungi using estimates from model 5 (based on validation data) where $r_{GC}(T) = \beta_{GC} \cdot r_{GC,culture}(T) = 0.6355 \cdot r_{GC,culture}(T)$, and $r_{OM}(T) = \beta_{OM} \cdot r_{OM,culture}(T) = 0.0263 \cdot r_{OM,culture}(T)$.

Unscaled (Plot A) and scaled fungal growth rates (Plot B) using model 5 estimates ($\beta_{GC} = 0.6355$ and $\beta_{OM} = 0.0263$) appear in Figure 3.7. Plot B would look similar for all of the model estimates because of the ratio between the growth rate scaling parameters was approximately 25:1 for all models. These plots show how *G. clavigera* persists in the mutualism despite warming conditions; its advantage under the bark allows it to grow faster than *O. montium* until the temperature reaches approximately 32°C, when it becomes too warm for *G. clavigera* to grow. This plot underscores the need to have accurate parameter estimates, specifically those that define the coldest and warmest temperatures where the two fungi can grow (T_0 and T_m from Eqn 3.1), as these most prominently distinguish the two fungi when their growth is scaled.

3.5. Conclusions

We have tested several hypotheses regarding the timing of mycangial packing of fungi during the MPB teneral adult feeding window and determined how growth rates under bark compare with growth rates measured in culture in the lab. Each hypothesis was tested by developing a mathematical representation and parameterizing the corresponding model using field observations of fungal species being carried by MPB attacking and emerging from trees. Model predictions were evaluated using the field data used in parameterization, in addition to an independent dataset of field observations. We found that while all models adequately predicted the proportion of fungi being carried from a tree when evaluated using the same data used for parameterization, the two mycangial packing hypotheses which corresponded to later mycangial packing, model 4 (mostly last fungi contacted) and model 5 (last fungi contacted) were most plausible. Our analyses therefore suggest that MPB may be more likely to pack their mycangia near the end of their teneral adult feeding window. In addition, estimated growth rate scaling parameters for the models suggest *G. clavigera* is as much as twenty-five times faster growing than *O. montium*, although the strength of this conclusion is in doubt due to anomalously low production of *O. montium* in observed trees. To the extent that this is true, however, it provides an explanation for how *G. clavigera* has maintained prevalence in the face of warming temperatures.

We derived a method, based on observed data, for combining models to describe two overlapping phenologies and incorporating a nontrivial interaction between them. This required connecting temporal timing predictions for MPB and predictions of length colonized by fungi using a colonization index C which allowed us to convert the length colonized by each fungus to a probability of the tree being colonized by one fungus or the other on a given day. In the specific case of MPB this allowed us to deduce cryptic growth rates of fungi under the bark and to determine that the fungi last fed upon are most likely to be dispersed (and therefore have the highest fitness). In general, however, this same approach could be used for systems with temperature dependent transmission of diseases and parasites, fertilization of plants by specialist pollinators, and efficacy of biocontrol agents against pests, to name a few. In all these systems, overlapping phenologies and unknown probabilities of interaction during a thermally controlled window of opportunity control eventual outcomes.

CHAPTER 4

ESTIMATING THE DEVELOPMENTAL THRESHOLDS OF POIKILOTHERMS

USING PRIOR KNOWLEDGE

4.1. Introduction

Over the past century, considerable attention has been focused on developing phenological models which tie the rate of development of an organism to environmental conditions such as temperature (Régnière et al., 2012; Krenek et al., 2011). In particular, modeling efforts have primarily focused on poikilotherms because of the higher correlation between life events and temperature in plants and cold-blooded animals such as insects (Régnière et al., 2012). A common approach when developing phenological models is to use laboratory data and field observations to relate temperature to the development rate of a species. Early models were linear due to ease of use, however, they lacked accuracy near thermal extremes which limited their utility (Campbell et al., 1974). To combat this, dozens of nonlinear models have been proposed to model development (or thermal performance) as a function of temperature in algae, fungi, arthropods, reptiles and protozoa (e.g., Logan et al., 1976; Logan, 1988; Sharpe and DeMichele, 1977; Schoolfield et al., 1981; Briere et al., 1999; Dauta et al., 1990; Ratkowsky et al., 1983; Smits et al., 2003; Stevenson et al., 1985; Krenek et al., 2011). These models are generally considered an improvement over linear models because they can be used to more accurately model the development of an organism across a realistic range of temperatures.

A common feature of many nonlinear development models is the inclusion of one or more biologically meaningful (ecophysiological) parameters to describe a species' development. These often include the lower and upper temperature threshold, T_0 and T_m, or the optimal temperature, T_{opt}. Though the exact definition of these terms vary, in this paper we will refer to the lower and upper temperature thresholds, T_0 and T_m, as the temperatures below and above which, respectively, development will stop. Optimal temperature, T_{opt}, will be used to describe the temperature at which peak development or the maximum growth rate occurs. These parameters are important for a number of reasons (for example, when

comparing performance between species or when investigating the effect of various climate change scenarios) and can have a strong effect on the shape of nonlinear development models or thermal performance curves.

While the specific shape of developmental curves may vary, a common theme in nonlinear development models is that development rates are zero for temperatures below the species- (or individual-) specific lower threshold, T_0, increase gradually with temperature to some peak occurring at T_{opt}, then development rates drop off sharply toward zero as the temperature approaches the upper development threshold, T_m (Krenek et al., 2011). These temperature thresholds are important and biologically meaningful, however, a practical issue with their use is that they are difficult to directly measure or observe. In the case of poikilotherms, development may be so slow at thermal thresholds as to appear nonexistent, possibly with no change occurring during the window of an experiment. In other organisms like bacteria and fungi, one may not be able to distinguish between no growth and very slow growth and high temperature studies are often plagued with contamination issues. Thus, these parameter values must be obtained with other non-biological parameter values using techniques like Maximum Likelihood Estimation (MLE). Side effects of common parameter estimation techniques are that the technique can become trapped in local minima (versus the global minimum), lessening the accuracy of parameter estimates, and there is often no formal method for incorporating knowledge of temperature thresholds obtained from failed laboratory experiments or other fieldwork and previous studies. Difficulty in estimating these thresholds is often further exaggerated by the scarcity of data near the lower temperature threshold and the rapid decrease in growth near the upper temperature threshold. Thus, there is a clear need for better methods for estimating temperature thresholds.

Fungi are among the most diverse and biologically important poikilothermic organisms on Earth. Despite their ubiquity and importance, and extreme environmental sensitivity, few models exist that can be used to accurately estimate their responses to temperature. Improved temperature threshold estimates for fungi are of particular interest at this time due to the need to better understand the effects global warming will have on biodiversity

and ecosystem function (Daufresne et al., 2009; Hill et al., 1999; Richardson and Schoeman, 2004; Ruess et al., 1999; Weitere et al., 2009).

Here we use mutualistic fungi associated with bark beetles to test whether the fit and ease of parameterization of growth rate curves can be improved. In particular, we focus on gaining accurate estimates of the lowest and warmest temperature where each fungus can grow. These fungi are critically important to their insect hosts; providing nutrients without which the hosts cannot survive. Thus, it is important to know their specific temperature thresholds in order to understand how they interact with their host beetles under variable environmental conditions. These beetle-fungi systems exhibit the following characteristics: 1) Most bark beetles involved in mutualisms with fungi carry two specific fungi. 2) These fungi are carried to pine trees by the beetles in summer and spend the following fall and winter colonizing their new host tree. This means that much of their growth could occur at temperatures near their respective lower developmental thresholds. 3) The fungi exhibit differential growth rates and thresholds in response to temperature which affects their relative prevalence with the host over time. 4) The fungi exert differential fitness effects on the host requiring an understanding of their individual dynamics to predict host dynamics. Improved estimates of developmental thresholds could improve the fit of growth rate curves that would lead, not only to more accurate models, but also to improved insight into the behavior and dynamics of each fungal species within a tree. Mathematically-derived temperature thresholds may also guide the design of experiments that would lead to the best improvements in model fit. This knowledge could then be applied to poikilothermic systems in general.

In this paper, we obtain parameter estimates (including estimates of T_0 and T_m) for four species of bark beetle associated fungi using a Bayesian-based algorithm called Metropolis-Hastings (MH). This algorithm is a Markov Chain Monte Carlo method (MCMC) which samples from a distribution of interest – in our case, a distribution of parameters for the observed data. This technique offers a number of benefits including the ability to explore the entire parameter space (rather than being trapped in local minima), the ability to tune

the algorithm for use with a particular dataset or function, and the ability to incorporate prior knowledge about the parameter values or valid parameter ranges. For additional comparison, we also use a technique similar to MLE in which the function to be optimized includes the likelihood as well as prior information. Parameter estimates obtained from these techniques will be compared against parameters obtained using MLE (implemented via a local, built-in optimization method) to determine whether improvements have been made in the quality of fit of the model or ease of obtaining parameters. The two primary goals of this work are to determine accurate temperature thresholds for the four fungal species as well as to determine whether the use of Bayesian techniques can lead to an improvement in the parameterization of nonlinear curves.

4.2. Methods

4.2.1. Fungal growth data

Radial growth observations from lab experiments (Moore, 2013; Dysthe et al., 2014) for four species of bark beetle associated fungi: *Grosmannia clavigera* and *Ophiostoma montium*, symbionts of the mountain pine beetle (MPB, *Dendroctonus ponderosae* Hopkins, Coleoptera: Curculionidae Scolytinae), and *Ceratocystiopsis brevicomi* and *Entomocorticum sp B.*, symbionts of the western pine beetle (WPB, *Dendroctonus brevicomis*), were used to develop our models. These two beetle-fungus symbioses are interesting because they involve three-way interactions whose outcomes are driven by temperature. In Chapter 2 we created a model for the growth of fungal symbionts in a tree and connected it with a model for beetle development and found that the overall future of the mutualism is highly dependent on temperature and that differences in the growth profiles of the fungi within the tree have the capability to stabilize or destabilize the mutualism, particularly in an era of climate change. As such, a more accurate understanding of the fungi's respective thermal performance characteristics would go a long way toward better understanding the dynamics of the entire mutualism.

MPB associated fungi

Grosmannia clavigera and *O. montium* are filamentous fungi that are only found in association with MPB (Adams et al., 2008). Along with MPB, these species inhabit pine forests from northern Mexico, through 12 U.S. states, and 3 Canadian provinces (Carroll et al., 2003). The fungi benefit the beetles by providing nutrients (Six and Paine, 1998; Bleiker and Six, 2007). In turn, the fungi benefit by obtaining transportation from the beetles from tree to tree. When new MPB adults leave a tree, they carry spores of the fungi in specialized structures called mycangia and then deposit the spores in a new tree as they construct egg galleries (Six and Paine, 1998). After the spores are deposited, the fungi begin to grow within the phloem layer and sapwood of the tree by forming dense mycelium networks (Six and Klepzig, 2004). From lab experiments, it is known that the radial rate of growth of both fungi is strongly dependent on temperature and that the fungi differ in terms of their temperature preferences and tolerances. Overall, it is thought that *G. clavigera* is the superior mutualist due to being slightly more virulent and a better first invader of a tree. *G. clavigera* also seems to grow better at cooler temperatures relative to *O. montium.*

WPB associated fungi

Ceratocystiopsis brevicomi and *E.* sp.B., associates of the WPB, are less well-studied than the MPB fungi. It is thought that these fungi are also critical for beetle nutrition because WPB feed in the outer bark, a tree tissue less nutritious than the phloem layer where MPB feed. Like the fungi associated with MPB, one fungus is thought to be a better partner than the other. While fitness effects of these fungi on the host beetle have not been studied, the symbiosis very likely functions like the nutritional mutualism between the southern pine beetle, *Dentroctonus frontalis* and its *Entomocorticum* and *Ceratocystiopisis* associates. The temperature tolerances of the WPB fungi also differ, potentially affecting the prevalence and effects of these fungi on the beetle.

4.2.2. Temperature-dependent growth experiments

MPB-associated fungi

Fungi were isolated from the mycangia of MPB emerging from lodgepole pine trees at three locations: Stump Hollow (Logan Canyon, UT), Lubrecht Experimental Forest (near Missoula, MT), and Vipond Park (in southwest MT) in the summer of 2010 and 2011. These fungi were identified and replicates of 51 isolates of *G. clavigera* (21, 18, and 12, respectively, from Stump Hollow, Lubrecht and Vipond Park) and 42 isolates of *O. montium* (23, 12, and 7 from the same sites, respectively) were grown on 2% malt extract agar in Petri dishes held at constant temperatures of 5, 10, 15, 22*, 25, and 30°C (22* indicates that replicates were grown at room temperature which was approximately 22°C). The plates were monitored daily and the amount of area colonized by the fungi in each culture was traced and measured. Area observations were converted to measurements of radius colonized and a line fitted to obtain a single radial growth rate for each culture (see Chapter 2) for further details). These data are presented in Figures 4.1 (all sites combined) and 4.2 (by site).

WPB-associated fungi

Thirteen isolates of *C. brevicomi* and 14 isolates of *E.* sp.B. were isolated from beetles collected from four areas that span the latitudinal range of the WPB (Southern California to Southern British Colombia) and grown on malt extract agar in Petri dishes held at 10, 15, 22, 28, and 34°C. As with the MPB-associated fungi, growth of the WPB-associated fungi were measured periodically, although in the case of these fungi, which are slow growing, measurements were made several days apart rather than daily. These area measurements were then converted to measurements of radius colonized and a line fitted to obtain a radial growth rate for the culture of each isolate (Figure 4.3).

MPB-associated fungi (past studies)

Several studies have assessed the growth of the fungal associates of MPB at different temperatures (Rice et al., 2008; Plattner et al., 2008). From these experiments we know
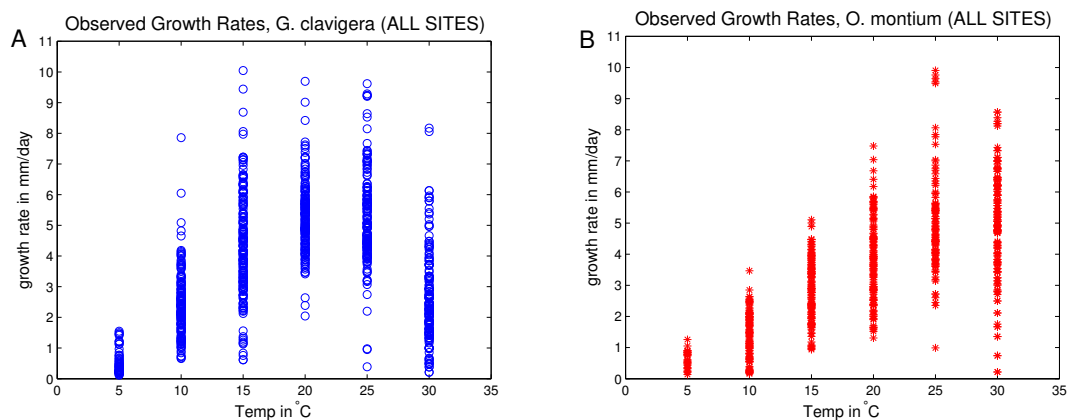
Fig. 4.1: Growth rates of MPB-associated fungi (mm/day) from Stump Hollow, Lubrecht and Vipond Park combined plotted against the temperature (°C) at which the fungi were grown (*G. clavigera*, Plot A; *O. montium*, Plot B)
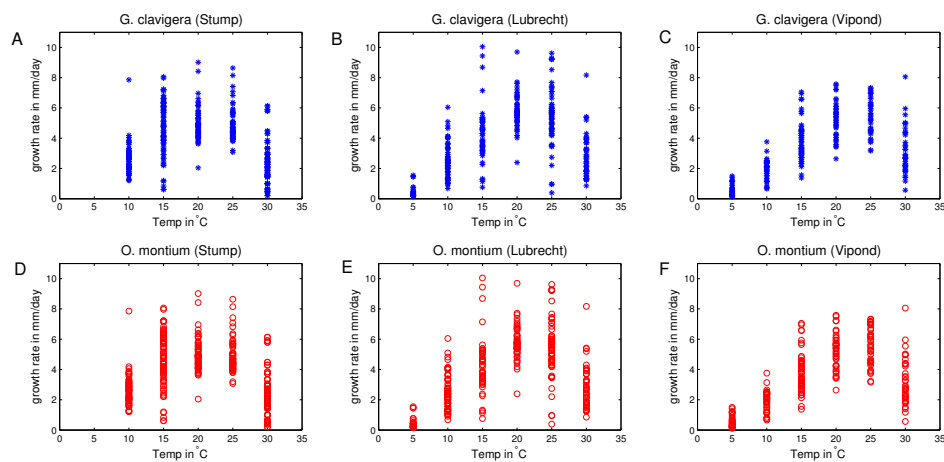
Fig. 4.2: Growth rate of MPB-associated fungi (mm/day) plotted against the temperature (°C) at which the fungi were grown. Growth rates for *G. clavigera* (Plots A-C) and *O. montium* (Plots D-F) are presented by site (Stump Hollow, Plots A,D; Lubrecht, Plots B,E; Vipond Park, Plots C,F).
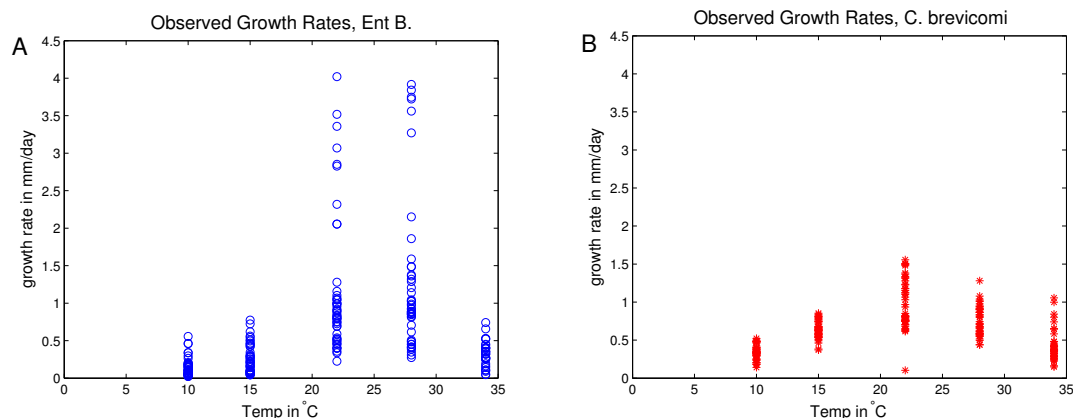
Fig. 4.3: Growth rates of WPB-associated fungi growth rate data in mm/day (*E.* sp.B., Plot A; *C. brevicomi*, Plot B) plotted against the temperature (in °C). A key difference to note is that the symbionts of the WPB are much slower growing than the symbionts of MPB (*G. clavigera* and *O. montium*) and that the growth of *E.* sp.B. exhibits much more variability at the higher temperatures.

that *G. clavigera* generally grows better at cool temperatures while *O. montium* continues growing at higher temperatures (Six and Paine, 1998; Solheim and Krokene, 1998). From studies conducted by Plattner et al. (2008), we know that *G. clavigera* isolates incubated at 4, 30, and 37°C were either unable to grow or grew poorly. Optimal growth for these isolates was observed to occur between temperatures of 20 and 25°C. Rice et al. (2008) also conducted growth experiments at temperatures ranging from 5 to 37°C as well as an experiment testing for survival at -20°C. They found that growth of *G. clavigera* and *O. montium* was inhibited at 5°C; that *G. clavigera* exhibited optimal growth between 20 and 25°C (with the exception of one isolate from Alberta that exhibited optimal growth at 15°C); and that *O. montium* exhibited optimal growth at 25°C. The optimal growth rate of the various isolates was found to occur between 8 and 17mm/day. In terms of upper temperature tolerances, growth of *G. clavigera* was found to drop off sharply at 30°C to less than 10% of its growth rate at 20°C while *O. montium* continued to grow well (at almost 90% of its growth rate at 20°C). As the temperature increased to 35 and 37°C, none of the isolates established, grew, or survived. With regards to cold-weather survival, they found that all *G. clavigera* isolates survived 3 months at -20°C whereas none of the *O. montium* isolates survived a week at this temperature.

From the results of these studies, it appears that the lower temperature threshold for both *G. clavigera* and *O. montium* lies somewhere below 10°C but above 4°C. The optimal growing temperature for *G. clavigera* likely lies between 20 and 25°C and the optimal temperature for *O. montium* likely lies around 25°C. Regarding upper temperature thresholds, the steep dropoff in growth rate for *G. clavigera* at 30°C with no growth at warmer temperatures (35, 37°C) indicates a threshold just above 30°C. The strong growth of *O. montium* at 30°C, but no growth at 35 and 37°C, also indicates its upper threshold lies somewhere just above above 30°C, though at a higher temperature than for *G. clavigera*. This information is used to quantify prior distributions for *G. clavigera* and *O. montium* in Section 4.3.2.

WPB-associated fungi (past studies)

The WPB-fungus mutualism has been less-well studied than the relationship between fungal symbionts of MPB and southern pine beetle. There is limited information available regarding the growth of WPB-associated fungi and their temperature tolerances. Two relevant studies on this system include a recent study by Davis et al. (2010) and an older study by Hsiau and Harrington (1997). Davis et al. (2010) recently isolated *E.* sp.B and *C. brevicomi* isolates from WPB in Coconino National Forest (AZ) and Plumas National Forest (CA). In this study, two replicates of each fungal isolate were incubated in a dark environment at temperatures of 5, 10, 15, 20, 25 and 28°C with fungal growth being traced every 48 hours for 15 days. Fungal growth rates were found to increase as temperature increased and then decline once temperature surpassed 28°C. The mean growth of the fungi at 5°C was found to be quite slow (0.074 ± 0.027mm/day for *C. brevicomi* and 0.057 ± 0.036mm/day for *E.* sp.B) and the optimal temperature (of the temperatures studied) for both fungi occurred at 25°C (Figure 4.4). Hsiau and Harrington (1997) also conducted a study to determine the optimal growth temperature of *C. brevicomi*. This study measured daily growth of the fungi incubated at temperatures ranging from 10 to 35°C at 5°C intervals. *C. brevicomi* was found to exhibit optimal growth between 25 and 30°C (with an average daily growth rate of 3.84 ± 0.25mm/day at 25°C and 3.84 ± 0.31mm/day
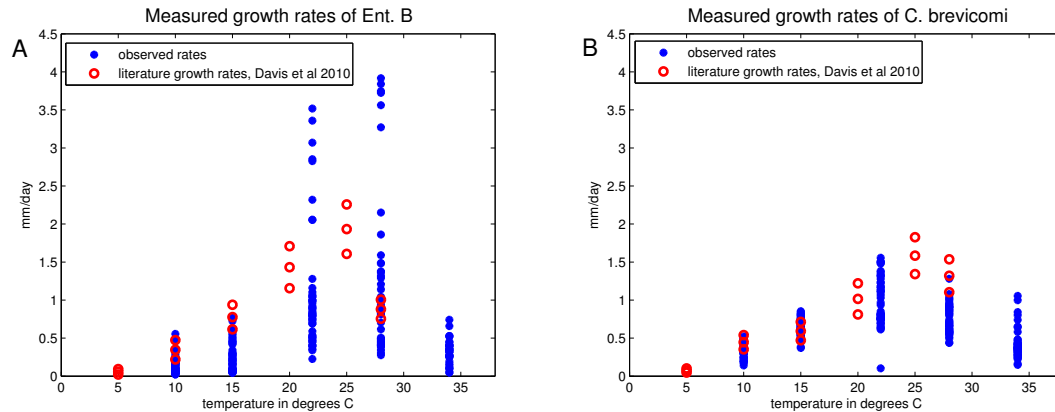
Fig. 4.4: Compilation of published (red o, Davis et al. 2010) and new (Dysthe, Bracewell, and Six, unpublished data) growth rate data (blue *) for WPB-associated fungi at various temperatures. This past data can be used to build prior distributions (quantifying our prior knowledge) for the lower and upper temperature thresholds, the optimal temperature for growth and the maximum growth rate.

at $30°C$).

These studies (and the knowledge that nonzero growth rates were observed at $34°C$ for our parameterization data) indicate that both $E.$ sp.B. and $C. brevicomi$ have a lower temperature threshold below $5°C$ and an upper temperature threshold above $34°C$. The optimal temperature occurs somewhere between 20 and $28°C$ for $E.$ sp.B. and between 20 and $30°C$ for $C. brevicomi$ (this range is broader because of the conflict between results in the studies listed above). This information is quantified in Section 4.3.2 to form prior distributions for parameters T_0, T_m and T_{opt} (for use with the Metropolis-Hastings algorithm).

4.3. Thermal performance curves

After reviewing dozens of nonlinear growth rate or thermal performance curves (Régnière et al., 2012; Krenek et al., 2011; Shi and Ge, 2010; Hansen et al., 2011), four curves were selected (shown in Table 4.1) based on criteria of shape, successful implementation in modeling development in other species, and the inclusion of both the lower and upper temperature development thresholds as parameters (which unfortunately eliminated many popular and successful curves from our study). These rate curves vary in terms of the number of parameters (ranging from 4-6) and the mathematical mechanisms that give them their shape.

The fact that the growth rate observations were skewed with higher growth rates observed closer to the (expected) upper temperature threshold means that the data requires at least four parameters for adequate representation (two parameters to represent the lower and upper temperature thresholds and two to help describe the location of the optimal growth rate).

The inclusion of additional parameters, sometimes called second order parameters, can be helpful to control other nuances in the curve such as concavity or the rate of increase at low temperatures. These additional parameters can come at a price, particularly when used to parameterize data with large or irregular variability. The Hansen and Régnière curves (R3 and R4 from Table 4.1) are excellent examples of this. The inclusion of parameters such as ω and Δ_m describe nuances in the appearance of the curve (such as the rate of increase of growth rate at low temperature and the width of the boundary layer between the optimal temperature and upper temperature threshold) that can improve the fit to data. Problems arise, however, when a parameter estimation technique begins exploring regions of parameter space that are unreasonable, such as allowing $\Delta_m \to 0$. The other parameters in the curve can help to mitigate the damage in fit; however, the resulting curve will likely exhibit characteristics that are unrealistic (see Figures 4.5 and 4.6, Plots C and D). Knowing that unrealistic parameter estimations are a risk, we chose to include the Hansen curve (R3) because it was used to parameterize *G. clavigera* and *O. montium* growth rates in Chapters 2 and 3 and we are interested in trying to improve the parameterization to determine if it could improve the fit of models for the MPB-fungi symbiosis to data. The Régnière curve (R4) was included primarily because it has the potential to fit data very well, however, it is often difficult to parameterize and we would like to determine whether the inclusion of prior information regarding parameter values can improve this process.

4.3.1. Parameterization techniques

Parameter estimation for the growth rate curves was performed using three different methods, 1) basic Maximum Likelihood Estimation (MLE) implemented via a built-in optimizer (the Nelder-Mead simplex algorithm, 'fminsearch' in MATLAB), 2) the Metropolis-

Table 4.1
Temperature-dependent development rate curves used to parameterize the growth of MPB-
and WPB-associated fungi. Each of these curves is only valid for predicting development
rate for temperatures T between the thermal development thresholds T_0 and T_m (measured
in degrees C).

Formulation	Details
(R1) $r(T) = BT(T - T_0)(T_m - T)^\omega$	Briere-2 4 parameters (B, T_0, T_m, ω) Briere et al. (1999)
(R2) $r(T) = \begin{cases} \frac{B}{T_{opt}-T_0}(T - T_{opt}) + r_{opt}, & T < B \\ \frac{B}{T_{opt}-T_m}(T - T_{opt}) + r_{opt}, & T > B \end{cases}$	Dogleg 4 parameters (B, T_0, T_m, T_{opt})
(R3) $r(T) = B\left(\left[e^{\omega(T-T_0)} - 1\right] - \left[e^{\omega(T_m-T_0)} - 1\right] e^{-(T_m-T)/\Delta_m}\right)$	Hansen 5 parameters $(B, T_0, T_m, \omega, \Delta_m)$ Hansen et al. (2011)
(R4) $r(T) = B\left[e^{\omega(T-T_0)} - \left(\frac{T_m - T}{T_m - T_0}\right) e^{-\omega(T-T_0)/\Delta_0}\right]$ $-B\left[\left(\frac{T-T_0}{T_m-T_0}\right) e^{\omega(T_m-T_0)-(T_m-T)/\Delta_m}\right]$	Régnière et al. (2012) 6 parameters $(B, T_0, T_m, \omega, \Delta_0, \Delta_m)$ Régnière et al. (2012)

Hastings algorithm (MH), and 3) "Bayesian-type" MLE (B-MLE) using a built-in optimizer. Method 1 has the simplest implementation of the three techniques and is a common approach for parameter estimation. Method 2 requires more extensive coding and specification of parameters and functions before it can be used, however it is based on a relatively simple algorithm. As a Bayesian technique it allows for formal incorporation of prior knowledge about reasonable or most likely parameter values. A major drawback is that it requires extensive amounts of computational time and user tuning. Method 3 is a hybrid of the first two, using a built-in optimizer to reduce coding and tuning requirements while still allowing formal incorporation of prior knowledge. These methods are described in detail below.

MLE via built-in optimizer

MLE takes its name because the goal is to maximize the likelihood, $\mathcal{L}(\theta|r_{obs})$, of the parameters θ given the data, r_{obs}. In practice, this is completed by minimizing the negative log likelihood of the data, $nLL(\theta|r_{obs}) = -\log\left(\mathcal{L}(\theta|r_{obs})\right)$. For our data, we assumed that the observed growth rates collected in Sections 4.2.2 and 4.2.2 had normal (additive) error and could be described by the equation

$$r_{obs} = r_{pred} + \varepsilon, \qquad \text{where} \qquad \varepsilon \sim N(0, \sigma^2).$$

This yielded a negative log likelihood of

$$nLL(\theta|r_{obs}) = \frac{n}{2}\log(2\pi\sigma^2) + \sum_{i=1}^{n} \frac{(r_{obs,i} - r_{pred})^2}{2\sigma^2},$$

where i is the index of the datapoint and n is the number of datapoints. Using 'fminsearch', MLE was implemented by providing the function to minimize, $nLL(\theta|r_{obs})$, and an initial guess θ (a vector of parameter values for the rate function and a variance parameter σ^2 corresponding to the error assumption). The optimizer then returned a vector-valued parameter estimate θ^*, the negative log likelihood of that estimate, and an exit flag of 1 or 0 (1 indicating that the method converged and 0 indicating that it did not converge). Advantages of this method are its ease of implementation and its speed; however, it may not

find the global optima.

The Metropolis-Hastings algorithm

The second technique we used attempts to remedy the shortcomings stated above. It is a statistical technique implemented via the Metropolis-Hastings (MH) algorithm. This algorithm was developed by Metropolis, Rosenbluth, Rosenbluth, Teller and Teller in 1953 and later generalized by Hastings in 1970 (Metropolis et al., 2004). This method is not an optimization technique, rather, it allows the user to sample from some target density function f (that is known up to a constant multiple, i.e., $f(\theta) \propto P(\theta)$) by generating samples from a proposal or candidate density $q(Y|\theta)$ and accepting or rejecting the samples based on a specific criteria. Instead of arriving at a single parameter estimate, MH results in a distribution for each parameter in the model. For purposes of parameter estimation, parameters can be chosen by selecting some summary statistic from each distribution (such as the mean or mode). Another option for parameterizing an individual-based model would be to draw parameters for each individual from the resulting MH distribution which would be a natural way to incorporate variability in growth characteristics between individuals.

To implement MH, a target density $f(\theta)$ is chosen. For our purposes, $f(\theta)$ represents the posterior distribution of the parameters given the rate function and the observed data. This is proportional to the likelihood of the data, $\mathcal{L}(\theta|r_{obs})$ (the function we optimized for MLE), times the prior distribution of the parameters, $Prior(\theta)$ (where prior knowledge about the system or parameters can be incorporated). That is,

$$Posterior \propto Likelihood \times Prior, \text{ or}$$

$$p(\theta|r_{obs}) \propto \mathcal{L}(\theta|r_{obs}) \times Prior(\theta). \tag{4.1}$$

After specifying a likelihood function and a prior distribution, the user must specify an initial vector of parameter values, θ_0, to be the first sample of the Markov chain and a proposal density $q(Y|\theta_t)$ which is used to suggest a candidate vector of new parameter values, Y, for the next value in the chain. MH determines whether to accept the new candidate

based on whether it is more or less likely than the previous value in the chain, θ_t. This is done by calculating the acceptance ratio α, defined to be $\alpha = f(Y)/f(\theta_t) = P(Y)/P(\theta_t)$ (since $f(\theta) \propto p(\theta)$). The new candidate is automatically accepted if it is more likely than the previous value ($\alpha \geq 1$) and accepted with probability α if $\alpha < 1$. If the new candidate is accepted, we set $\theta_{t+1} = Y$, otherwise we reject the candidate and set $\theta_{t+1} = \theta_t$. This procedure is then repeated a large number of times to generate a Markov Chain. Once completed, the effects of the initial guess are mitigated by removing a large number of samples from the beginning of the chain (commonly called the burn-in period). The remaining chain represents a collection of samples from our target distribution: the posterior distribution of the parameters given the data. While many characteristics of the posterior distribution on each parameter could be used, we chose the sample mean to represent the final estimate for this technique.

There are two key differences between MH and MLE. First, MLE optimizes a function and results in a single parameter estimate whereas MH samples from a distribution (rather than minimizing it) and results in a chain of samples from the target distribution. Second, MH allows for the specification of prior distributions for each parameter. This is where the user can include prior knowledge about a given parameter (based on their knowledge of the system being parameterized) to help ensure the algorithm does not result in overly spurious parameter estimates and to ensure the reasonable area of parameter space is the area being explored. MH is further described in Table 4.2.

"Bayesian-type" MLE with built-in optimizer

The final parameterization technique we tested for this paper was essentially MLE with a built-in optimizer (described in Section 4.3.1), however, rather than maximizing the likelihood, we maximized the posterior likelihood (i.e., the product of the likelihood times the prior distribution as shown in Eqn 4.1). This was implemented by minimizing the quantity

$$nLL(\theta|r_{obs}) - \log\left(Prior(\theta)\right).$$

This caused the optimizer to search for parameter values which minimize the negative log

Table 4.2
Metropolis-Hastings Algorithm.

Metropolis-Hastings Algorithm
To obtain a distribution of samples from the posterior distribution $p(\theta|r)$ where θ is a vector of parameters and r represents the observed data, we make the assumption that

$$p(\theta|r) \propto \mathcal{L}(\theta|r)Prior(\theta)$$

where $\mathcal{L}(\theta|r)$ is the likelihood of the data given the parameters and $Prior(\theta)$ is the prior distribution of the parameters. I.e.,

Posterior probability $\propto$ Likelihood $\times$ Prior probability.

Thus, we 'know' our posterior distribution (the distribution we wish to sample from) to within a constant and can use Metropolis Hastings.

To implement the technique, the user must specify:
- The form of the error in the data - which determines the likelihood function $\mathcal{L}(\theta|r)$
    (see Section 4.3.1)
- The prior distribution of the parameters (see Section 4.3.2)
    Can be vague or uninformed, or, in the case of biologically meaningful parameters,
    a more informative prior may be used
- Initial parameter guess θ_0
- A proposal density $q(Y|\theta_t)$ with which to generate new samples (parameter guesses)
    (the average stepsize between parameter estimates can be tuned to raise or lower
    the accept-reject ratio α)
- Length of the chain
- Length of the burn-in period for the chain

The algorithm proceeds as follows:
1. Provide initial parameter guess θ_0
2. Generate $Y \sim q(Y|\theta_t)$
3. Calculate acceptance probability $\alpha = \frac{p(Y)}{p(\theta_t)} \frac{q(\theta_t|Y)}{q(Y|\theta_t)}$
4. Let
$$\theta_{t+1} = \begin{cases} Y, & \text{with probability } \alpha \\ \theta_t, & \text{with probability } 1-\alpha) \end{cases}$$

(the new sample is always accepted if $\alpha \geq 1$ and it may be accepted if $\alpha < 1$.
5. Repeat steps 2-4.

likelihood of (as in MLE) that were also commensurate with prior knowledge of the system. Among the advantages of this method are that it is fast and easy to implement (like MLE), does not require a high number of user inputs (just the prior distribution rather than the prior distribution, proposal distribution, length of chain and burn-in period), and can utilize prior knowledge to so that the method will converge to more realistic regions of parameter space (like MH). This is very important when estimating the lower and upper temperature thresholds, as a significant amount of prior knowledge exists regarding their location. As with MLE implemented via a local optimizer, however, the method may still fail to converge or converge to a local optimum depending on the initial choice of parameters.

4.3.2. Tuning Metropolis Hastings

As outlined in the MH algorithm (Table 4.2), use of MH requires specification of initial parameters, proposal density, likelihood function, prior distribution of parameters, length of chain and length of burn-in period. For consistency, initial parameters and the likelihood function were chosen to be the same for all three parameterization techniques. The other components were chosen to best ensure that the acceptance probability of new samples was in the vicinity of 25% (which was most affected by the stepsize between samples – governed by the proposal density – and the choice of prior distributions) and to allow for convergence of the chain. The proposal density, $q(Y|\theta_t)$, was selected to be a normal random walk in which the stepsize for the various parameters was commensurate to the magnitude of those values or some proxy for the possible range of values the parameters could take on (i.e., the lower and upper temperature thresholds were allowed to take a much larger step between samples than the value of an empirical parameter whose magnitude ranged from 10^{-3} to 10^{-4}). That is, each component of the new sample Y was selected by taking (normal) random steps from the previous sample, i.e.,

$$Y_i = \theta_{t,i} + \varepsilon_i W_i \cdot s \quad \text{where} \quad \varepsilon_i \sim N(0,1),$$

where W was a vector of positive numbers loosely representing the range in values each parameter could take on and $s \in (0,1)$ was a stepsize which could be adjusted to obtain

the desired acceptance ratio (high stepsizes led to large steps between parameters and, often, lower acceptance probabilities while smaller stepsizes often led to higher acceptance probabilities). The parameter s tended to need adjusting when switching between rate functions or estimating parameters for a different fungal dataset.

Choice of prior distributions

As shown in Eqn 4.1 of Section 4.3.1, the distribution to be sampled over in Metropolis-Hastings includes the effects of a prior distribution describing each of the parameters included in the fungal growth rate curves (Table 4.4) as well as a parameter, σ, representing the error between the observations and the values predicted by the growth rate curves. Because of previous experiments, we chose somewhat informative prior distributions for the lower and upper temperature thresholds, T_0 and T_m, as well as the optimal temperature T_{opt}. For the other parameters, B, b, ω, α, and σ, since we did not have an a priori estimate of where they lie, we chose a less informative prior, mostly to ensure the parameters would only take on positive values.

The prior distribution for each model was specified by assuming that each of the model parameters was independent so that $Prior(\theta)$ could be written as the product of distributions describing the individual parameters. Normal distributions were used to describe the range of temperature parameters T_0 and T_m and a truncated normal was used for T_{opt} (to ensure $T_{opt} \in (T_0, T_m)$). Parameters for these normal distributions were chosen after reviewing recent growth studies involving the various fungi (Section 4.2.2). For the remaining empirical parameters, a Gamma(α, β) distribution with shape parameter α and an inverse scale (or rate) parameter β (with support on $x \in (0, \infty)$) was chosen for its broad and fairly uninformative shape. This distribution constrained the parameters to take on only positive values while providing little information about the actual value so that the data could more strongly influence the parameter estimation.

Further tuning of MH

Additional tuning of MH was required to select an appropriate length of chain (how many samples to obtain) and an appropriate burn-in period (number of initial samples

Table 4.3
Information from previous studies (Section 4.2.2) used to set prior distributions for temperature parameters. These prior distributions were used with the Metropolis-Hastings algorithm and with B-MLE.

Summary of prior information regarding temperature parameters				
	E. sp.B.	*C. brevicomi*	*G. clavigera*	*O. montium*
T_0	Lies below 5°C	Lies below 5°C	Lies below 10°C (unable to grow/ grew poorly at 4°C; Plattner et al., 2008; inhibited at 5°C; Rice et al., 2008)	Lies below 10°C (inhibited at 5°C; Rice et al., 2008)
T_{opt}	20-28°C	20-30°C	20-25°C	Around 25°C
T_m	>34°C	30-34°C	>30°C and <35-37°C	>30°C (though likely higher than *G. clavigera* threshold) and <35-37°C

Table 4.4
Prior distributions and parameters used for MH and B-MLE. B^* indicates the prior for B used with the Dogleg curve (R2) which, for this curve, is the optimal (fastest) growth rate for the fungi. For the remaining curves, the prior for B was chosen to be Gamma(1, .5).

Summary of Prior Distributions (and parameters) used with MH				
	T_0	T_{opt}	T_m	Other
E. sp.B.	$N(4, 2^2)$	$N(24, 3^2)$	$N(36, 2^2)$	Gamma(1,.5) $B^* \sim$ Gamma(2,.5) $\kappa \sim$ Gamma(100,.5)
C. brevicomi	$N(4, 2^2)$	$N(24, 3^2)$	$N(36, 2^2)$	Gamma(1,.5) $B^* \sim$ Gamma(1.5,.5) $\kappa \sim$ Gamma(100,.5)
G. clavigera	$N(5, 5^2)$	$N(22.5, 2^2)$	$N(32, 2^2)$	Gamma(1,.5) $B^* \sim$ Gamma(6,.5) $\kappa \sim$ Gamma(100,.5)
O. montium	$N(5, 4^2)$	$N(25, 2^2)$	$N(32, 2^2)$	Gamma(1,.5) $B^* \sim$ Gamma(6,.5) $\kappa \sim$ Gamma(100,.5)

to discard). Since there is no formula to determine the proper length of chain and burn-in period, we generally erred on the conservative side by selecting relatively long chains (100,000–200,000) and discarding high numbers of samples (40,000–100,000) to ensure convergence. Visual indicators of convergence and a proper acceptance ratio were checked by plotting chains of samples for each of the various parameters. From these plots we were able to verify that the sample chain was exploring the parameter space (and not holding constant at a single value or a small range of values) and to ensure that it was not exploring samples in such a way that indicated it had not reached a good region of parameter space (i.e., samples trending down or up which might indicate the method was still overcoming the effect of a poor initial guess).

4.3.3. Comparison of methods

As stated earlier, the two primary goals of this work were to determine accurate temperature thresholds for the four fungal species as well as to determine whether the use of Bayesian techniques could lead to an improvement in the parameterization of nonlinear curves. To evaluate this second question, we conducted a number of trials. First, all four growth rate curves were roughly parameterized to evaluate their ability to fit the fungus growth data, i.e., a visual fit of the data to the curves was obtained by adjusting parameters by hand to provide an initial guess. This initial guess was sent to the parameter estimation technique (and perturbed as necessary to ensure convergence for MLE and B-MLE), however, we did not attempt to verify whether the global minima had been found. After analyzing the fit (using visual inspection and the Bayesian Information Criterion, BIC, described below) of the various parameterized curves, more in-depth tests were conducted by uniformly selecting initial values for temperature thresholds from a broad region (-10 to 10°C degrees for T_0 and 30 to 40°C for T_m) and perturbing the remaining parameters (from the initial guess discussed above). These perturbed initial parameters were then fed into each of the three methods as an initial guess and the methods were repeated 100 times. Convergence information, consistency of parameter estimates, visual fit and BIC are compared in Section 4.4.2. Finally, using BIC as a criterion, the best rate curve for each dataset

was chosen. This is discussed in Section 4.4.3.

4.4. Results

4.4.1. Initial results of parameterization (all functions)

Initial parameter estimates obtained for the various fungal growth rate curves revealed an interesting range of behavior (Tables 4.5–4.8, Figures 4.5 and 4.6) ranging from well-behaved parameterizations (Plot A in Figures 4.6 and 4.5) to pathological behavior caused by near-zero (Plots C and D in Figures 4.6 and 4.5) or negative parameter (Figure 4.5, Plot A) estimates and biologically unreasonable temperature thresholds (Figure 4.6, Plot D and Figure 4.5, Plots B and D). Temperature threshold estimates for each fungus varied between growth rate curves (and also between parameter estimation techniques). All three parameter estimation techniques produced (generally) reasonable parameter estimates for curves R1 and R2 (with the exception of several estimates obtained for *O. montium* using MLE; see Tables 4.5–4.8 and Figure 4.5, Plots A and B). As the number of parameters in the rate curve increased, the parameter estimation techniques had more difficulty.

To quantify the actual fit of the rate curves to the data, the Bayesian Information Criterion (BIC) was calculated for each rate function, fungus, and parameter estimation technique (Table 4.9). BIC is a criteria for goodness of fit that is similar to AIC, however, it penalizes model complexity more heavily. It estimates the probability that the posterior probability of a model is true, so a lower BIC is considered to be more likely the true model. BIC is defined as

$$BIC = -2\log(\mathcal{L}) + \log(n)k,$$

where n is the number of datapoints and k is the number of parameters in the model. From these calculations, we found that overall, The Briere-2 and Dogleg curves (R1 and R2) performed better than the Hansen and Régnière curves (R3 and R4) and that MLE occasionally performed quite well, achieving the lowest BIC for several of the functions. On the whole, however, it was a more volatile estimation method, occasionally resulting

Table 4.5
Parameter estimates for *G. clavigera* (Stump Hollow dataset) using MLE (row 1 of each cell), MH (row 2), and B-MLE (row 3). 0* indicates the parameter estimate neared machine precision, i.e., zero.

Parameter estimates for *G. clavigera*							
	T_0	T_m	B				σ^2
R1	0.71;	34.61;	0.0003;	1.42;			1.67;
Briere-2	-3.72;	32.89;	0.0008;	1.06;			1.65;
$r(T_0, T_m, B, \omega)$	-0.66	33.68	0.0005	1.25			1.66
R2	-2.74;	34.63;	5.98;	22.71;			1.75;
Dogleg	-1.96;	34.78;	6.02;	22.39;			1.78;
$r(T_0, T_m, B = r_{opt}, T_{opt})$	-1.43	34.66	6.06	22.37			1.74
R3	2.78;	30.00;	13.87;	0.016;	0*;		1.63;
Hansen	-3.70;	32.02;	6.17;	0.045;	8.80;		1.68;
$r(T_0, T_m, B, \omega, \Delta_m)$	-0.39	30.00	15.25	0.013	0*		1.21
R4	-5.95;	30.00;	4.66;	0.008;	1.31;	0.02;	3.36;
Régnière	-6.15;	28.98;	2.45;	0.026;	0.51;	0.54;	3.35;
$r(T_0, T_m, B, \omega, \Delta_0, \Delta_m)$	2.50	29.58	5.37	0*	0*	0.26	2.89

in extremely high (poor) BICs. We found that altering the MLE setup to include prior knowledge (B-MLE) did result in less volatility in BIC values and fewer instances of unrealistic parameter values. B-MLE was also able to achieve good parameter estimates for the simpler rate curves (R1 and R2) with low BIC values. As the number of variables in the rate curve increased, however, B-MLE also produced some extremely poor BIC values (i.e., for *G. clavigera* and *O. montium* with the Hansen curve, R3; see Table 4.9). MH seemed to be the most consistent method. It did not often achieve the lowest BIC for a given dataset or rate curve, however, the inclusion of prior knowledge and the ability to tune the method to ensure it adequately explored the parameter space did seem to insulate it from achieving extremely poor BICs. Another detail to note is that the MH estimates were achieved with one run of the algorithm whereas the MLE and B-MLE estimates (included in Tables 4.5–4.8) leading to these BIC estimates were sometimes the result of running the algorithm more than 10 times before achieving convergence.

Table 4.6
Parameter estimates for *O. montium* (Stump Hollow dataset) using MLE (row 1 of each cell), MH (row 2), and B-MLE (row 3). 0* indicates the parameter estimate neared machine precision, i.e., zero.

Parameter estimates for *O. montium*							
	T_0	T_m	B				σ^2
R1	15.92;	275.90;	-0.0288;	-6.66;			17.99;
Briere-2	-4.31;	34.24;	0.0025;	0.46;			1.80;
$r(T_0, T_m, B, \omega)$	-4.46	34.11	0.0025	0.46			1.79
R2	-3.50;	115.00;	5.71;	32.94;			1.86;
Dogleg	1.54;	34.10;	5.92;	29.18;			1.81;
$r(T_0, T_m, B = r_{opt}, T_{opt})$	1.64	33.39	5.95	29.30			1.76
R3	-0.09;	30.74;	19.11;	0.0092;	0.45;		1.77;
Hansen	-2.07;	32.65;	5.15;	0.0279;	1.85;		1.82;
$r(T_0, T_m, B, \omega, \Delta_m)$	2.56	30.00	2.28	0.0552	0*		1.11
R4	-2.52;	40.97;	1.48;	0.0390;	0.0032;	0.0705;	1.94;
Régnière	0.23;	30.84;	1.80;	0.0349;	0.5049;	5.89;	1.91;
$r(T_0, T_m, B, \omega, \Delta_0, \Delta_m)$	-3.86	32.21	2.01	0.0283	0.7841	0*	1.78

Table 4.7
Parameter estimates for *C. Brevicomi* using MLE (row 1 of each cell), MH (row 2), and B-MLE (row 3). 0* indicates the parameter estimate neared machine precision, i.e., zero.

Parameter estimates for *C. brevicomi*							
	T_0	T_m	B				σ^2
R1	-1.91;	29.64;	0.0007;	0.47;			0.07;
Briere-2	3.22;	38.46;	4.27E-5;	1.43;			0.04;
$r(T_0, T_m, B, \omega)$	3.38	39.27	2.97E-5	1.52			0.04
R2	3.22;	41.56;	1.04;	23.00;			0.04;
Dogleg	4.70;	41.98;	1.06;	21.21;			0.04;
$r(T_0, T_m, B = r_{opt}, T_{opt})$	3.56	40.72	1.05	22.93			0.04
R3	4.05;	30.80;	5.82;	0.0098;	3.47;		0.07;
Hansen et al. (2011)	1.05;	36.41;	3.56;	0.0209;	10.83;		0.04;
$r(T_0, T_m, B, \omega, \Delta_m)$	1.80	36.41	4.65	0.0161	10.70		0.04
R4	2.54;	28.00;	0.70;	0.0098;	2.09;	11.97;	0.08;
Régnière et al.	3.23;	30.83;	0.48;	0.0247;	0.99;	12.32;	0.09;
$r(T_0, T_m, B, \omega, \Delta_0, \Delta_m)$	3.52;	33.95;	0.92;	0*	0*	4.59	0.08

Table 4.8
Parameter estimates for *E*. sp.B. using MLE (row 1 of each cell), MH (row 2), and B-MLE (row 3). 0* indicates the parameter estimate neared machine precision, i.e., zero.

Parameter estimates for *E*. sp.B.							
	T_0	T_m	B				σ^2
R1	9.28;	34.32;	0.0008;	0.63;			0.42;
Briere-2	6.32;	34.27;	0.0008;	0.52;			0.43;
$r(T_0, T_m, B, \omega)$	5.46	34.05	0.0010	0.38			0.42
R2	12.97;	36.09;	1.61;	25.68;			0.41;
Dogleg	10.05;	37.21;	1.51;	24.26;			0.44;
$r(T_0, T_m, B = r_{opt}, T_{opt})$	8.93	36.53	1.47	25.70			0.43
R3	6.17;	34.00;	2.63;	0.02;	0*;		0.42;
Hansen	6.34;	34.52;	1.51;	0.04;	3.26;		0.44;
$r(T_0, T_m, B, \omega, \Delta_m)$	5.51	34.00	0.89	0.04	0*		0.42
R4	0.19;	13.59;	0.0032;	0.33;	2.08;	14.87;	1.06;
Régnière	3.76;	33.25;	0.2035;	0.08;	2.08;	1.17;	0.47;
$r(T_0, T_m, B, \omega, \Delta_0, \Delta_m)$	1.08	34.00	0.0045	0.21	2.76	9.91	0.47

Table 4.9
Comparison of $\Delta\text{BIC} = \text{BIC} - \text{BIC}_{low}$. Recall that $\text{BIC} = -2\log(\mathcal{L}) + \log(n)k$ (where n is the number of datapoints and k is the number of parameters in the model).

Comparison of ΔBIC across models, fungi, and parameter estimation techniques				
	MLE	**MH**	**B-MLE**	
R1	0;	8.8;	0.1;	*E*. sp.B.
Briere-2	964.0;	13.0;	8.6;	*C. brevicomi*
$r(T_0, T_m, B, \omega)$	0;	2.6;	2.4;	*G. clavigera*
	143.7	7.8	3.0	*O. montium*
R2	22.9;	23.6;	23.9;	*E*. sp.B.
Dogleg	26.8;	6.4;	6.4;	*C. brevicomi*
$r(T_0, T_m, B = r_{opt}, T_{opt})$	2.2;	15.5;	9.5;	*O. montium*
	0	4.8	1.2	*G. clavigera*
R3	242.0;	33.5;	227.9;	*E*. sp.B.
Hansen	0;	48.6;	135.7;	*C. brevicomi*
$r(T_0, T_m, B, \omega, \Delta_m)$	7.0;	42.6;	8.0;	*G. clavigera*
	143.7	24.3	17.4	*O. montium*
R4	268.3;	267.3;	250.3;	*E*. sp.B.
Régnière et al.	49.9;	25.6;	36.8;	*C. brevicomi*
$r(T_0, T_m, B, \omega, \Delta_0, \Delta_m)$	217.1;	26.8;	41.0;	*G. clavigera*
	184.8	192.6	190.3	*O. montium*

Fig. 4.5: Comparison of the various rate curve fits for *O. montium* for MLE (solid red curve), MH (using the mean of the samples collected after the burn-in period, dashed blue curve) and B-MLE (dotted black curve). Here we see reasonable fits for the Briere-2 curve (R1; Plot A) and with MH and B-MLE for the Dogleg curve (R2; Plot B). Pathological behavior was also exhibited for this dataset, however. This can be seen in the unrealistically high upper temperature threshold obtained by MLE for the Dogleg curve ($T_m = 115.00$), the sharp corner in the B-MLE parameterization for the Hansen curve (R3, Plot C) and the exponential shape of the MLE parameterization for the Régnière curve (R4; Plot D, possibly caused by three parameters having nearly zero values).
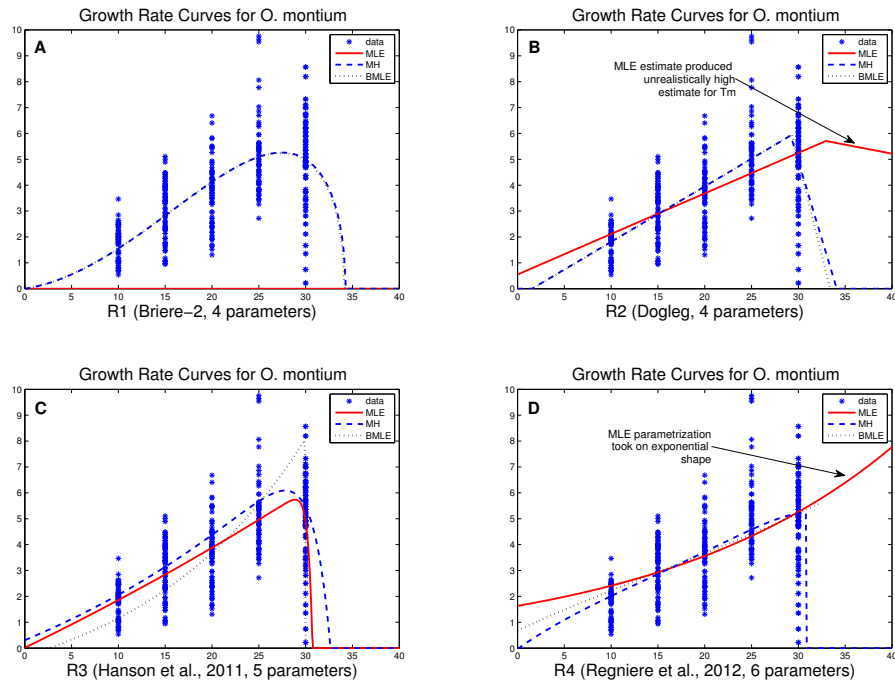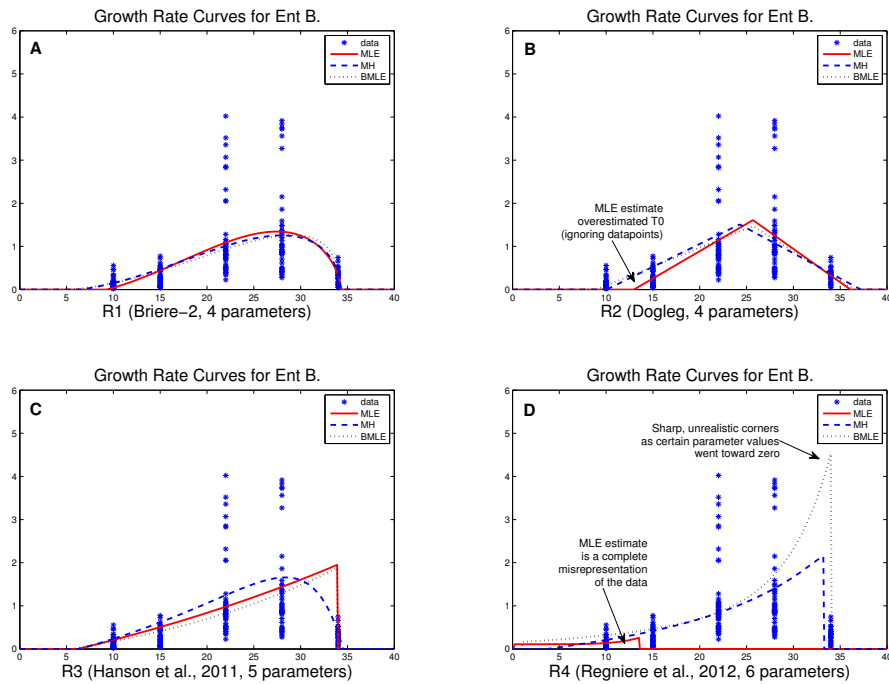
Fig. 4.6: Comparison of the various rate curve fits for *E.* sp.B. using MLE (solid red curve), MH (using the mean of the samples collected after the burn-in period, dashed blue curve) and B-MLE (dotted black curve). Here we see slight differences in fits obtained for the Briere-2 and Dogleg curves (R1 and R2; Plots A and B) though it seems that MLE has discounted the growth rate observations collected at 10°C. Fits for the Hansen curve (R3; Plot C) and the Régnière curve (R4; Plot D) display more pathological behavior with sharp corners obtained for MLE and B-MLE fits for the Hansen curve (R3) and with all techniques for the Régnière curve (R4). These can be partly attributed to $\Delta_m \sim 0$ in the Hansen curve and other parameter values becoming small in the Régnière curve. In Plot D, we also see that MLE has converged to a poor region of parameter space with $T_m = 13.59$ which is clearly not realistic.

4.4.2. In-depth test of parameterization methods

Briere-2 function (R2) to parameterize G. clavigera and O. montium data

Using the Briere-2 function with a normal error assumption, MLE, MH and B-MLE were applied to *G. clavigera* and *O. montium* data collected at Stump Hollow 100 times with variable initial parameters. Overall, MLE failed to converge 49% of the time with *G. clavigera* data and 75% of the time with *O. montium* data. In addition, half of the "convergent" iterations for *G. clavigera* and all but one for *O. montium* had actually converged to a local, rather than global, minimum (resulting in a BIC nearly 1000 higher than for many other non-convergent iterations) which led to extremely poor and widely varied parameter estimates. In contrast, MH resulted in stable parameter estimates with low standard deviation between estimates. Bayesian-type MLE resulted in slightly higher convergence than MLE (converging 58 of 100 times versus 51 of 100 for *G. clavigera* and 59 of 100 versus 25 of 100 for *O. montium* data) though its estimates were also highly varied. To get a better idea of the quality of the estimates and see how the variability in parameters affected the shape and appearance of the growth rate curves, the (convergent) parameterized rate curves for each technique were plotted with their respective data (Figure 4.7). Here we see a high degree of inconsistency between both MLE and B-MLE estimates and relatively consistent, smooth, rate curves obtained via MH.

Hansen function (R3) to parameterize O. montium and C. brevicomi

The in-depth parameterization test was also applied to *O. montium* data collected at Stump Hollow and *C. brevicomi* with the Hansen rate curve (R3). This revealed similar results. MLE failed to converge 56% of the time for *O. montium* and 80% of the time for *C. brevicomi* while B-MLE failed to converge 55% of the time for *O. montium* and 77% of the time for *C. brevicomi*. As with the parameter estimates obtained with the Briere-2 curve (R3), MLE and B-MLE estimates varied widely and, in general, produced inconsistent and poor fits (Figure 4.8, Plots A, C, D and F). MH estimates also exhibited variability, though parameter values were much more consistent and created reasonable looking rate curves (Figure 4.8, Plots B and E).

Fig. 4.7: Spread in rate curves after obtaining one hundred MLE (Plots A, B), MH (Plots C, D), and B-MLE (Plots E, F) parameter estimates for *G. clavigera* and *O. montium* (Stump Hollow dataset) using the Briere-2 (R1) curve, normal error, and random initial parameter estimates. Only convergent parameter estimates are plotted for MLE and B-MLE.
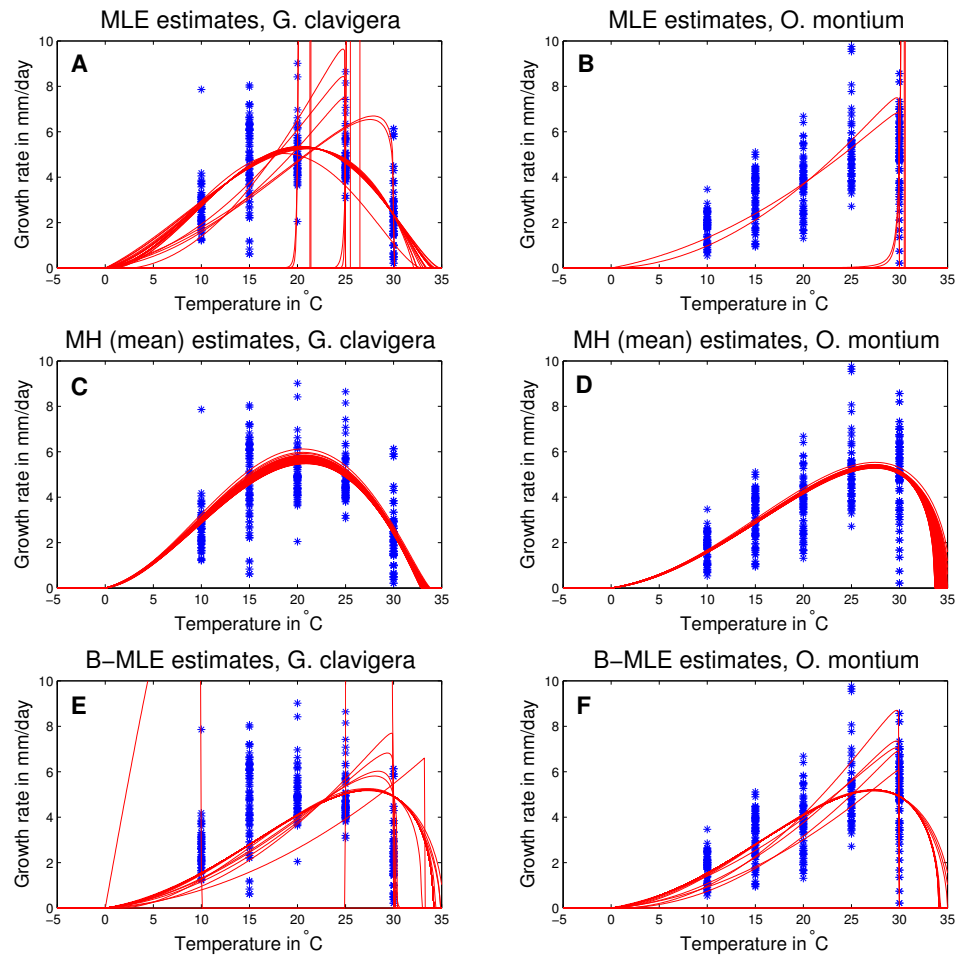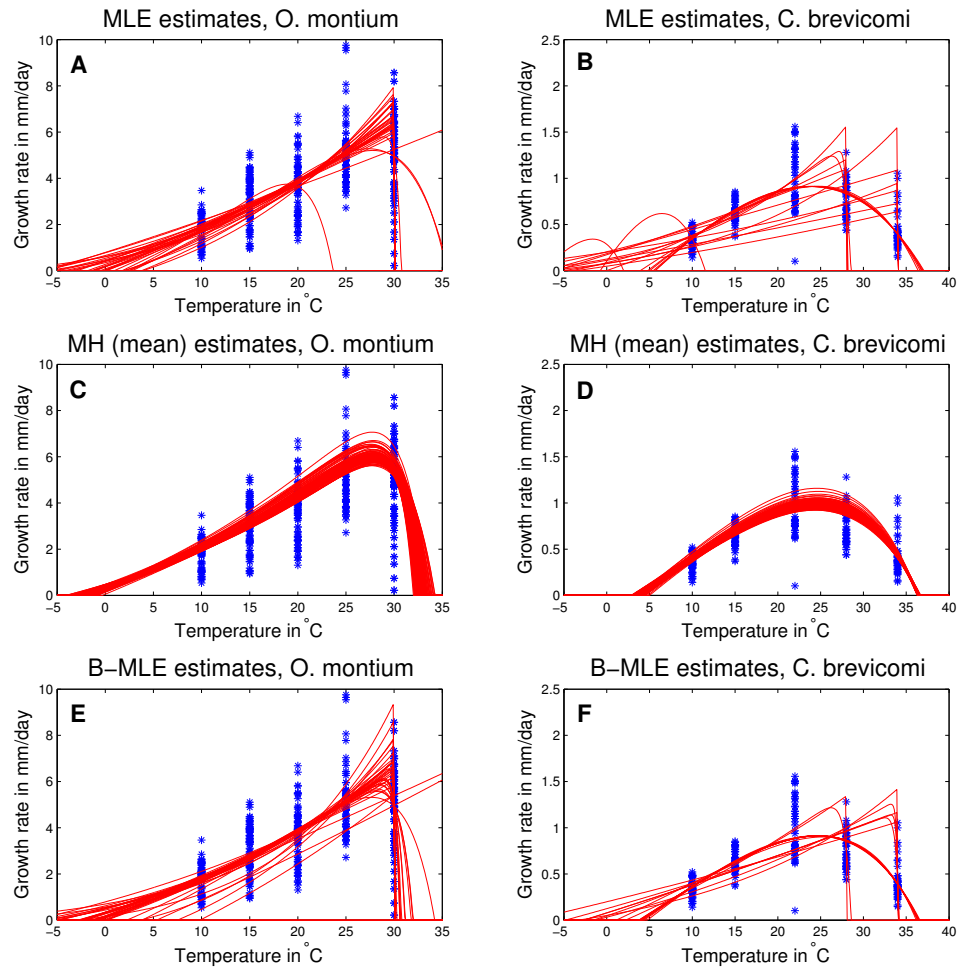
Fig. 4.8: Spread in rate curves after obtaining one hundred MLE (Plots A, B), MH (Plots C, D), and B-MLE (Plots E, F) parameter estimates for *O. montium* (Stump Hollow dataset) and *C. brevicomi* using the Hansen (R3) curve, normal error, and random initial parameter estimates. Only convergent parameter estimates are plotted for MLE and B-MLE.

Table 4.10

Best rate curve and parameter estimates for each fungus based on a criteria of BIC.

Best parameters and rate curves for the fungal datasets					
	T_0	T_m	B		
E. sp.B. (R1, Briere-2, MLE)	9.28	34.32	0.0008	$\omega = 0.63$	
C. brevicomi (R2, Dogleg, MLE)	3.22	41.56	$B = r_{opt} = 1.04$	$T_{opt} = 23.00$	
G. clavigera (R1, Briere-2, MLE)	0.71	34.61	0.0003	$\omega = 1.42$	
O. montium (R3, Hansen, MLE)	-0.09	30.74	19.11	$\omega = 0.0092$	$\Delta_m = 0.45$

4.4.3. Overall parameter estimates from the three parameterization methods

Using BIC as the criteria for best parameter estimates, we found that *G. clavigera* was best parameterized using the Briere-2 curve (R1) with temperature thresholds of $(T_0, T_m) = (0.71, 34.61)$ while *O. montium* was best parameterized with the Hansen curve (R3) with temperature thresholds of $(T_0, T_m) = (-0.09, 30.74)$ (Table 4.10, Figure 4.9). For WPB-associated fungi, we found that the Briere-2 (R1) curve provided the best fit to *E*. sp.B. data while the Dogleg (R2) curve provided the best fit to *C. brevicomi*. The respective temperature thresholds for these fungi were $(T_0, T_m) = (9.28, 34.32)$ and $(T_0, T_m) = (3.22, 41.56)$ (Table 4.10, Figure 4.9), indicating that *C. brevicomi* has a much wider range of temperatures where it can grow.

4.5. Discussion

Based on a cursory application of the various parameterization techniques, we found that for each dataset, parameter estimates were sensitive to the rate curve, choice of prior distribution, and parameterization method. Overall, MLE performed well when estimating curves with lower numbers of parameters though it often had to be repeated more than 10 times to achieve convergence. Even convergent applications of MLE experienced difficulty in terms of estimating unrealistic temperature thresholds (i.e., the lower temperature threshold for *E*. sp.B., both thresholds for *O. montium* using the Briere-2 curve (R1), and
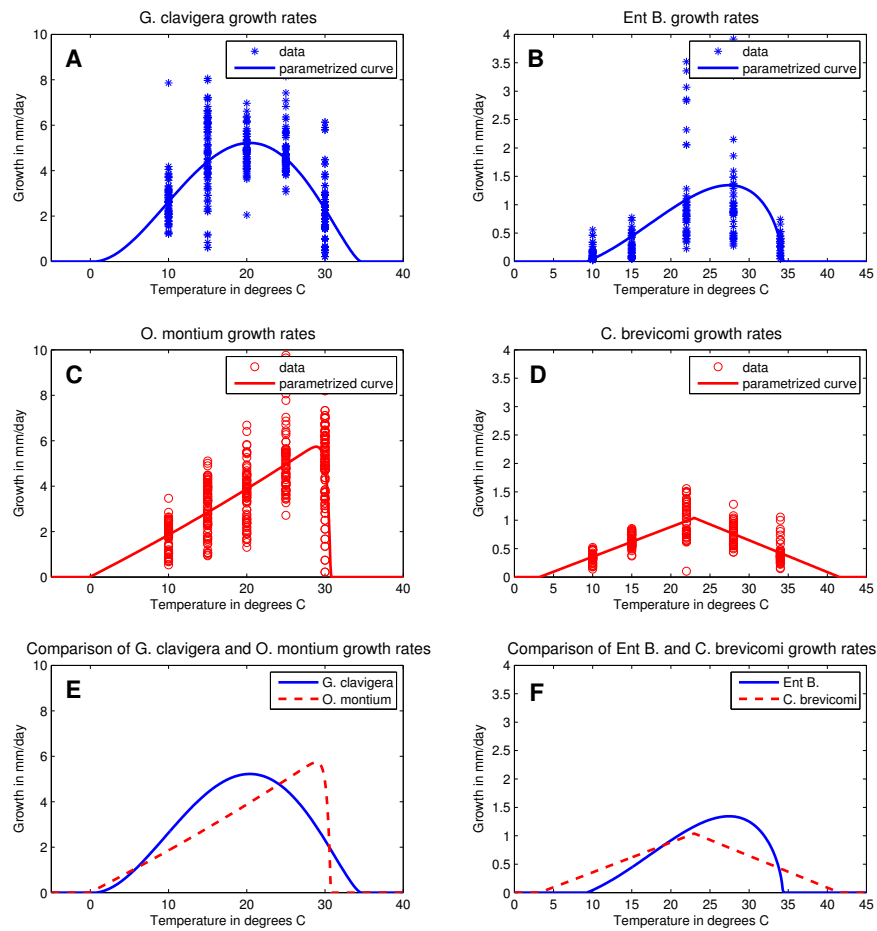
Fig. 4.9: Comparison of the observed data and the best parameterized rate curves for each fungus (Plots A-D) using the curves and parameters shown in Table 4.10. Plot E overlays the rate curve for MPB-associated fungi and Plot F overlays WPB-associated fungi. Here we see that while the temperature thresholds for *O. montium* (the warm-loving fungus associated with MPB) lie below those of *G. clavigera* (the cool-loving fungus with MPB), the overall growth characteristics reflect known behavior of the fungi.

the upper temperature threshold for *O. montium* using the Dogleg curve (R2); see Tables 4.5-4.8), allowing estimates to be nearly zero or negative, or resulting in drastically different parameter values given small perturbations in the initial guess. As the number of parameters increased (the Hansen and Régnière curves; R3 and R4), MLE (occasionally) experienced even more difficulty and had the potential to completely misrepresent the data (see Figures 4.5-4.8).

B-MLE utilized the same optimizer as MLE, however, the inclusion of prior knowledge regarding T_0 and T_m successfully prevented unrealistic parameter estimates for the temperature thresholds and negative estimates for the remaining parameters. This allowed B-MLE to regularly achieve good parameter estimates for the curves with four parameters (Briere-2 and Dogleg, R1 and R2) though it still suffered from lack of convergence and inconsistency (see Figures 4.7 and 4.8), and often resulted in overly angular/choppy rate curves (Figures 4.5-4.8). MH, also including prior knowledge (as well as allowing user tuning to ensure adequate exploration of the parameter space) was the most consistent of the techniques. It did not always achieve the lowest BIC value; however, it seemed most able to accommodate variable, messy data. MH provided reasonable parameter estimates and visually well-fitting rate curves for the Briere-2, Dogleg and Hansen curves (R1, R2, and R3 which had up to five parameters). As with the other techniques, MH struggled to parameterize the Régnière curve (R4) in that the fits obtained were angular and slightly underestimated the upper temperature threshold.

Taken together, we see why MLE is often the parameterization method of choice. It is fast, easy, and often accurate. In parameterizing the various rate curves and datasets with different structure and amounts of variability, we also found limitations of MLE. It is sensitive to the choice of initial parameters and may fail to converge. It can also run off to regions of parameter space that are invalid and achieve terrible fits. This indicates that MLE requires a significant amount of user knowledge and input after the fact to obtain good parameter estimates. That is, the user must not only ensure that MLE has converged, but also that the parameter values it has converged to are reasonable or the technique

must be repeated. B-MLE can improve consistency somewhat, however, failure to converge and converging to a local minima is still a concern so the user must again exercise caution in trusting parameter estimates. MH, on the other hand, was quite consistent. From a standpoint of repeatability, MH is desirable in that it requires the user to be extremely clear from the outset regarding their knowledge of previous parameters and how much weight they wish this knowledge to have relative to the data (versus secretly discarding undesirable parameter estimates after the fact). That said, MH did struggle when the number of parameters in the function were increased. This could likely be remedied with improved prior knowledge. This prior knowledge could affect the algorithm in terms of having a more informative prior distribution on the parameters as well as allowing the user to specify more reasonable step-sizes for the proposal distribution.

Overall, based on ease of parameterization and quality of fit (ΔBIC, shown in Table 4.9), R1 and R2, the Briere-2 and Dogleg rate curves best approximated the fungus growth rate data. Overall, the Briere-2 (R1) provided the best fit for *G. clavigera* and *E.* sp.B. and the Dogleg (R2) provided the best fit for *C. brevicomi*. For *O. montium*, the best rate curve was either the Dogleg or the Hansen curve (R2 or R3), depending on the method used for parameterization. MLE was able to achieve the lowest BIC for *O. montium* using the Hansen curve (R3), though when prior knowledge was included (MH, B-MLE), the Dogleg curve (R2) achieved the best fits. This could partly be due to the prior distribution on T_m (i.e., $T_m \sim N(32, 2^2)$) causing MH and B-MLE to provide more weight to parameter estimates for T_m that were closer to 32 (MLE estimated that T_m was 30.74). The data for *O. montium* also exhibited an extremely high degree of variability, especially for measurements taken at $30°$C which makes it difficult to distinguish between the performance of the rate curves.

4.6. Conclusions

Though many techniques are available for parameterizing functions to data, the best technique will often depend on the complexity of the function and the variability and size of the dataset. In this paper, we used nonlinear functions having four to six parameters

to describe moderately large datasets containing a few hundred observations with high amounts of variability and parameterized the functions using three techniques: MLE, MH, and B-MLE. For these functions and datasets, MH was clearly the superior method in terms of consistency and requiring the user to formally specify any biases from the outset. MLE and B-MLE were occasionally able to attain better fits to the data (as measured by BIC), however, this often required perturbing initial parameters more than 10 times to achieve convergence and then knowing whether the convergent parameters and resulting fit were reasonable or whether the method needed to be repeated again. MH, on the other hand, consistently resulted in adequate fits using one run of the algorithm. Considering today's atmosphere where repeatability and reproducibility of scientific experiments (Stodden, 2010; Vanschoren et al., 2012) is prized, the ability to produce consistent parameter estimates and fully justify any user bias are more important than ever. This makes techniques such as MH increasingly attractive.

CHAPTER 5

SUMMARY AND CONCLUSIONS

In this work we utilized mathematical tools to create and validate two models describing the interactions of three species with overlapping phenologies. These models incorporated previous models or approaches for MPB development and new models for fungus growth in a tree and were parameterized using direct and indirect observations (i.e., fungus growth rates collected in an artificial medium as well as records of attacking and emerging MPB and the fungus they were carrying). We posit that predictions about the system as a whole will be made stronger when considering their overlapping phenologies. MPB success is thought to depend on nutritional benefits obtained from feeding on fungus colonized phloem at different stages in its development. Due to differences between its fungal symbionts, the degree of MPB success will also depend on fungal timing. Thus, in order to best predict or understand the future of the MPB-fungus system, inclusive models that quantify the likelihood of fungal presence at the appropriate time are essential.

In Chapter 2 we developed an individual-based model describing the growth of fungal lesions on a one-dimensional ring of tree circumference. Using the assumption that the fungi would not actively compete, we allowed the fungus lesions to grow at a rate based on temperature and then stop when they reached another lesion (mimicking the finite space available to colonize within a host tree). Using this model for fungal growth, we combined its predictions with a median model for MPB development. This allowed us to predict when the median MPB adult would emerge from a tree based on an observed record of hourly temperatures so that we could determine the proportion of each fungus that would be carried to a new host tree the following year. Finally, we utilized this combination of models to test whether different forms of variability in temperature could explain the relatively stable dynamics between MPB, *G. clavigera* and *O. montium* over time. Using observed temperature records from the Sawtooth National Wildlife Refuge and a higher elevation site, Railroad Ridge, as well as simulated temperature records formed from these datasets, we tested whether intra-year variability (variability over the course of a single

year), inter-year variability (variability between years), or variability due to a portion of the MPB population periodically transitioning between thermal regions could explain the continued presence of both fungi in the mutualism. We found that cooler years favored *G. clavigera* and warmer years favored *O. montium* (which was expected based on known growth profiles exhibited by the fungi). In general, however, temperature records from the SNRA tended to consistently favor *O. montium* while the temperatures at RRR consistently favored *G. clavigera*. When viewed over a long period of time, this generally resulted in a loss of one fungus from the mutualism.

An unexpected result of the MPB fungus simulations was that the distance between fungal lesions (determined by the density of attacking MPB) could also influence the proportion of each fungi over time. We found that closely spaced lesions (due to high densities of attacking MPB) could also stabilize the mutualism. Regarding temperature variability, however, we found that only large-scale variability in temperature, such as from portions of the MPB population periodically transitioning between different thermal environments, was enough to stabilize the mutualism over a long period of time. Regarding the future of the mutualism as a whole, the simulations conducted in Chapter 2 seemed to indicate that in the face of increasing temperatures, *G. clavigera* would be slowly displaced from the mutualism due to its preference for cooler temperatures relative to *O. montium*.

In Chapter 3, we adapted the fungal growth model from Chapter 2 and then compared its predictions against real world observations of MPB and fungus exiting the tree. This model included several changes: 1) the fungal growth model was restructured so that it was deterministic (rather than stochastic) and the cumulative growth of all fungal lesions was tracked (rather than the growth of lesions individually), 2) the model incorporated two parameters describing how the growth of *G. clavigera* and *O. montium* scaled from a Petri dish to a tree, 3) a distributional approach was used to determine the TA feeding window (rather than calculating the date of emergence for the median MPB), and 4) five submodels were introduced to describe a spectrum of possible various interactions between MPB and fungi within the host tree. These changes resulted in a number of benefits,

they significantly reduced computational time, provided the ability to track fungus lesions that began growing on different days (as they would in a tree), and allowed us to compare predictions with observed MPB emergence data (difficult with the previous model because it modeled too few individuals). This model was then parameterized and tested using real-world MPB attack and emergence observations collected from 2010 to 2011 and 2011 to 2012.

After parameterizing and testing the models, we found that while dynamics between years were different, the models which assigned the fungi in the mycangia of MPB based on the fungi present in the tree just prior to emergence performed best. This indicates that fungus present at the end of the teneral adult feeding window just prior to MPB emergence from a host tree is more important than the fungus present during earlier phases of the feeding window. We also found that the growth of the two fungi scale very differently from a Petri dish to a live tree. *G. clavigera*, known to be more virulent and better able to tolerate low oxygen conditions (such as those in a freshly attacked tree) grew approximately 25 times more quickly than *O. montium*. However, these exact numbers were directly influenced by observations from study trees in which very low numbers of beetles were observed exiting with *O. montium*.

Since MPB success is strongly tied to the success of its symbionts and Chapters 2 and 3 seemed to predict different outcomes from the mutualism in terms of whether both fungi will be maintained, we revisited the parameterization of the fungal growth rate curves in Chapter 4. Fungal growth rate curves are used by both models to predict how fast each fungus will grow as a function of temperature. The format of these curves can vary widely; however, nonlinear curves are generally preferred because they more accurately represent the growth of the fungi over a broad range of temperatures. These curves formed the basis of the fungal growth model, determining how fast the fungi can colonize the host tree. We wanted to see whether the fungal growth rate curves used in Chapter 3 could be improved upon to better distinguish the growth of each species and to better explain fungal emergence for both the parameterization and validation dataset. To do this, we selected four possible rate

curves used to model the growth of other cold-blooded organisms and then parameterized the curves using maximum likelihood estimation (MLE), Metropolis Hastings (MH), and Bayesian "MLE" (B-MLE) to best fit observed growth rates for mountain pine beetle and western pine beetle associated fungi collected in an artificial medium. The intent was to test whether the inclusion of prior information, allowed in MH and B-MLE, could improve the fit of the data or the reliability of the parameter estimation technique. What we found is that MLE is a good technique; it often produces very good parameter estimates as quantified by the Bayesian Information Criterion. On the other hand, MLE did not consistently achieve good parameter estimates. Often, the method had to be repeated and results discarded due to lack of convergence or convergence to a poor region of parameter space. This made MLE highly unreliable and indicates that some degree of expert knowledge is required (after the fact) to obtain good, trustworthy parameters. The inclusion of prior knowledge in B-MLE did help to remedy these issues, though it still had the potential to converge to poor regions of parameter space and obtain very unrealistic fits to the data. Finally, using MH, we found that we could achieve much more consistent and realistic fits, though as the number of parameters increased, the method also resulted in more variable parameter estimates. We assess that this could be remedied by increasing the precision in the prior distribution for the parameters (by leaning more heavily on prior knowledge regarding several parameters in the rate curve).

Overall, the most significant portions of this work are the development of a framework for connecting models describing the phenology of various species to better understand how the system will act as a whole and introducing the use of prior knowledge when estimating fungal growth rate curves. Using the notion of a colonization index, we were able to combine different forms of output from phenology models (i.e., translating predictions of length colonized by fungi to predictions of the proportion of a tree colonized so that these could be combined with temporal predictions for MPB development) to arrive at an accurate model for the combined dynamics of three interacting species. In addition, since fungal growth rates at various temperatures formed the basis of our models, introducing Bayesian param-

eter estimation greatly improved the ease of parameterization as well as the consistency of the estimates (across rate curves and fungal datasets).

In an era of warming climate, researchers are interested in whether the MPB-fungus relationship will remain stable, or whether one fungus will be displaced from the mutualism. Since the fungi differ substantially in their benefits to the beetle, the loss of one fungi could greatly affect the ability of MPB (for better or worse) to spread across landscapes. Our models seem to indicate that if the rate of fungal growth in a tree is proportionate to that measured in an artificial medium (i.e., with the growth of both fungi scaling in the same way), then one symbiont will likely be lost from the mutualism unless portions of MPB periodically transition to different thermal areas. When parameterizing the MPB-fungus model to data, however, it seemed much more likely that the fungus growth rates observed in an artificial medium will scale differently for each species with *G. clavigera* gaining a substantial advantage over *O. montium* in a tree. This seems to indicate that *G. clavigera* will likely not be lost from the mutualism any time soon, though the accuracy of our growth rate scaling parameters was slightly suspect due to the oddities in our dataset, in which extremely low numbers of MPB were observed to be emerging with *O. montium*. In reality, it is likely that some combination of results from Chapter 2 and Chapter 3 will occur. We assess that the growth rate scaling parameters of the fungi do differ, though not by as great a margin. As a result, it is likely that *O. montium*, the warm-loving fungus, will experience greater success in warmer climates while *G. clavigera*, through its greater virulence, will also continue to persist in the mutualism.

REFERENCES

Adams, A. S., Six, D. L., 2007. Temporal variation in mycophagy and prevalence of fungi associated with developmental stages of *Dendroctonus ponderosae* (coleoptera: Curculionidae). Environ. Entomol. 36 (1), 64–72.

Adams, A. S., Six, D. L., Adams, S. M., Holben, W. E., 2008. In vitro interactions between yeasts and bacteria and the fungal symbionts of the mountain pine beetle (*Dendroctonus ponderosae*). Microb. Ecol. 56 (3), 460–466.

Bentz, B., Vandygriff, J., Jensen, C., Coleman, T., Maloney, P., Smith, S., Grady, A., Schen-Langenheim, G., 2013. Mountain pine beetle voltinism and life history characteristics across latitudinal and elevational gradients in the western United States. For. Sci. 60 (2), 000–000.

Bentz, B. J., Logan, J. A., Amman, G. D., 1991. Temperature-dependent development of the mountain pine beetle (coleoptera: Scolytidae) and simulation of its phenology. Can. Entomol. 123 (05), 1083–1094.

Bentz, B. J., Regniere, J., Fettig, C. J., Hansen, E., Hayes, J., Hicke, J., Seybold, S., 2010. Climate change and bark beetles of the western United States and Canada: direct and indirect effects. BioScience 60 (8), 602–613.

Bentz, B. J., Six, D. L., 2006. Ergosterol content of fungi associated with *Dendroctonus ponderosae* and *Dendroctonus rufipennis* (coleoptera: Curculionidae, scolytinae). Ann. Entomol. Soc. Am. 99 (2), 189–194.

Bleiker, K. P., Six, D. L., 2007. Dietary benefits of fungal associates to an eruptive herbivore: Potential implications of multiple associates on host population dynamics. Environ. Entomol. 36 (6), 1384–1396.

Briere, J. F., Pracros, P., Le Roux, A. Y., Pierre, J. S., 1999. A novel rate model of temperature-dependent development for arthropods. Environ. Entomol. 28 (1), 22–29.

Burnham, K. P., Anderson, D. R., 2002. *Model Selection and Multimodel Inference: A Practical Information-Theoretic Approach*. Springer, New York.

Calabrese, J. M., Fagan, W. F., 2004. Lost in time, lonely, and single: reproductive asynchrony and the Allee effect. Am. Nat. 164 (1), 25–37.

Campbell, A., Frazer, B., Gilbert, N., Gutierrez, A., Mackauer, M., 1974. Temperature requirements of some aphids and their parasites. J. Appl. Ecol. 11 (2), 431–438.

Carroll, A. L., Taylor, S. W., Régnière, J., Safranyik, L., 2003. Effect of climate change on range expansion by the mountain pine beetle in British Columbia. In: *Mountain Pine Beetle Symposium: Challenges and Solutions, Oct. 30-31, 2003. Kelowna BC. Natural Resources Canada, Information Report BC-X-399, Victoria* pages 223–232.

Chen, H., Walton, A., 2011. Mountain pine beetle dispersal: spatiotemporal patterns and role in the spread and expansion of the present outbreak. Ecosphere 2 (6), art66.

Cook, S. P., Shirley, B., Zambino, P., 2010. Nitrogen concentration in mountain pine beetle larvae reflects nitrogen status of the tree host and two fungal associates. Environ. Entomol. 39, 821–826.

Cudmore, T. J., Björklund, N., Carroll, A. L., Staffan Lindgren, B., 2010. Climate change and range expansion of an aggressive bark beetle: evidence of higher beetle reproduction in naïve host tree populations. J. Appl. Ecol. 47 (5), 1036–1043.

Cullingham, C., Cooke, J., Dang, S., Davis, C., Cooke, B., Coltman, D., 2011. Mountain pine beetle host-range expansion threatens the boreal forest. Mol. Ecol. 20 (10), 2157–2171.

Daufresne, M., Lengfellner, K., Sommer, U., 2009. Global warming benefits the small in aquatic ecosystems. Proc. National Academy of Sciences 106 (31), 12788–12793.

Dauta, A., Devaux, J., Piquemal, F., Boumnich, L., 1990. Growth rate of four freshwater algae in relation to light and temperature. Hydrobiologia 207 (1), 221–226.

Davis, T. S., Hofstetter, R. W., Klepzig, K. D., Foster, J. T., Keim, P., 2010. Interactions between multiple fungi isolated from two bark beetles, *Dendroctonus brevicomis* and *Dendroctonus frontalis* (coleoptera: Curculionidae). J. Yeast and Fungal Research 1 (7), 118–126.

de la Giroday, H. M. C., Carroll, A. L., Aukema, B. H., 2012. Breach of the northern Rocky Mountain geoclimatic barrier: initiation of range expansion by the mountain pine beetle. J. Biogeogr. 39 (6), 1112–1123.

Dysthe, C., Bracewell, R., Six, D., 2014. Growth rates of western pine beetle associated fungi. Unpublished raw data.

Goodsman, D. W., Erbilgin, N., Lieffers, V. J., 2012. The impact of phloem nutrients on overwintering mountain pine beetles and their fungal symbionts. Environ. Entomol. 41 (3), 478–486.

Gross, R. S., Werner, P. A., 1983. Relationships among flowering phenology, insect visitors, and seed-set of individuals: experimental studies on four co-occurring species of goldenrod (solidago: Compositae). Ecol. Monogr. 53 (1), 95–117.

Hansen, E. M., Bentz, B. J., Powell, J. A., Gray, D. R., Vandygriff, J. C., 2011. Prepupal diapause and instar IV developmental rates of the spruce beetle, *Dendroctonus rufipennis* (coleoptera: Curculionidae, scolytinae). J. Insect Physiol. 57 (10), 1347–1357.

Harrington, T. C., 1993. *Ceratocystis and Ophiostoma: Taxonomy, ecology, and pathogenicity* chapter Diseases of conifers caused by species of Ophiostoma and Leptographium., pages 161–172. The American Phytopathological Society Press, St. Paul.

Harrington, T. C., 2005. *Ecological and Evolutionary Advances in Insect-Fungal Associations* chapter Ecology and evolution of mycophagous bark beetles and their fungal partners, pages 257-291. Oxford University Press, Oxford.

Hicke, J. A., Logan, J. A., Powell, J. A., Ojima, D. S., 2006. Changing temperatures influence suitability for modeled mountain pine beetle (*Dendroctonus ponderosae*) outbreaks in the western United States. J. Geophys. Res. 111 (G02019).

Hill, J. K., Thomas, C. D., Huntley, B., 1999. Climate and habitat availability determine 20th century changes in a butterfly's range margin. Proceedings of the Royal Society of London. Series B: Biological Sciences 266 (1425), 1197–1206.

Hsiau, P. T.-W., Harrington, T. C., 1997. Ceratocystiopsis brevicomi sp. nov., a mycangial fungus from *Dendroctonus brevicomis* (coleoptera: Scolytidae). Mycologia 89 (4), 661–669.

Kaspari, M., Pickering, J., Longino, J. T., Windsor, D., 2001. The phenology of a Neotropical ant assemblage: evidence for continuous and overlapping reproduction. Behav. Ecol. Sociobiol. 50 (4), 382–390.

Klepzig, K., Adams, A., Handelsman, J., Raffa, K., 2009. Symbioses: A key driver of insect physiological processes, ecological interactions, evolutionary diversification, and impacts on humans. Environ. Entomol. 38 (1), 67–77.

Krenek, S., Berendonk, T. U., Petzoldt, T., 2011. Thermal performance curves of *Paramecium caudatum*: A model selection approach. Eur. J. Protistol. 47 (2), 124–137.

Krokene, P., Solheim, H., 1998. Pathogenicity of four blue-stain fungi associated with aggressive and nonaggressive bark beetles. Phytopathology 88 (1), 39–44.

Logan, J., Wollkind, D., Hoyt, S., Tanigoshi, L., 1976. An analytic model for description of temperature dependent rate phenomena in arthropods. Environ. Entomol. 5 (6), 1133–1140.

Logan, J. A., 1988. Toward an expert system for development of pest simulation models. Environ. Entomol. 17 (2), 359–376.

Logan, J. A., Bentz, B. J., 1999. Model analysis of mountain pine beetle (coleoptera: Scolytidae) seasonality. Environ. Entomol. 28 (6), 924–934.

Logan, J. A., Powell, J. A., 2001. Ghost forests, global warming, and the mountain pine beetle (coleoptera: Scolytidae). Am. Entomol. 47 (3), 160.

Meddens, A. J., Hicke, J. A., Ferguson, C. A., 2012. Spatiotemporal patterns of observed bark beetle-caused tree mortality in British Columbia and the western United States. Ecological Applications 22 (7), 1876–1891.

Metropolis, N., Rosenbluth, A. W., Rosenbluth, M. N., Teller, A. H., Teller, E., 2004. Equation of state calculations by fast computing machines. J. Chemical Physics 21 (6), 1087–1092.

Molnár, P. K., Kutz, S. J., Hoar, B. M., Dobson, A. P., 2013. Metabolic approaches to understanding climate change impacts on seasonal host-macroparasite dynamics. Ecology Letters 16 (1), 9–21.

Moore, M. L., 2013. *The effects of temperature on fungal symbionts in the mountain pine beetle-fungus multi-partite symbiosis.* PhD thesis The University of Montana, Missoula.

Murali, K., Sukumar, R., 1994. Reproductive phenology of a tropical dry forest in Mudumalai, southern India. J. Ecol. 82 (4), 759–767.

Paine, T., Raffa, K., Harrington, T., 1997. Interactions among scolytid bark beetles, their associated fungi, and live host conifers. Annu. Rev. Entomol. 42 (1), 179–206.

Plattner, A., Kim, J. J., DiGuistini, S., Breuil, C., 2008. Variation in pathogenicity of a mountain pine beetle–associated blue-stain fungus, *Grosmannia clavigera*, on young lodgepole pine in British Columbia. Canadian J. Plant Pathology 30 (3), 457–466.

Powell, J. A., Bentz, B. J., 2009. Connecting phenological predictions with population growth rates for mountain pine beetle, an outbreak insect. Landscape Ecol. 24, 657–672.

Powell, J. A., Bentz, B. J., 2014. Phenology and density-dependent dispersal predict patterns of mountain pine beetle (*Dendroctonus ponderosae*) impact. Ecol. Model. 273, 173–185.

Powell, J. A., Logan, J. A., 2005. Insect seasonality: circle map analysis of temperature-driven life cycles. Theor. Popul. Biol. 67 (3), 161–179.

Raffa, K. F., 2001. Mixed messages across multiple trophic levels: the ecology of bark beetle chemical communication systems. Chemoecology 11 (2), 49–65.

Raffa, K. F., Aukema, B. H., Bentz, B. J., Carroll, A. L., Hicke, J. A., Turner, M. G., Romme, W. H., 2008. Cross-scale drivers of natural disturbances prone to anthropogenic amplification: the dynamics of bark beetle eruptions. BioScience 58 (6), 501–517.

Raffa, K. F., Berryman, A. A., 1983. The role of host plant resistance in the colonization behavior and ecology of bark beetles (coleoptera: Scolytidae). Ecol. Monogr. 53 (1), 27–49.

Ratkowsky, D., Lowry, R., McMeekin, T., Stokes, A., Chandler, R., 1983. Model for bacterial culture growth rate throughout the entire biokinetic temperature range. J. Bacteriol. 154 (3), 1222–1226.

Régnière, J., Powell, J., Bentz, B., Nealis, V., 2012. Effects of temperature on development, survival and reproduction of insects: Experimental design, data analysis and modeling. J. Insect Physiol. 58 (5), 634–647.

Rice, A., Thormann, M., Langor, D., 2008. Mountain pine beetle-associated blue-stain fungi are differentially adapted to boreal temperatures. For. Pathol. 38, 113–123.

Richardson, A. J., Schoeman, D. S., 2004. Climate impact on plankton ecosystems in the Northeast Atlantic. Science 305 (5690), 1609–1612.

Ruess, L., Michelsen, A., Schmidt, I. K., Jonasson, S., 1999. Simulated climate change affecting microorganisms, nematode density and biodiversity in subarctic soils. Plant and Soil 212 (1), 63–73.

Safranyik, L., Carroll, A. L., Regniere, J., Langor, D. W., Riel, W. G., Shore, T. L., B. Peter, B. J. C., Nealis, V. G., Taylor., S. W., 2010. Potential for range expansion of mountain pine beetle into the boreal forest of North America. Can. Entomol. 142 (05), 415–442.

Safranyik, L., Carroll, A. L., Wilson, B., 2007. *The mountain pine beetle: a synthesis of biology, management and impacts on lodgepole pine* chapter The biology and epidemiology of the mountain pine beetle in lodgepole pine forests. Canadian Forest Service.

Sambaraju, K. R., Carroll, A. L., Zhu, J., Stahl, K., Moore, R. D., Aukema, B. H., 2012. Climate change could alter the distribution of mountain pine beetle outbreaks in western Canada. Ecography 35 (3), 211–223.

Schneider, C., Rasband, W., Eliceiri, K., 2012. NIH Image to ImageJ: 25 years of image analysis. Nat. Methods 9, 671–675.

Schoolfield, R., Sharpe, P., Magnuson, C., 1981. Non-linear regression of biological temperature-dependent rate models based on absolute reaction-rate theory. J. Theor. Biol. 88 (4), 719–731.

Sharpe, P. J., DeMichele, D. W., 1977. Reaction kinetics of poikilotherm development. J. Theor. Biol. 64 (4), 649–670.

Shi, P., Ge, F., 2010. A comparison of different thermal performance functions describing temperature-dependent development rates. J. Therm. Biol. 35 (5), 225–231.

Six, D., 2012. Ecological and evolutionary determinants of bark beetle-fungus symbioses. Insects 3 (339-366).

Six, D., Bentz, B., 2007. Temperature determines symbiont abundance in a multipartite bark beetle-fungus ectosymbiosis. Microb. Ecol. 54, 112–118.

Six, D., Paine, T., 1998. Effects of mycangial fungi and host tree species on progeny survival and emergence of *Dendroctonus ponderosae* (coleoptera: Scolytidae). Environ. Entomol. 27 (6), 1393–1401.

Six, D. L., Klepzig, K. D., 2004. Dendroctonus bark beetles as model systems for studies on symbiosis. Symbiosis 37 (1), 207–232.

Smits, N., Brière, J.-F., Fargues, J., 2003. Comparison of non-linear temperature-dependent development rate models applied to *in vitro* growth of entomopathogenic fungi. Mycological Research 107 (12), 1476–1484.

Solheim, H., Krokene, P., 1998. Growth and virulence of mountain pine beetle associated blue-stain fungi, *Ophiostoma clavigerum* and *Ophiostoma montium*. Can. J. Bot. 76 (4), 561–566.

Stevenson, R. D., Peterson, C. R., Tsuji, J. S., 1985. The thermal dependence of locomotion, tongue flicking, digestion, and oxygen consumption in the wandering garter snake. Physiol. Zool. 58 (1), 46–57.

Stodden, V., 2010. The scientific method in practice: reproducibility in the computational sciences.

Taylor, S., Carroll, A., Alfaro, R., Safranyik, L., 2007. *The mountain pine beetle: a synthesis of biology, management and impacts on lodgepole pine* chapter Forest, climate and mountain pine beetle outbreak dynamics in western Canada. Canadian Forest Service.

Upadhyay, H., 1981. A Monograph of Ceratocystis and Ceratocystiopsis. University of Georgia Press, Athens.

Vanschoren, J., Blockeel, H., Pfahringer, B., Holmes, G., 2012. Experiment databases. Machine Learning 87 (2), 127–158.

Weitere, M., Vohmann, A., Schulz, N., Linn, C., Dietrich, D., Arndt, H., 2009. Linking environmental warming to the fitness of the invasive clam *Corbicula fluminea*. Global Change Biology 15 (12), 2838–2851.

Wood, D. L., 1982. The role of pheromones, kairomones, and allomones in the host selection and colonization behavior of bark beetles. Annu. Rev. Entomol. 27, 411–446.

APPENDIX

Multiple Author Release for Doctoral Dissertation

I, Melissa Moore, as coauthor of the work entitled "The role of temperature variability in stabilizing the mountain pine beetle-fungus mutualism" hereby authorize Audrey L. Addison to submit said work to Utah State University as all or part of a dissertation in partial fulfillment of the requirements for a doctoral degree.

I further authorize Audrey Addison to execute the following Dissertation Agreement* with ProQuest Information and Learning, Ann Arbor, Michigan.

<div align="center">Dissertation Agreement*</div>

Though my graduate school, I agree to supply you, ProQuest Information and Learning, with my dissertation and with an abstract of 350 words or less. I grant you the nonexclusive right to reproduce and distribute my dissertation in and from microform or electronic format, along with the right to reproduce and distribute my abstract in any format. I represent to you that the dissertation and the abstract are my original work, do not infringe any rights of others, and that I have the right to make these grants. You agree to offer copies of my dissertation for sale, and to publish an abstract of my dissertation in Dissertation Abstracts International. You also agree to pay me a royalty of ten percent, on sales of copies of my dissertation, for any calendar year when such sales equal seven (7) copies or more. In order to be eligible for such royalties in any calendar year, I agree that my obligation is to notify you of any change of address at least once during the subsequent two calendar years.

Date: _5/2/14_

Signature: _____

Multiple Author Release for Doctoral Dissertation

I, Diana L. Six, as coauthor of the works entitled "The role of temperature variability in stabilizing the mountain pine beetle-fungus mutualism" and "Connecting predictions for symbiotic fungal prevalence to temperature and mountain pine beetle development" hereby authorize Audrey L. Addison to submit said work to Utah State University as all or part of a dissertation in partial fulfillment of the requirements for a doctoral degree.

I further authorize Audrey Addison to execute the following Dissertation Agreement* with ProQuest Information and Learning, Ann Arbor, Michigan.

Dissertation Agreement*

Though my graduate school, I agree to supply you, ProQuest Information and Learning, with my dissertation and with an abstract of 350 words or less. I grant you the nonexclusive right to reproduce and distribute my dissertation in and from microform or electronic format, along with the right to reproduce and distribute my abstract in any format. I represent to you that the dissertation and the abstract are my original work, do not infringe any rights of others, and that I have the right to make these grants. You agree to offer copies of my dissertation for sale, and to publish an abstract of my dissertation in Dissertation Abstracts International. You also agree to pay me a royalty of ten percent, on sales of copies of my dissertation, for any calendar year when such sales equal seven (7) copies or more. In order to be eligible for such royalties in any calendar year, I agree that my obligation is to notify you of any change of address at least once during the subsequent two calendar years.

Date: _4/30/14_

Signature: _____

ELSEVIER LICENSE
TERMS AND CONDITIONS
Apr 23, 2014

This is a License Agreement between Audrey L Addison ("You") and Elsevier ("Elsevier") provided by Copyright Clearance Center ("CCC"). The license consists of your order details, the terms and conditions provided by Elsevier, and the payment terms and conditions.

All payments must be made in full to CCC. For payment instructions, please see information listed at the bottom of this form.

Supplier	Elsevier Limited The Boulevard,Langford Lane Kidlington,Oxford,OX5 1GB,UK
Registered Company Number	1982084
Customer name	Audrey L Addison
Customer address	1435 E 700 N Logan, UT 84321
License number	3375000679217
License date	Apr 23, 2014
Licensed content publisher	Elsevier
Licensed content publication	Journal of Theoretical Biology
Licensed content title	The role of temperature variability in stabilizing the mountain pine beetle–fungus mutualism
Licensed content author	A.L. Addison,J.A. Powell,D.L. Six,M. Moore,B.J. Bentz
Licensed content date	21 October 2013
Licensed content volume number	335
Licensed content issue number	
Number of pages	11
Start Page	40
End Page	50
Type of Use	reuse in a thesis/dissertation
Portion	full article
Format	electronic
Are you the author of this Elsevier article?	Yes
Will you be translating?	No

Title of your thesis/dissertation	Beetles, Fungi and Trees: A story for the ages? Modeling and projecting the multipartite symbiosis that exists between the mountain pine beetle, Dendroctonus ponderosae, and its fungal symbionts, Grosmannia clavigera and Ophiostoma montium
Expected completion date	May 2014
Estimated size (number of pages)	130
Elsevier VAT number	GB 494 6272 12
Permissions price	0.00 USD
VAT/Local Sales Tax	0.00 USD / 0.00 GBP
Total	0.00 USD

Terms and Conditions

INTRODUCTION

1. The publisher for this copyrighted material is Elsevier. Byclicking "accept" in connection with completing this licensingtransaction, you agree that the following terms and conditions apply to thistransaction (along with the Billing and Payment terms and conditionsestablished by Copyright Clearance Center, Inc. ("CCC"), at the timethat you opened your Rightslink account and that are available at any time at http://myaccount.copyright.com).

GENERAL TERMS

2. Elsevier hereby grants you permission to reproduce the aforementionedmaterial subject to the terms and conditions indicated.

3. Acknowledgement: If any part of the material to be used (for example,figures) has appeared in our publication with credit or acknowledgement toanother source, permission must also be sought from that source. If suchpermission is not obtained then that material may not be included in yourpublication/copies. Suitable acknowledgement to the source must be made, eitheras a footnote or in a reference list at the end of your publication, asfollows:

"Reprinted from Publication title, Vol /edition number, Author(s), Title ofarticle / title of chapter, Pages No., Copyright (Year), with permission fromElsevier [OR APPLICABLE SOCIETY COPYRIGHT OWNER]." Also Lancet special credit -"Reprinted from The Lancet, Vol. number, Author(s), Title of article, PagesNo., Copyright (Year), with permission from Elsevier."

4. Reproduction of this material is confined to the purpose and/or media forwhich permission is hereby given.

5. Altering/Modifying Material: Not Permitted. However figures andillustrations may be altered/adapted minimally to serve your work. Any otherabbreviations, additions, deletions and/or any other alterations shall be madeonly with prior written authorization of Elsevier Ltd. (Please contact Elsevierat permissions@elsevier.com)

CURRICULUM VITAE

Audrey Addison

1435 E 700 N, Logan, UT 84321

(907) 632-4432

audrey.smith@aggiemail.usu.edu

RESEARCH INTERESTS:

Applying mathematics to real-world problems. Mathematical ecology, developing and parameterizing models, numerical analysis, simulation, parallelization, optimization.

EDUCATION:

Ph.D., Mathematics

Utah State University, Logan, UT, May 2014

Advisor: James Powell

Dissertation Title: Beetles, Fungi and Trees: A story for the ages? Modeling and projecting the multipartite symbiosis between the mountain pine beetle, *Dendroctonus ponderosae*, and its fungal symbionts, *Grosmannia clavigera* and *Ophiostoma montium*.

M.S., Mathematics

Utah State University, Logan, UT, May 2014

Advisor: James Powell

Thesis Title: Developing a density-based approach to modeling sexual dimorphism and adaptive speciation.

B.S., Mathematics

University of Alaska Anchorage, Anchorage, AK, May 2004

Minor: Aviation Technology

TEACHING EXPERIENCE:

Instructor of Record, Utah State University:

Responsible for all aspects of teaching delivery and assessment.

Elements of Algebra (MATH 0900, Fall 2008)

Intermediate Algebra (MATH 1010, Spring 2010)

College Algebra (MATH 1050, Spring 2012)

Trigonometry (MATH 1060, Spring 2011)

Calculus Techniques (MATH 1100, Spring 2009, Fall 2010)

Calculus I (MATH 1210, Fall 2011)

Calculus II (MATH 1220, Fall 2010, Fall 2013)

Calculus III (MATH 2210, Fall 2012)

Ordinary Differential Equations* (MATH 2280, Spring 2013)

*one of two graduate students (out of 40) chosen to teach this course,

is generally reserved for faculty.

Guest Lecturer, Utah State University:

Methods of Applied Mathematics** (graduate level course), Fall 2013

**distance ed course, required use of instructional technology/recording devices

RESEARCH PUBLICATIONS:

A.L. Addison, J.A. Powell, D.L. Six, M. Moore, B.J. Bentz. *The role of temperature variability in stabilizing the mountain pine beetle-fungus mutualism.* Journal of Theoretical Biology, Volume 335, 21 October 2013, Pages 40-50.

In review: **A.L. Addison**, J.A. Powell, B.J. Bentz, D.L. Six. *Connecting predictions for symbiotic fungal prevalence to temperature and mountain pine beetle development.*

Unpublished manuscript: *Estimating the developmental thresholds of poikilotherms using prior knowledge.* A.L. Addison, included as part of Ph.D. Dissertation.

Unpublished manuscript: *Evolving Models: A density-based approach to modeling sexual dimorphism and adaptive speciation.* A.L. Addison, M.S. Thesis.

SERVICE:

Founding President, Utah State University SIAM Student Chapter, Oct 2012-Dec 2013

Member, Utah State University Math Biology Group

Member, Utah State University AMS Student Chapter

COMPUTER SKILLS:

Languages & Software: MATLAB, C++, R, *Mathematica*, Maple, Microsoft Office (including Access and SQL)

FUNDING INVOLVEMENT:

Travel grant ($500), SIAM, July 2013

Primary organizer for SIAM Student Chapter Fundraiser ($680), Utah State University, January 2013

Travel grant, housing and meal allowance ($1500), Mathematical Biosciences Institute, The Ohio State University, July 2011

TALKS, PRESENTATIONS AND CONFERENCES:

SEG Conference, September 2013, attended High Performance Computing Course.

SIAM Annual Meeting, July 2013,

funded to attend and represent Utah State University's SIAM Student Chapter.

MAA Conference, March 2013, Inter-mountain chapter,

Oral Presentation: "A tale of two fungi."

NGAUS Conference, September 2012, Selected to represent the 176th Wing

as an Officer Professional Development candidate at the 2012 National Guard

Association of the United States Conference.

Inter-mountain Graduate Research Symposium, March 2012,

Oral Presentation on modeling the mountain pine beetle - fungus mutualism.

Mathematical Biosciences Institute Summer Graduate Program,

July 2011, workshop in ecology and evolution.

Competitive entrance, given funding to attend.

Inter-mountain Graduate Research Symposium, March 2010,

Poster Presentation on density-based ecological modeling approaches for adaptive

speciation and sexual dimorphism.

MAA Conference, March 2010, Oral presentation on density-based

ecological modeling approach.

AWARDS AND ACTIVITIES:

USU Department of Mathematics and Statistics

Graduate Researcher of the Year, 2014;

Award given to one PhD student per department to recognize outstanding

performance by a graduate student. One selected out of more than 30 PhD students.

Nominated for the USU College of Science

Graduate Researcher of the Year, 2014

SIAM Certificate of Recognition for outstanding efforts and accomplishments

on behalf of the USU SIAM Chapter, April 2013.

Pat Tillman Military Scholar, class of 2010.

$3,000 award for four academic years. 2010-2014.

National Guard "All Guard" Biathlete, 2004, 2005.

OTHER PROFESSIONAL EXPERIENCE:

Air Force Intelligence Officer, *Jan 2006-present*

Provide training and threat information to five diverse flying squadrons,

commanders, and support personnel. Develop training plans; maintain programs;

supervise/mentor newer officers.

Ranking intelligence officer on two OEF deployments (Africa and Afghanistan).

Rescue Coordination Center Controller, *Sep 2004-Jan 2006*

Coordinated search and rescue activities for downed aircraft throughout Alaska.

Command Post Controller, *Mar 2001-Sep 2004*

Lone controller in comm hub of the base; provided interagency coordination.